Strål
säkerhets
myndigheten
Swedish Radiation Safety Authority

Authors: Adrian Bath
Hans-Peter Hermansson

Research

# 2009:28

# Biogeochemistry of Redox at Repository Depth and Implications for the Canister

Report number: 2009:28 ISSN: 2000-0456
Available at www.stralsakerhetsmyndigheten.se

**Title:** Biogeochemistry of Redox at Repository Depth and Implications for the Canister
**Report number:** 2009:28.
**Authors:** :Adrian Bath and Hans-Peter Hermansson
**Date:** August 2009.

This report concerns a study which has been conducted for the Swedish Radiation Safety Authority, SSM. The conclusions and viewpoints presented in the report are those of the author/authors and do not necessarily coincide with those of the SSM.

## SSM perspective

### Background

The present groundwater chemical conditions at the candidate sites for a spent nuclear fuel repository in Sweden (the Forsmark and Laxemar sites) and processes affecting its future evolution comprise essential conditions for the evaluation of barrier performance and long-term safety. This report reviews available chemical sampling information from the site investigations at the candidate sites, with a particular emphasis on redox active groundwater components and microbial populations that influence redox affecting components. Corrosion of copper canister material is the main barrier performance influence of redox conditions that is elaborated in the report. One section addresses native copper as a reasonable analogue for canister materials and another addresses the feasibility of methane hydrate ice accumulation during permafrost conditions. Such an accumulation could increase organic carbon availability in scenarios involving microbial sulphate reduction.

### Purpose of Project

The purpose of the project is to evaluate and describe the available knowledge and data for interpretation of geochemistry, microbiology and corrosion in safety assessment. A conclusive assessment of the sufficiency of information can, however, only be done in the future context of a full safety assessment.

### Results

The authors conclude that SKB's data and models for chemical and microbial processes are adequate and reasonably coherent. The redox conditions in the repository horizon are predominantly established through the $SO_4^{2-}$/HS- and $Fe^{3+}/Fe^{2+}$ redox couples. The former may exhibit a more significant buffering effect as suggested by measured Eh values, while the latter is associated with a lager capacity due to abundant Fe(II) minerals in the bedrock. Among a large numbers of groundwater features considered in geochemical equilibrium modelling, Eh, pH, temperature and concentration of dissolved sulphide comprise the most essential canister corrosion influences. Groundwater sulphide may originate from sulphide minerals and ongoing sulphate reduction as indicated by SRB populations, and may be limited by organic carbon availability. Another possible route for sulphate reduction is by coupling with anaerobic me-

thane oxidation. However, during present day conditions methane levels at Forsmark and Laxemar are probably too low for any essential sulphide production by that route. Methane hydrate could accumulate in fractures and repository void spaces beneath permafrost, but the potential impacts would be minimised by low porosity in crystalline rocks down to and below repository depth.

### Future work

A more detailed understanding of geochemical processes at repository depth may be needed to establish a firm basis for evaluation of groundwater corrodent concentrations. The same ranges of processes also need to be analysed in more detail for scenarios involving major climate change.

### Project Information

Project manager: Bo Strömberg
Project reference: SSM 2008/280
Project number: 200810237 and 200810238

# Content

# Executive summary

This report reviews the available biogeochemical data and the resulting models for redox-controlling systems in the near field geosphere at repository depth at SKB's two candidate deep repository sites at Forsmark and Laxemar. It focuses particularly on the processes that control present and future concentrations of $HS^-$ which is the main species of reduced sulphur in these conditions and is a corrodant of copper metal. Data and models for the near field are the main consideration here because these define the boundary conditions for how corrosion conditions will evolve in the EBS, i.e. in the bentonite buffer between the interface with rock and the rim of a canister. Processes in the buffer itself are not considered in depth because they are the focus of other work being carried out for SSM.

Data reported by SKB for populations of microorganisms in water samples, assumed to be reasonably representative of in situ groundwaters, are compiled. The main patterns and relationships among the main types of microbes and hydrochemical parameters are discussed. In addition, data from similar investigations at the Finnish site at Olkiluoto can be compared with data from Forsmark and Laxemar. Overall, comparison of the three sites indicates a coherent biogeochemical model that covers the range of conditions. Organic carbon (DOC) availability is an important constraint on reduction reactions.

A survey of literature for biogeochemical models for sulphate ($SO_4^{2-}$) reduction in organic-rich sediments provides some indication of reduction rates, but uncertainties and variability are large. It can be concluded that $SO_4^{2-}$ reduction by DOC is relatively rapid when it is mediated by microbial activity. Transferring that conclusion to the geosphere conditions at the crystalline rock sites requires some caution because of the constraints of low DOC, low microbe populations and other geochemical aspects such as salinity. The general significance of the biogeochemical pathway for $SO_4^{2-}$ reduction involving methane ($CH_4$), i.e. anaerobic oxidation of $CH_4$, remains inconclusive, but it is likely to be minor or negligible with the present low $CH_4$ abundance at repository depth at Forsmark and Laxemar whereas it is considered to be more likely at the Finnish site at Olkiluoto at which concentrations of $CH_4$ are many orders of magnitude higher. Relevant data for concentrations of $CH_4$ and $H_2$ in groundwaters at the sites are sparse; data are not available for acetate.

SSM's compilation of SKB's reported hydrochemical data for pH, $E_h$ and redox-active solutes is updated. Geochemical modelling is used to evaluate the effect of adjusting pH values for the possibility that $CO_2$ outgassed at time of sampling and thus caused pH values to drift upwards. Geochemical modelling is also used to calculate theoretical electrochemical potentials, $E_h$ values, for the $SO_4^{2-}/HS^-$ and $Fe(OH)_3/Fe^{2+}$ redox couples ($Fe^{3+}/Fe^{2+}$ couple is also modelled but $Fe^{3+}$ data are too uncertain for that calculated $E_h$ to have any reliability). Comparison shows that site-measured $E_h$ values are most usually closer to the electrochemical potential calculated for the $SO_4^{2-}/HS^-$

couple. The potential for the $Fe(OH)_3/Fe^{2+}$ couple is usually lower, i.e. more negative $E_h$ values. This provides further evidence that $SO_4^{2-}$ reduction is active, presumably because of mediation by SRB. Other lines of interpretation, and the fact that $Fe^{2+}$ is much more abundant in the total system than $SO_4^{2-}$ or $HS^-$ because of the $Fe^{II}$ reservoir in minerals, suggest that long-term stability of reducing conditions is likely to depend on $Fe^{2+}$ redox reactions.

Maximum HS concentration in near-field groundwater will be attenuated by precipitation of ferrous sulphide. That control is likely to persist into the future if $Fe^{2+}$ buffering by water-rock reaction with mineral sources of $Fe^{II}$ continue and pH conditions remain stable. Modelling of geochemical equilibrium confirms that FeS rather than $FeS_2$, pyrite, is the control for present $HS^-$ concentrations in near-field groundwaters. However pyrite is an accessory mineral in bentonite and presumably is a significant buffer of redox in the EBS. If pyrite were to control the concentration of $Fe^{2+}$ at a very low level in the bentonite, then $HS^-$ concentration could in theory be proportionately higher in equilibrium with FeS, though SKB provides evidence that production of $HS^-$ in situ would be inhibited in highly compacted bentonite.

Biogeochemical conditions at the EBS-rock interface in the initial period after closure of a repository could be affected by higher temperatures (typically 40-60°C for 1000 years) and higher radiation. These transients will be precursors for the evolution of near-field conditions in the long term.

The scenarios for long-term variations of biogeochemical conditions away from those presently observed, and the potential impact of those changes on production of corrodants in the near field, are considered. The most significant changes would probably be either greater penetration of fresh water recharge carrying greater amounts of DOC and possibly also increasing microbial numbers and activity, or increasing salinity and influx of greater amounts of $SO_4^{2-}$ to the near field. Both possibilities could increase $HS^-$ production outside the EBS which would cause a greater diffusive flux of $HS^-$ into the EBS. If $HS^-$ will be limited by precipitation of FeS then $HS^-$ concentration is unlikely to exceed 0.1 to 1 mg/L. This is a reasonable interpretation, but needs to consider possibilities that availability of reactive $Fe^{2+}$ buffered by mineral $Fe^{II}$ declines or whether there could be a big change of pH.

The stability of copper metal in terms of $HS^-$ concentration and other ambient hydrochemical parameters is examined by thermodynamic analysis and displayed in $E_h$-pH space in Pourbaix diagrams. Corrosion of copper by $HS^-$ could form rather complex products in the Cu-S-H-O system and the effectiveness of immunity or passivation would be variable depending on those products. The effect of salinity, i.e. increasing $Cl^-$, is to increase the vulnerability of copper at a given $E_h$; increasing temperature has a similar effect, as does decreasing pH.

Pourbaix diagrams constructed to take account of additional solutes Fe, Cl, N and $CO_3$ investigate what controls the immune areas and solid equilibria that influence corrosion. Amongst the issues is the potential effect of $NH_3$ on corrosion although present natural concentrations are well below levels that would have an impact.

There are a rather small number of native copper occurrences in ore deposits and of more minor occurrences worldwide that represent the preservation ('immunity') of metallic copper against corrosion in those specific geological and geochemical settings. Evidence about long-term stability or corrosion/alteration of copper metal in these various conditions is assessed. In most if not all cases, geochemical conditions have probably remained fairly constant and protective of the copper metal for much of their geological ages. Exposure of native copper to 'active' open-system biogeochemical fluctuations and processes has happened for rather shorter periods of time. Alteration ('corrosion') products probably originate from these periods of exposure. It is not presently possible to infer the relationship of these alteration products to either specific environmental conditions (e.g. groundwater compositions) or timescales.

Stability fields of copper metal in natural conditions, plus the areas in $E_h$-pH space where passivating oxides are stable, are examined with Pourbaix diagrams for complex geochemical systems. Mixed Cu-Fe oxides are indicated but these probably form only at high temperatures and are thus not relevant. Previous work on these issues for SKN and SKI concluded that reaction kinetics and metastable sulphide phases are probably important alongside the thermodynamic equilibria.

In conclusion, this report has found that SKB's data and models for biogeochemistry of redox at repository depth provide a reasonably coherent understanding of how concentrations of corrodant solutes are controlled in the near field. Data for *in situ* conditions are rather sparse but are judged to be just adequate to underpin the interpretations, considering the difficulties of sampling. Some data have yet to be reported and there are data gaps or large uncertainties in some of the more 'difficult' biogeochemical parameters. Relationships and spatial variabilities of parameters are not clear cut, therefore interpretations are tentative. The central theme of the biogeochemical model is that microbial mediation causes redox reactions to achieve equilibrium much faster than they would otherwise. Therefore the system will be reactive to external changes, e.g. increase of methane concentrations, and also will be internally buffered by water-rock reactions, e.g. reactions with mineral sources of $Fe^{II}$. The models provide a basis for prognosis of the biogeochemical effects in scenarios for evolution of the system at repository depth. SKB's long-term safety case in SR-Site should be evaluated in terms of its robustness to those scenarios on the basis of redox equilibria, outside the EBS and probably also inside the EBS, being reached relatively quickly and also on the basis of fluxes and mass budgets of chemical and microbial species.

# 1. Introduction and scope

Intellisci Ltd (Adrian Bath) and Studsvik Nuclear AB (Hans-Peter Hermansson) have collaborated since 2004 supporting SSM (and formerly SKI) in the evaluation of geochemical data reported by SKB from their deep repository site investigations at Forsmark (Östhammar) and Simpevarp-Laxemar (Oskarshamn). In addition, the collaboration has involved the scientific review of some geochemical issues that might influence post-closure performance of the engineered barrier system, primarily understanding of the present and likely future redox conditions and control in groundwaters at repository depth.

The present document describes the tasks carried out during 2008 within the collaborative work. The work is a continuation and development of geochemical review and modelling carried out in the 2006-7 programmes of work on "Variability and Uncertainties of Key Hydrochemical Parameters for SKB Sites" and "Impacts of Future Glaciations on Geochemical Conditions at Repository Depth: Review of SKB's Approach". These tasks were reported in SKI research reports [1, 2].

The task descriptions below give an overview of the present collaborative work.

1. Review site-specific and generic literature from SKB, SKI, Posiva and other research (including underground labs and other tunnels/mines) on biogeochemistry in geosphere at repository depth of redox and corrodants: dissolved oxygen (DO), sulphide ($HS^-$), iron species ($Fe^{2+}$, $Fe^{3+}$), N species, methane ($CH_4$), hydrogen ($H_2$).
2. Carry out modelling of redox processes, including considerations of microbial mediation of reactions and of other effects such as solute transport and mass budgets on concentrations of corrodants (especially sulphide) in vicinity of deposition holes.
3. Investigate potential impacts of changing corrodant and other geochemical conditions ($HS^-$, $Cl^-$, N species, $CH_4$, $H_2$, DO, DIC) on the stability of components in the EBS, particularly of copper.
4. Review literature and other information about the occurrence and geochemical stability/alteration of native copper, particularly with respect to ambient biogeochemical conditions including redox species, salinity, microbial populations, DIC.
5. Review electrochemical basis of natural analogues of native copper.
6. Evaluate experimental and theoretical evidence for copper stability/instability under natural aqueous conditions, oxic or anaerobic.

# 2. Issues addressed

Knowledge of electrochemical redox conditions in groundwaters at repository depth at the present time has been a target for geochemistry in SKB's site characterisation projects at Forsmark (Östhammar) and Simpevarp-Laxemar (Oskarshamn). Knowledge of the factors that promote redox stability and that control possible redox fluctuations in the short-term after closure and through long-term future environmental changes will need to be demonstrated in SR-Site. The important redox conditions for long-term repository performance are those that control the abundance and supply of corrodants, i.e. redox-sensitive species and other solutes, to the outer surfaces of canisters.

In the short term after closure, these conditions around the canisters will likely be the product of biogeochemical interactions between groundwaters and engineered barrier system (EBS) components, principally buffer and backfill materials. In the longer term, natural redox conditions may predominate within the EBS. For either case, the microbiological and geochemical processes that control corrodant species should be understood. If and when canisters are eventually breached and radionuclides released, redox conditions will play an important role in speciation and mobility of some radionuclides as well as affecting some sorbing solids.

Redox conditions, i.e. electrochemical tendency to reduction or oxidation of solutes and specifically the activity of electrons and abundances of oxidising or reducing corrodants, are the general issue. The potential for transport of dissolved oxygen, which is an oxidising corrodant towards copper, in groundwater flow to repository depth, and the geochemical attenuation and consumption of any such oxygen especially under enhanced flow conditions such as in sub-glacial hydrological conditions, was considered in [2, 3, 4].

This report focuses on the biogeochemical processes that control abundances of corrodants, primarily sulphide, in reducing conditions. Microorganisms play a potential key role by mediating these processes, e.g. the reduction of dissolved sulphate to sulphide.

Biogeochemical conditions in a future repository should therefore be considered in the context of:

(a) Naturally-occurring microorganisms and sources of redox-active geochemical species at repository depth: carbon as a microbial energy source and other electron donors, i.e. reducing agents; sulphate and other terminal electron acceptors, i.e. oxidised solutes.

(b) Additions and changes to these natural biogeochemical systems arising from 'introduced materials' in the repository: for example, introduction of labile organic carbon and of microorganisms could be a relatively significant perturbation to the natural system which has low organic carbon abundance and microbial activity.

(c) Scenarios for future changes in these groundwater conditions: groundwater composition changes over time, either towards higher or lower total salinities and with corresponding changes of sulphate and possibly also of other redox-active solutes; changes of abundances of dissolved organic carbon and/or of microorganisms due to changing surface environment; changes of dissolved methane concentrations from either deep geosphere or shallow biosphere origins.

The implications for repository performance of biogeochemical conditions in groundwaters around a repository volume are assessed by modelling the chemical thermodynamics of redox development and resulting reactions that would corrode copper canisters. In addition, the possible implications of reaction mediation, specifically kinetics of redox transformations, by micro-organisms are considered.

Insights into these geosphere processes and their potential effect on corrosion of copper might be provided by study of occurrences of 'native' copper and of the geochemical conditions in which naturally-occurring copper has survived for geological timescales in its metallic form, i.e. resisting corrosion. The second part of this report provides information on such occurrences, albeit rare, and discusses the issues relating to apparent stability of copper in these cases.

# 3. Contents of this report

Chapters 1 and 2 provide an introduction to the scope and background of this report. In particular, the scope is limited primarily to biogeochemical conditions in the near-field geosphere at the outside of the Engineered Barrier System (EBS). EBS issues are considered in detail in reviews and reports in other SSM projects. The scope also focuses on chemically reducing conditions in the near field and the production and control of the main relevant corrodant which is sulphide ($HS^-$). Scenarios for oxidising conditions and specifically the potential penetration of dissolved oxygen (DO) to repository depth and its geochemical attenuation have been considered in a previous report by these authors.

Chapter 4 summarises microbial and associated hydrochemical data from groundwater sampling operations at SKB's sites at Forsmark and Laxemar-Simpevarp. Tables of these data are in Appendix A. The biogeochemical significance of, and uncertainties in interpreting, these rather sparse data are discussed.

Chapter 5 looks at what is available from the literature for constructing models for biogeochemical processes and for calibrating the rates at which the processes might operate in the crystalline rock environment of interest. SKB has a qualitative geomicrobiology model and also has quantitative geochemical models for evolution of near-field and EBS chemistry including pH and redox ($E_h$) which have various simplifications, mainly that of equilibrium, and do not attempt to couple the microbial effects on reaction kinetics. Microbiological models in the literature for $SO_4^{2-}$ reduction in shallow sedimentary geochemical systems are evaluated as indicators for processes in the very different conditions of deep crystalline rock groundwaters.

Chapter 6 presents an updated compilation of pH, $E_h$ and redox-related geochemical data that SKB has reported for Forsmark and Laxemar. The tabulated data are in Appendix B. It also reports the results of geochemical modelling of redox couples so that calculated $E_h$ and measured *in situ* $E_h$ values can be compared and conclusions drawn concerning what controls the measured $E_h$ and what biogeochemical processes are likely to control long-term redox stability or variation. Then the possible scenarios for long-term variations of hydrochemistry and of redox-active species are discussed qualitatively and possible impacts identified in the context of the biogeochemical models.

Chapter 7 puts the potential variations of near-field compositions of redox-active solutes, and thus potential variations of chemistry in the EBS, in the context of direct effects on copper corrosion. This is done by means of thermodynamic calculations and illustration of corrosion-related solution-solid equilibria in $E_h$-pH space as Pourbaix diagrams. Some points arising from these are discussed, mainly concerning the sensitivity of corrosion processes to other variables in these complex natural geochemical systems.

Chapter 8 presents a brief review of information about native copper occurrences worldwide. It considers whether these provide 'analogue' information that could be useful in understanding long-term corrosion resistance. It also considers how much information is available about the specific biogeochemical conditions that account for the preservation and alteration/corrosion of these occurrences. Thermodynamic modelling and Pourbaix diagrams are used to illustrate the complexity of redox conditions and equilibria involved.

Chapter 9 presents a summary of the main points and conclusions arising in this review. Some issues that are relevant in review and evaluation of SR-Site are offered to SSM.

There are five appendices: A contains details of the microbiological analyses and associated geochemical data from Forsmark and Laxemar-Simpevarp, and also comparable data from Äspö and Olkiluoto; B contains the spreadsheet that tabulates the redox-related hydrochemical data from SKB reports; C presents an extended review and assessment of information that is pertinent to the question of whether methane hydrate ice could form in permafrost in these rock environments and what if any impact it could have; D contains additional Pourbaix diagrams for variations of the main parameters in the Fe-S-O-H system that supplement Figure 6 in Chapter 7; E also contains additional Pourbaix diagrams for variations of the main parameters in subdivisions of the Cu-Fe-Cl-N-S-C-H-O system, supplementing Figures 7 to 12 in Chapter 7.

# 4. Biogeochemistry in Fennoscandian crystalline rocks

## 4.1 Data for microorganisms at Forsmark and Laxemar-Simpevarp

The main methods that have been used to analyse microorganisms in deep water samples from these sites are (a) counting total numbers of cells by the AODC (acridine orange direct count) method, and (b) measuring most probable numbers (MPN) of cultivable cells of the main types of anaerobic microorganisms by incubating inoculations of suitable media and analysing for metabolic products or substrate consumption. The populations of cultivable microorganisms as measured by (b) are generally a small fraction of the total microorganism numbers as measured by (a).

It has been suggested that microorganisms with MPN populations $>10^3$ $mL^{-1}$ in water samples might have high biogeochemical influence, whereas lower populations down to 50 $mL^{-1}$ are considered to have possible or low influence on groundwater chemistry. It is probable, however, that microbial population densities on fracture surfaces are considerably higher than densities in corresponding groundwaters, and therefore that these 'sorbed' or 'biofilm' microorganisms play a very significant role in biogeochemical reactions. There is no information about populations and biogeochemical activities of sorbed microorganisms in Fennoscandian crystalline rocks.

Prior to the present investigations at Forsmark and Simpevarp/Laxemar, total cell numbers in deep groundwaters in the Fennoscandian Shield were considered to be typically $10^5$ to $10^6$ $mL^{-1}$ (cells per millilitre) and generally independent of depth over the range of interest, to around 1000 m [5, 6]. Populations of sulphate-reducing bacteria (SRB) were estimated to be mostly in the range 100-10000 $mL^{-1}$. It was suggested that there might be a correlation between SRB prevalence and fracture-filling iron sulphide [7]. It was also suggested that SRB numbers decline in the most saline groundwaters, but evidence for this was inconclusive [5].

The recent investigations, of which there are details in Appendix A, have indicated slightly lower populations of microorganisms. Reliable estimates for total numbers of cells in deep groundwater samples from Äspö HRL, Forsmark and Laxemar are in the range $4.5x10^4$ to $1.7x10^5$ $mL^{-1}$ [8].

Some comments on the biogeochemical data that are compiled in Tables A1 and A2 in Appendix A are:

– SKB's site descriptive model (SDM) v2.1 'R' reports generally have only graphical illustrations of microbiological data, so it has been necessary to

obtain raw data values for KFM06A & 07A and KLX03A samples from SKB's 'P' reports (in which likely data ranges for 95% confidence are also given);
- Hydrochemical data for $E_h$ and redox-active solutes are not available for some samples with microbiological data, e.g. all KFM06A samples and KLX03/196;
- There are no 'historical' MPN data for anaerobes, and only estimates of total cell numbers, for KLX01 & 02 samples, so the only data for the Laxemar sub-area are from four KLX03 samples.
- The reproducibility of the samplings and microbiological analyses is not well enough known, although evidence is presented in 'P' reports and in [8] that analytical reproducibility may be within a factor of 2. However the issue of 'in-borehole' sample contamination, especially by mixing with residual drilling or flushing water, also should be taken into account (data for % of drilling/flushing water are in Tables A1 and A2).

Cultivable SRB populations in repository-depth groundwaters at Forsmark and Laxemar-Simpevarp, as measured by an appropriate MPN (most probable number) method, have been found to be rather lower than previously suggested: <0.2 to 500 $mL^{-1}$, with one outlier of 3000 $mL^{-1}$ in a sample from Äspö [8]. SRB numbers in Forsmark water samples are low, <2 $mL^{-1}$, down to repository depth and appear to have an inverse correlation with $SO_4^{2-}$ concentrations which is not evident in samples from Laxemar-Simpevarp, but in both cases there are too few data to draw any firm conclusion. The depth trends of $SO_4^{2-}$ concentrations at the two sites are different: at Forsmark, $SO_4^{2-}$ reaches a maximum of about 600 mg/L in brackish marine waters at 500-600 m depth and decreases with increasing salinity below that, whereas at Laxemar, $SO_4^{2-}$ increases in correlation with Cl reaching a maximum of 700-800 mg/L in saline waters at 1000 m depth.

## 4.2 Discussion of biogeochemical data

The numbers of water samples from Forsmark, Laxemar and Olkiluoto with fairly complete data for microorganism populations and inorganic solutes are low. Microbial data may have variable and quite high uncertainties as to how representative they are of in situ conditions, although evaluation of replicate samplings and analyses gives some degree of confidence about reproducibility [8]. Some tentative interpretations draw the information together and give an idea of biogeochemical processes:

- In most water samples that were analysed for microorganisms, the numbers (MPN values) of the analysed anaerobes were generally low. According to SKB's criteria, these low numbers are of low or negligible influence in mediating the relevant reactions. The numbers in only a few samples were sufficiently high to have significant influence, so the inferences that follow relate to a low proportion of a small number of samples. Therefore the inferred relationship between microorganisms and redox conditions appears to be heterogeneous and is uncertain.

- Comparing microbiological data from Forsmark and Laxemar-Simpevarp, the numbers of SRB have similar ranges and variability between the two areas, except for an isolated 'historical' analysis for a sample from KLX01 which has to be regarded cautiously.

- The numbers of acetogens are generally rather higher in Laxemar-Simpevarp samples than in Forsmark samples, but there are not enough data to justify an interpretation of such differences. Three samples from KLX03 have significantly high numbers of acetogens and one of these (which is from repository depth range) also had significant numbers of methanogens and SRB. One sample from Forsmark, KFM03A/943, has notably high numbers of acetogens and SRB. Acetogens might facilitate sulphate reduction via the oxidation of DOC or methane to acetate which SRB then utilise. Population numbers of acetogens broadly correlate with hydrogen concentrations which suggests that acetogens are active.

- Populations of methanogens are mostly low, with MPN >100 $mL^{-1}$ in two samples from Forsmark and one from Laxemar. This indicates that in situ methane production does not occur to a significant extent. Therefore observed low concentrations of dissolved methane probably have an external source, i.e. deep-seated 'geogas'.

- The much higher present-day $CH_4$ at Olkiluoto does not correlate with an increase in SRB numbers, though it does correspond to very low sulphate concentrations below 400 m depth.

From sparse data, Pedersen et al have tentatively inferred that SRB and the reduction of $SO_4^{2-}$ dominate from about 100 m depth down to repository depth range and also in a deeper zone to ~900 m depth at Laxemar, with organic carbon and acetate respectively as the carbon sources (this is a similar model to that for Forsmark). DOC in these groundwaters is typically in the range 1.4 to 21 mg/L. It had previously been observed in hydrochemical interpretation that evidence of $SO_4^{2-}$ reduction (i.e. lowered $SO_4^{2-}$ and raised $HCO_3^-$ concentrations) in Äspö groundwaters tends to correspond with high contents of DOC, >10 mg/L [9]. There is no evidence to suggest that SRB use $CH_4$ rather than, or in addition to, DOC or acetate as the carbon source in groundwaters at Forsmark and Laxemar.

This contrasts with Olkiluoto where it is thought that $CH_4$ might be involved in $SO_4^{2-}$ reduction. This is based on the changes of both $SO_4^{2-}$ and $CH_4$ concentrations that are observed at 300-400 m depth, although there is no direct evidence for anaerobic $CH_4$ oxidation.

Unfortunately there are no data for acetate concentrations at any of these sites. It would be interesting to know how these vary within and between sites, in view of the role that acetogens and acetate might have in $SO_4^{2-}$ reduction.

## 4.3 Experiments on oxygen consumption

Studies of microbial oxygen reduction in the Redox Zone, REX and Microbe-REX experiments in the Äspö HRL focused on the transient proliferation of aerobic microbes due to perturbation of an anaerobic groundwater regime by the introduction of oxygen [9, 10, 11, 12].

The Microbe-REX study comprised laboratory experiments to measure total respiration rates and oxygen reduction rates in groundwater samples from the Äspö HRL tunnel, attributing reactions primarily to methane-oxidising bacteria (methanotrophs) [11]. Total cell counts in the unperturbed groundwater samples were $10^3$-$10^6$ cells $mL^{-1}$. After introduction of oxygen, cell counts were similar or higher, presumably due to introduction of aerobic bacteria. Dissolved $CH_4$ concentrations were measured in the range 1-$10^3$ µM and $H_2$ in the range 0.1-10 µM. Analyses of groundwater samples from close to the tunnel wall showed that a major part of the microbial populations was methane- and hydrogen-oxidising bacteria, up to $2x10^5$ cells $mL^{-1}$. Laboratory experiments indicated $O_2$ reduction rates, mediated by those aerobic bacteria, from 0.3 to 4.5 µM $O_2$ per day. It was concluded that $CH_4$ oxidation is one of the processes in the attenuation of $O_2$ that would be introduced during repository excavation and operation, and perhaps also during a future glaciation. However the main process that would consume DO in infiltrating groundwaters down to repository depth is considered to be the oxidation of ferrous iron, $Fe^{II}$, released from iron-containing minerals. The modelling of this oxygen-consumption and redox-buffering process is described briefly in Section 5.1 below.

Rates of $Fe^{II}$ oxidation by $O_2$ were studied by in situ and laboratory experiments in the REX project which also identified the roles of $CH_4$ and $H_2$ in depleting oxygen in this environment [9]. The experiments focused on the rates of $O_2$ depletion by reaction with $Fe^{II}$-minerals on fracture surfaces, which may be mediated by Fe-oxidising microbes. For the fracture mineral conditions in the samples from Äspö HRL, the experimental rate of $O_2$ depletion was between 50 and $1.3x10^6$ µM $O_2$ per day, i.e. comparable or greater than the rate of depletion in the Microbe-REX experiments.

## 4.4 Experiments on sulphate reduction

Initial evidence of SRB facilitating the reduction of $SO_4^{2-}$ in groundwaters at these sites came from limited experimentation with groundwater from KLX01. Using lactate as the C source, the rate of $HS^-$ production by unattached SRB was measured as 8-114 µmol $m^{-3}d^{-1}$ and by SRB attached in a biofilm was 0.2-9 µmol $m^{-2}d^{-1}$ [13]. These empirical results are not directly comparable because the former rate is per water volume whilst the latter rate is per surface area, but they suggest that (a) SRB attached as biofilms to mineral surfaces are more efficient at producing $HS^-$ than when not attached,

and (b) that up to 290 µg of $H_2S$ per day could be produced by SRB in a biofilm per $m^2$ of the surfaces of a fracture with 1mm aperture. It is noted that these experimental rates were apparently not constrained by available carbon because an artificial source, i.e. lactate, was added. Thus the rates would be expected to represent an upper limit relative to unperturbed natural conditions where DOC and/or bacteriogenic acetate is the sole C source, although the study described below suggests otherwise.

Observations made during a 90-day closed loop circulation 'MICROBE' experiment in a fracture 43.8 m from the tunnel wall at 447 m depth in Äspö HRL, provided in situ evidence for sulphate reduction coupled with acetate production and consumption in unperturbed deep groundwaters [8]. Interpreted rates of production of $HS^-$ and acetate ($HA^-$) during the main part of the MICROBE experiment were 0.08 mg($HS^-$)$L^{-1}d^{-1}$ and 0.14 mg($HA^-$)$L^{-1}d^{-1}$. The $HS^-$ production rate converts to 2400 µmol $m^{-3}d^{-1}$ which surprisingly is several orders of magnitude higher than the rate in experiments (described above) where lactate was the C source. Rates broadly corresponded with the measured cell populations of SRB and acetogens in solution which were inferred to be indicative of much larger populations of active microbes attached to fracture surfaces in biofilms. It is speculated that the higher rate of $HS^-$ production in the in situ experiment compared with lab experiments could be due to the difficulty of maintaining reducing anaerobic conditions in the latter case, and perhaps also to a greater propensity for active biofilms in the former case.

There is a general inference that microorganisms attached to rock surfaces in biofilms have greater population density and are expected to be more active in microbially-mediated redox transformations such as $HS^-$ production than microorganisms dispersed in groundwater. This means that analyses of cell populations in water are just a proxy indicator of relative levels of biogeochemical activity. Moreover it is likely that some rock surfaces are better microbiological hosts than others, for example surfaces with labile redox-active elements such as Fe. Rock surfaces that have been 'contaminated' by deposits of insoluble organic carbon from substances introduced by repository construction would probably stimulate the highest levels of microbiological activity.

# 5. Models for biogeochemical processes in the geosphere

## 5.1 Consumption of dissolved oxygen

Numerical models for the consumption of $O_2$ in: (a) shallow groundwaters in fractures, involving reactions with dissolved organic carbon and with fracture minerals; (b) saturated backfill, involving reactions with organic carbon and with $Fe^{II}$ and sulphide minerals; (c) rock between surface and repository depth and around a repository; and (d) saturated bentonite buffer, have been reported by [10, 12, 14, 15, 16].

Reducing reactions and reactants involved in consumption of oxygen in geosphere rocks are distinct from those involved in sulphide production, and they have been reviewed in detail for SSM elsewhere [3, 4]. So only a brief summary of the reactions and of the involvement of microorganisms in oxygen consumption is provided here.

In (a) and (b), the kinetics of $O_2$ reaction have taken account of microbial mediation. In (c) the rate of $O_2$ consumption in a transmissive fracture is constrained by the rate of $Fe^{II}$ release by dissolution of fracture-filling biotite or chlorite, as per the model of Guimerà et al [17, 18] which does not contain any microbial enhancement of dissolution rates. SKB's approach to modelling the attenuation of DO in transmissive fractures has been reviewed for SSM in [2, 3, 4]. The reviews conclude that SKB's geochemical model has uncertainties that potentially make the resulting predictions of $O_2$ consumption non-conservative. The uncertainties occur in assumed maxima for downwards sub-glacial water velocity and DO concentrations, and also in the kinetics of release of $Fe^{2+}$ from biotite or chlorite. Modelling shows that an uncertainty range of two orders of magnitude in the reaction kinetics is significant in terms of $O_2$ attenuation. Along with uncertainties about the duration of anomalous sub-glacial hydraulic conditions, it can be concluded that there is a low but non-negligible probability of DO reaching repository depth. Whether that oxygen could then have any impact on copper canisters would depend on the performance of the near-field rock barrier and of the bentonite buffer.

In (d), the consumption of $O_2$ in buffer is constrained kinetically by the rate of in-diffusion and in mass budget terms by the amount of pyrite present in compacted bentonite, i.e. not making any assumptions about microbial involvement.

Grandia et al's model for $O_2$ consumption in saturated backfill [14] considers a reference case in which pyrite in backfill is the early phase with reducing capacity (RDC), and several sub-cases involving ± pyrite, ± siderite, ± organic matter and biotite as the only $Fe^{II}$ containing phase. Whilst microbial activity is implicated in the consumption of $O_2$ by organic matter, and a suitable kinetic formula for this has been adopted form the REX project [9], it has been suggested that microbial mediation of pyrite oxidation is significant only for a narrow pH-$O_2$ field which is acidic with $Fe^{3+}$ rather than $O_2$ as the principal oxidizer and is therefore not significant for conditions in backfill [14].

## 5.2 Microbial production of sulphide

### 5.2.1 Sulphate reduction in crystalline rock groundwaters

The model proposed by SKB for $SO_4^{2-}$ reduction in groundwaters at Forsmark and Laxemar utilises short chain organic acids, such as acetate (which are produced by acetogenic bacteria) as the normal sources of carbon and energy for SRB [8, 19]. The sequence of reactions is:

- Production of acetate from $H_2$ and $CO_2$, mediated by autotrophic acetogens;
- Reduction of $SO_4^{2-}$ by acetate (possibly coupled with $H_2$) or by DOC, mediated by SRBs;
- Control of dissolved $HS^-$ by reaction with $Fe^{2+}$ to precipitate FeS and $FeS_2$.

The general implication of this model is that the sulphide production rate potentially has a number of constraining factors: the fluxes of $SO_4^{2-}$, DOC and $H_2$ and possibly also of $CH_4$, as well as the viability and activity of acetogens, SRB and maybe also methanogens. It is inferred that the generally low populations of these microorganisms reflects the low concentrations and fluxes of the main energy sources, i.e. DOC and $H_2$. Equally, it is evident that the overall constraint on sulphide production is the flux of dissolved $SO_4^{2-}$ (assuming that sources of $SO_4^{2-}$ by mineral sulphide oxidation are relatively minor). This appears to have been the case at Olkiluoto where sulphate has been depleted in deep groundwaters, and it may be happening below repository depth range at Forsmark where $SO_4^{2-}$ decreases. Within repository depth range at both Forsmark and Olkiluoto, where $SO_4^{2-}$ remains at moderate concentrations, it seems that other factors are limiting the process, e.g. supply of naturally-occurring DOC and/or $H_2$.

It is likely that natural DOC will be enhanced in the vicinity of a repository by organic substances that would be introduced during construction and operation. From an estimated inventory of such organics, and by consideration of degradation pathways, maximum amounts of $HS^-$ that could be produced by SRB activity in deposition tunnels and other cavities in the repository have been estimated [19]. These amounts are 1.22 and 36 μM respectively, which equate to dissolved concentrations of 0.06 and 1.2 mg($HS^-$) $L^{-1}$. The same calculation was referred to in SKB's SR-Can to infer that "the maximum amount of sulphide that can be generated microbially is ~10 moles for

each deposition hole, which, if it was able to react completely with the canister, would be equivalent to a corrosion of less than 10 μm if distributed evenly" [15]. The reasoning behind this interpretation of the original information is not provided.

In addition to the constraint on microbial activity posed by availability of energy sources, DOC and $H_2$, there is the basic constraint on microbial viability which is posed by the availability and mass transfer of nutrients that are necessary for cell growth. These nutrients include nitrogen and phosphate compounds. Minerals and groundwaters at repository depth in crystalline rocks are extremely poor suppliers of nutrients, i.e. an 'oligotrophic' environment. Dissolved nitrogen, mainly as $NH_4^+$, is reported in the SKB hydrochemical database at concentrations up to mg/L level; the higher concentrations of $NH_4^+$ in this range are found in groundwaters that are dominated by the brackish Littorina water component. Dissolved phosphate occurs at the μg/L level or below detection limit. Lower typical concentrations of N and P are quoted for Laxemar and Forsmark groundwaters in [8]; the reason for the discrepancy is not explained. A future evolution of groundwater composition at repository depth in which the concentrations of N and P were significantly higher is not envisaged, so nutrient supply will persist in the long term as a constraint on biogeochemical reactions.

In summary, the biogeochemical factors that need to be taken into account of prognosing the likely maximum rate of production and maximum concentration of $HS^-$ in geosphere groundwaters at repository depth are:

- $SO_4^{2-}$ concentration and inwards flux of $SO_4^{2-}$-containing groundwaters;
- Population and viability of SRB and acetogens;
- Concentration and inwards flux of DOC that is one of the sources of C to acetogens and SRB;
- Temperature, salinity, minor nutrients (N & P compounds) and other environmental factors that affect microbial proliferation and activity;
- Concentration and production rate of $Fe^{2+}$ from dissolution of Fe-oxide or Fe-containing aluminosilicate minerals, mediated by IRB, which reacts with $HS^-$ to precipitate FeS and $FeS_2$, and thus limits dissolved $HS^-$. Specifically, the availability of these sources of $Fe^{II}$ near to deposition holes and the rate of supply of $Fe^{2+}$ might need more consideration.

### 5.2.2 Rates of sulphate reduction

The rate of $SO_4^{2-}$ reduction, mediated by SRB, is dependent on several factors: population and activity of SRB, temperature, concentration of $SO_4^{2-}$, concentration of available labile DOC, and concentrations of other electron acceptors that might compete for electrons produced by DOC oxidation. There is not much literature on kinetic modelling of $SO_4^{2-}$ reduction, and moreover all of this literature refers to biogeochemical conditions in sediments and sedimentary rocks, in which carbon and nutrient sources are generally higher than in crystalline rocks. So the studies of $SO_4^{2-}$ reduction ki-

netics described in the following paragraphs have generally assumed that DOC is not the limiting factor, and may not be directly relevant to the carbon-poor and nutrient-poor geosphere environment of interest here. If organic C is sparse, SRB utilise $H_2$ or acetate as energy sources for $SO_4^{2-}$ reduction, and there is little if any research on the kinetics of these reactions.

In the literature on $SO_4^{2-}$ reduction in organic-rich sediments, it is coupled to the rate of DOC oxidation, e.g. [20, 21]:

$$2CH_2O + SO_4^{2-} + H^+ \rightarrow 2CO_2 + HS^- + 2H_2O$$

Utilization of DOC for microbial metabolism is represented by a Monod rate expression [21]:

$$R_i = R_{max} \frac{[EA]}{[EA]_{lim}} \text{ for } [EA] < [EA]_{lim}$$

where [EA] is the concentration of the electron acceptor, i.e. $SO_4^{2-}$ in this case, $[EA]_{lim}$ is a limiting concentration above which the rate of reduction is independent of [EA], and $R_{max}$ is the rate of DOC oxidation where $[EA] \geq [EA]_{lim}$. When several competing electron acceptors and related microbes are present, the total rate of DOC oxidation, $R_c$ comprises the sum of the rates for individual EAs:

$$R_C = \sum_{i=1}^{i=n} R_i$$

The fractional concentrations of each EA to $R_c$ depends on the relative energetics of each pathway and the interactions/suppressions among the various microbes.

In experiments with artificial labile organic substrates, $SO_4^{2-}$ reduction rates varied from 0.007 - 0.17 kg $m^{-3}$ $h^{-1}$, depending on initial $SO_4^{2-}$ concentration which was varied from 1000 – 10000 mg/L [22].

$[EA]_{lim}$ for $SO_4^{2-}$ reduction has a range of literature values from 0.001 to 1.6 mM [20, 21]. The first order rate constant for oxidation of DOC, $k^{DOC}$, is in the wide range of $10^{-7}$ to $10^{-3}$ $yr^{-1}$ [20, 21], i.e. the rate of DOC oxidation overall is:

$$R^{DOC} = k^{DOC} [DOC]$$

So that if DOC is, for example, 0.1mM, then $R^{DOC}$ is likely to be in the range $10^{-3}$ to $10^2$ mM $yr^{-1}$. If $SO_4^{2-}$ is the dominant electron acceptor (as it is in the deep geosphere) and exceeds 90 mg/L (i.e. 1mM, or possibly less), then the corresponding rate of $SO_4^{2-}$ reduction mediated by SRB will be in the range $10^{-8}$ to $10^2$ mM $yr^{-1}$. The lower part of this range is probably appropriate for the deep geosphere. These reduction rates are considerably lower than the empirical rate reported from experiments with labile organic matter which are above 600 mM $yr^{-1}$ [22].

There has been a lot of interest in the question of whether SRBs compete with methanogens, or whether $SO_4^{2-}$ reduction and methanogenesis are mutually exclusive in biogeochemical terms [23, 24] and in what conditions $SO_4^{2-}$ reduction might be driven by anaerobic oxidation of methane, AOM [25, 26]:

$$CH_4 + SO_4^{2-} \rightarrow HCO_3^- + HS^- + H_2O$$

In AOM, SRB do not utilise $CH_4$ directly, but form a consortium with archaea (single-celled microorganisms without nuclei) to cause $SO_4^{2-}$ reduction [25, 27]. Studies of AOM have found that the rate of $SO_4^{2-}$ reduction may be very high where $CH_4$ abundance is not limiting, e.g. up to 5 µmol $cm^{-3}$ $d^{-1}$ [26], or very low where $CH_4$ is not abundant (<1 nmol $cm^{-3}$ $d^{-1}$).

In cases where DOC is not the electron donor, the Monod rate expression is not appropriate for $SO_4^{2-}$ reduction kinetics. The Michaelis-Menten kinetics equation has been suggested for use [28]:

$$R = R_{max} \frac{[EA]}{[EA] + K_M}$$

where R is the rate of $SO_4^{2-}$ reduction, $R_{max}$ is a maximum reduction rate (presumably similar to $[EA]_{lim}$ in the Monod equation), [EA] is concentration of electron acceptor (here $SO_4^{2-}$), and $K_m$ is the Michaelis constant for the particular microbially-mediated reaction. Reaction rates for $SO_4^{2-}$ reduction, derived like those above from surficial sedimentary systems, of 2.5 x $10^{-12}$ mol $SO_4^{2-}$ $d^{-1}$ $cell^{-1}$ [27].

For a deep location with only 100 SRB cells per mL, this would correspond to a rate of about 0.1 mM $SO_4^{2-}$ per year. This is roughly in the middle of the range of $SO_4^{2-}$ reduction rates inferred above (i.e. $10^{-8}$ to $10^2$ mM $yr^{-1}$) for the cases where DOC is the electron donor. It would mean, if representative, that the microbially-mediated reduction of most or all of available $SO_4^{2-}$ (e.g. 96 mg/L or 1mM) could occur within a relatively short timescale. This indicates that $HS^-$ production would be constrained by $SO_4^{2-}$ flux and by $SO_4^{2-}$ concentrations and not by reduction kinetics.

# 6. Geochemical conditions at the EBS interface

## 6.1 Introduction

SKB's knowledge and understanding of the possible range of chemical conditions in the Engineered Barrier System (EBS), i.e. in a bentonite buffer around copper canisters and in the tunnel backfill, were set out in SR-Can [29, 30, 31]. Those reports were reviewed by SKI's EBS Review Group which concluded [32]:

> "Redox conditions in the buffer and backfill will be established through heterogeneous reactions between solutes in groundwater, and major and minor solid phases in the bentonite/clay. The degree to which pH is buffered and redox poised by the solid phases will depend on mass balance (are there enough buffering minerals present?), mass action (is the solubility of buffering minerals high enough?), and kinetics (is the reaction rate of buffering minerals fast enough?)."
>
> and
>
> "Regarding redox buffering, SKB refers to the roles potentially played by siderite and pyrite, and concludes that siderite dominates redox behaviour [29]. The presence of sulphate/sulphide in groundwater and iron in montmorillonite is apparently ignored, again seemingly without consideration of mass balance, mass action, and kinetic constraints. SKB believes that sulphate/sulphide will not be relevant due to the non-viability of sulphate reducing bacteria in highly compacted bentonite. The other possible redox couple acting in the system, $Fe^{II}$ /$Fe^{III}$ has been tested by SKB [30], but the conditions expected in the system do not reach the $Fe^{II}$/$Fe^{III}$ boundary. Therefore SKB concludes that the equilibrium with pyrite and siderite (as occurs with present-day groundwaters in Forsmark [30]) is the principal control of redox in the near field."

This section of the present report is concerned with the chemical conditions in the near field at the interface with the EBS. The chemical composition and especially pH and redox of near-field groundwaters have to be characterised and understood as bounding conditions for the evolution of buffer and backfill. Predictions of future stability or sensitivity to externally-driven changes of groundwater compositions, supported by palaeohydrogeological evidence, will also be expected from SKB in SR-Site. Some of the issues that SSM should be aware of during review of SR-Site are considered here.

There is a brief overview in Section 6.3.2 of the modelling that has been carried out by SKB and SKI to simulate the production of $HS^-$ at the outer

rim of the EBS and its transport through the EBS. The focus of this report is on biogeochemistry in the geosphere and at the EBS interface, rather than on processes in the EBS. Chemical evolution of the buffer and backfill is the focus of work being carried out for SSM on alternative models for groundwater-bentonite reactions, as indicated in the extracts above from the SR-Can EBS review.

## 6.2 pH and redox in near-field groundwaters

Hydrochemical data that were available up to the data freeze for SKB's v1.2 Site Descriptive Models as used in SR-Can were reviewed for SKI in [1]. The approach used in that report to assess the variability and uncertainties in the hydrochemical data reported by SKB has been used again here with an updated hydrochemical data set.

Geochemical modelling with PHREEQC [33] is used for two purposes connected with uncertainties and bias in pH and $E_h$: (i) to adjust pH to compensate for $CO_2$ outgassing on the basis of an assumption that in situ groundwater should be at equilibrium with calcite, and (ii) to evaluate the hypothetical $E_h$ on the basis of assumed control by $Fe^{3+}/Fe^{2+}$, $Fe(OH)_3/Fe^{2+}$ and $SO_4^{2-}/HS^-$ redox couples.

Adjusting the reported pH to compensate for $CO_2$ outgassing has been done by using the mixing-reaction mode of the computer program to simulate titration of $CO_2$ back into the water until calcite equilibrium is reached. Of course, if a solution is already saturated or over-saturated with calcite, then this does not work. However the majority of sample analyses are over-saturated which supports the hypothesis that $CO_2$ outgassing might have caused rising pH and over-saturation with respect to calcite.

These calculations have been carried out with current groundwater data from Forsmark and Laxemar, and also from the v1.2 SDM for Simpevarp and the Äspö HRL. Data for Forsmark and Laxemar were taken from the v1.2 data set and also from 'P' reports of preliminary data from samples obtained and analysed after the 1.2 data freeze and from a printout of data in SKB's SICADA database that was requested by SKI and delivered from SKB in early 2008 (note: data originating from SICADA have taken precedence over data from identical samples in P reports, where there are discrepancies). A compilation of all data used for the following calculations is in Appendix B.

The resulting adjusted pH values are shown in Table 1, in the column headed 'Model pH at $SI_c$ =0'. Adjusted pH data for Forsmark and Laxemar samples are typically 0.2 to 0.7 pH units lower than the measured values.

$E_h$ was calculated according to the thermodynamics of the redox couples $SO_4^{2-}/HS^-$, $Fe^{3+}/Fe^{2+}$ and $Fe(OH)_3/Fe^{2+}$:

$E_h$ $[SO_4^{2-}/HS^-]$ =

$$2.303\frac{RT}{F}\left[\frac{1}{8}\left(-\log K_T\right)+\frac{9}{8}\left(\log a_{H+}\right)+\frac{1}{8}\left(\log a_{SO4}\right)-\frac{1}{8}\left(\log a_{HS}\right)\right]$$

$$\text{where } \log K_T = \log K_{298} - \frac{\Delta H}{2.303R}\left(\frac{1}{T^\circ K} - \frac{1}{298}\right)$$

$$\log K_{298}[SO_4^{2-}/HS^-] = -33.65 \text{ and}$$
$$\Delta H[SO_4^{2-}/HS^-] = 60.14 \text{ kcal mol}^{-1}$$

$$E_h\,[Fe^{3+}/Fe^{2+}] = 2.303\frac{RT}{F}\left[-\log K_T + \log a_{Fe3+} - \log a_{Fe2+}\right]$$

$$\log K_{298}[Fe^{3+}/Fe^{2+}] = -13.02 \text{ and}$$
$$\Delta H[Fe^{3+}/Fe^{2+}] = 9.68 \text{ kcal mol}^{-1}$$

The calculation for the $Fe(OH)_3/Fe^{2+}$ couple was done with thermodynamic data for the solubility of amorphous $Fe(OH)_3$ suggested by Grenthe et al. [34], based on a study of redox in deep groundwaters from various of SKB's early exploratory sites:

$$E_h\,[Fe(OH)_3/Fe^{2+}] = E_o^{*} - 2.303\frac{RT}{F}\left[3pH + \log\left[Fe^{2+}\right]\right]$$

$$\text{where } E_o^{*} = 0.771 + 2.303\frac{RT}{F}\log K_S^{*}$$
$$\log K_S^{*} = -1.1$$

SKB have not analysed $Fe^{3+}$ directly because concentrations are so low that analyses using conventional methods would be unreliable for the purpose of redox calculation. $Fe^{3+}$ concentrations used here were obtained by subtraction of $Fe^{2+}$ from $Fe_{total}$. In a few cases $Fe^{2+} \geq Fe_{total}$ and therefore no value can be given for $Fe^{3+}$. It is evident that calculating $Fe^{3+}$ as the very small difference between two much bigger very similar values gives rise to very large uncertainty so that these calculated values for $Fe^{3+}$ are generally invalid.

Measured and modelled redox values for groundwater samples from the Forsmark, Laxemar and Simpevarp/Äspö/Ävrö areas are compiled in Table 2. $E_h$ data and redox modelling results for Forsmark and Laxemar are shown in Figures 1 and 2 respectively, excepting $E_h(Fe^{3+}/Fe^{2+})$ which are invalid calculations for the reason discussed above.

If redox couples are modelled using the adjusted pH values (i.e. the pH values in the right hand column of Table 1), slightly different $E_h$ values are obtained because of the intrinsic pH dependence of the $SO_4^{2-}/HS^-$ and $Fe(OH)_3/Fe^{2+}$ redox couples, and also the effect of pH on speciation for all of the redox equilibrium calculations. The adjusted pH values are lower than the measured pH values. The results are illustrated in Figures 3 and 4.

***Table 1.*** *Data for pH adjustment calculations based on assumption that in situ waters are saturated with respect to calcite.*

| Sample | Depth, m | pH[1] | pH[2] | pH[3] | $HCO_3^-$ mg/L | Sat Index (calcite) | Log $P_{CO2}$ | Mod pH at $SI_c$= 0 |
|---|---|---|---|---|---|---|---|---|
| *Forsmark* | | | | | | | | |
| KFM01A/115 | 110.1-120.77 | 7.68 | 7.62 | 7.47 | 61 | 0.22 | -3.1 | 7.43 |
| KFM01A/180 | 176.8-183.9 | 7.41 | 7.41 | 7.60 | 99 | 0.20 | -2.7 | 7.21 |
| KFM01D/432 | 428.5-435.6 | 8.10 | 8.10 | 7.55 | 36 | 0.65 | -3.8 | 7.38 |
| KFM01D/572 | 568.0-575.1 | 8.40 | 8.10 | 7.40 | 20 | 0.60 | -4.3 | 7.63 |
| KFM02A/512 | 509-516.08 | 6.83 | 6.93 | 7.18 | 125 | -0.17 | -2.0 | n/a |
| KFM03A/452 | 448.5-456.6 | 7.29 | 7.27 | 7.42 | 93 | 0.13 | -2.5 | 6.98 |
| KFM03A/642 | 639-646.12 | 7.38 | 7.48 | 7.55 | 22 | -0.16 | -3.3 | n/a |
| KFM03A/943 | 939.5-946.6 | 7.32 | 7.53 | 7.78 | 9 | -0.29 | -3.7 | n/a |
| KFM06A/357 | 353.5-360.6 | 6.91 | 7.33 | 7.41 | 48 | -0.21 | -2.7 | n/a |
| KFM07A/925 | 848-1001.6 | 8.04 | 8.05 | 8.00 | 6 | 0.19 | -4.7 | 7.84 |
| KFM08A/687 | 683.5-690.64 | 8.00 | 8.00 | 7.79 | 10 | 0.14 | -4.3 | 7.88 |
| KFM08D/673 | 669.7-676.8 | 8.40 | 8.30 | 8.14 | 7 | 0.33 | -4.9 | 7.95 |
| KFM10A/302 | 298-305.1 | 8.10 | 8.20 | | 21 | 0.24 | -3.9 | 7.77 |
| KFM10A/483 | 478-487.5 | 7.70 | 7.70 | 7.13 | 169 | 0.69 | -2.7 | 7.01 |
| KFM11A/451 | 447.5-454.64 | 7.53 | 7.54 | 7.58 | 24 | -0.09 | -3.4 | n/a |
| *Laxemar* | | | | | | | | |
| KLX01/458 | 456-461 | 8.60 | 8.70 | 8.20 | 78 | 0.91 | -4.0 | 7.70 |
| KLX01/691 | 680-702.11 | 7.80 | | 8.10 | 24 | 0.10 | -3.7 | 7.65 |
| KLX03/412 | 408-415.3 | 8 | | 7.89 | 189 | 0.72 | -2.9 | 7.27 |
| KLX03/742 | 735.5-748.04 | 7.5 | | 7.41 | 34 | -0.02 | -3.2 | n/a |
| KLX08/202 | 197-206.65 | 8.1 | 8.4 | 8.29 | 296 | 0.30 | -2.9 | 7.94 |
| KLX08/398 | 396-400.87 | 8 | 8.3 | 8.32 | 290 | 0.14 | -2.8 | 8.01 |
| KLX08/481 | 476-485.62 | 7.6 | 8.1 | 7.87 | 32 | -0.06 | -3.5 | n/a |
| KLX08/614 | 609-618.51 | 8.4 | 8.4 | 8.19 | 21 | 0.34 | -4.3 | 8.00 |
| KLX13A/435 | 432-439.16 | 8.5 | 8.3 | 8.33 | 75 | 0.23 | -3.6 | 8.16 |
| KLX13A/503 | 499.5-506.66 | 8.2 | 8.1 | 8.10 | 87 | 0.13 | -3.3 | 8.00 |
| KLX17A/426 | 416-437.51 | 8 | 8 | 7.92 | 118 | 0.16 | -3.0 | 7.82 |
| KLX17A/671 | 642-701.08 | | 8.3 | 8.36 | 238 | 0.10 | -3.0 | 8.21 |
| *Simpevarp, Äspö, Ävrö* | | | | | | | | |
| KSH01A/161 | 156.5-167 | | 8.17 | 7.36 | 25 | 0.36 | -4.0 | 7.75 |
| KSH01A/253 | 245-261.5 | | 8.08 | 7.34 | 17 | 0.22 | -4.1 | 7.79 |
| KSH01A/556 | 548-565 | | 8.15 | 7.63 | 11 | 0.12 | -4.4 | 8.02 |
| KAS02/208 | 202-214.5 | | 7.5 | 7.4 | 71 | 0.27 | -2.9 | 7.23 |
| KAS02/532 | 530-535 | | 7.73 | 8 | 10 | -0.13 | -4.0 | n/a |
| KAS03/131 | 129-134 | | 8 | 8 | 61 | 0.12 | -3.4 | 7.89 |
| KAS03/931 | 860-1002.06 | | 8 | 8.1 | 11 | 0.40 | -4.5 | 7.66 |
| KAS04/338 | 334-343 | | | 8 | 69 | 0.68 | -3.4 | 7.28 |
| KAS04/460 | 440-480.98 | | 8.1 | 8.1 | 21 | 0.42 | -4.1 | 7.94 |
| KAV01/422 | 420-425 | | 6.9 | 7.35 | 186 | 0.05 | -2.2 | 7.30 |
| KAV01/526 | 522-531 | | 7 | | 81 | -0.34 | -2.2 | n/a |
| KAV01/560 | 558-563 | | 7.2 | | 42 | -0.17 | -2.8 | n/a |

pH[1] = pH measured with borehole Chemmac system

$pH^2$ = pH measured with surface Chemmac system; these values were used as the basis for modelling the pH adjustment for KSH samples.

$pH^3$ = pH measured in laboratory; these values were used as the basis for modelling the pH adjustment for all samples except the KSH samples.

n/a = no adjustment of pH because Sat Index <0.

***Table 2.*** *Measured $E_h$ and redox-sensitive solutes and results from geochemical modelling of $E_h$ for the $SO_4^{2-}/HS^-$, $Fe^{3+}/Fe^{2+}$, and $Fe(OH)_3/Fe^{2+}$ redox couples for groundwater samples from boreholes at Forsmark, Simpevarp, Äspö and Ävrö.*

| Sample | Depth, m | $E_h$ (1) | pH (4) | $SO_4^{2-}$ mg/L | $HS^-$ (5) mg/L | $Fe_{tot}$ mg/L | $Fe^{2+}$ mg/L | $E_h$ $SO_4$/HS | $E_h$ 2) $Fe^{3+}/Fe^{2+}$ | $E_h$ (3) $Fe(OH)_3/Fe^{2+}$ |
|---|---|---|---|---|---|---|---|---|---|---|
| *Forsmark* | | | | | | | | | | |
| KFM01A/115 | 110.1-120.8 | -195 | 7.65 | 316 | <0.03 | 1.00 | 0.953 | -203 | 180 | -274 |
| KFM01A/180 | 176.8-183.9 | -188 | 7.41 | 547 | <0.03 | 0.54 | 0.475 | -188 | 239 | -218 |
| KFM01D/432 | 428.5-435.6 | -263 | 8.10 | 125 | 0.01 | 2.08 | 2.040 | -236 | | -378 |
| KFM01D/572 | 568.0-575.1 | -260 | 8.25 | 38 | 0.01 | 1.24 | 1.230 | -251 | | -394 |
| KFM02A/512 | 509-516.08 | -143 | 6.88 | 498 | 0.01 | 1.85 | 1.840 | -157 | 219 | -174 |
| KFM03A/452 | 448.5-456.6 | -176 | 7.28 | 511 | 0.05 | 1.10 | 1.110 | -187 | 181 | -227 |
| KFM03A/642 | 639-646.12 | -196 | 7.43 | 197 | | 0.23 | 0.233 | | | -224 |
| KFM03A/943 | 939.5-946.6 | -245 | 7.42 | 74 | 0.060 | 0.22 | 0.208 | -216 | 172 | -230 |
| KFM06A/357 | 353.5-360.6 | -155 | 7.12 | 157 | | | | | | |
| KFM07A/925 | 848-1001.6 | 9 | 8.04 | 99 | 0.171 | 0.19 | 0.162 | -254 | | -315 |
| KFM08A/687 | 683.5-690.6 | -209 | 8.00 | 92 | 0.006 | 0.72 | 0.726 | -235 | | -344 |
| KFM08D/673 | 669.7-676.8 | -260 | 8.35 | 101 | <0.006 | <0.006 | 0.006 | -257 | | -282 |
| KFM10A/302 | 298-305.1 | -281 | | 215 | 0.027 | 1.45 | 1.430 | -230 | | -350 |
| KFM10A/483 | 478-487.5 | -258 | 7.70 | 400 | 0.065 | 15.30 | 15.4 | -213 | | -359 |
| KFM11A/451 | 447.5-454.6 | -203 | 7.53 | 264 | 0.012 | 0.25 | 0.240 | -199 | | -231 |
| *Laxemar* | | | | | | | | | | |
| KLX01/458 | 456-461 | -280 | 8.65 | 106 | 0.460 | 0.04 | 0.040 | -283 | | -379 |
| KLX01/691 | 680-702.1 | -265 | 7.80 | 351 | 2.500 | 0.03 | 0.029 | -232 | | -213 |
| KLX03/412 | 408-415.3 | -270 | 8.00 | 127 | 0.007 | 0.44 | 0.429 | -229 | | -329 |
| KLX03/742 | 735.5-748 | -220 | 7.50 | 398 | 0.006 | 0.92 | 0.903 | -194 | | -260 |
| KLX08/202 | 197-206.65 | -266 | 8.25 | 13 | 0.004 | 0.12 | 0.112 | -246 | | -335 |
| KLX08/398 | 396-400.87 | -245 | 8.15 | 14 | 0.037 | 1.02 | 1.020 | -251 | | -384 |
| KLX08/481 | 476-485.62 | -210 | 7.85 | 132 | 0.008 | 0.28 | 0.275 | -225 | | -307 |
| KLX08/614 | 609-618.51 | -239 | 8.40 | 145 | 0.010 | <0.01 | <0.005 | -262 | | |
| KLX13A/435 | 432-439.16 | -287 | 8.40 | 37 | 0.003 | 0.01 | <0.006 | -262 | | |
| KLX13A/503 | 499.5-506.6 | -277 | 8.15 | 46 | <0.006 | 0.05 | 0.044 | -251 | | -322 |
| KLX17A/426 | 416-437.51 | -297 | 8.00 | 24 | 0.019 | 0.89 | | -240 | | |
| KLX17A/671 | 642-701.1 | -303 | 8.3 | 6 | <0.006 | 0.69 | 0.682 | -256 | | -394 |
| *Simpevarp, Äspö, Ävrö* | | | | | | | | | | |
| KSH01A/161 | 156.5-167 | -257 | 8.17 | 32 | | 1.413 | 1.397 | | 69 | -367 |
| KSH01A/253 | 245-261.5 | -160 | 8.08 | 51 | | 1.318 | 1.296 | | 76 | -364 |
| KSH01A/556 | 548-565 | -173 | 8.15 | 230 | | 0.523 | 0.511 | | 111 | -323 |
| KAS02/208 | 202-214.5 | -257 | 7.5 | 106 | 0.500 | 0.502 | 0.483 | -211 | 185 | -244 |
| KAS02/532 | 530-535 | -308 | 7.73 | 550 | 0.180 | 0.244 | 0.240 | -229 | | -282 |
| KAS03/131 | 129-134 | -275 | 8 | 31 | 0.710 | 0.125 | 0.123 | -247 | | -302 |
| KAS03/931 | 860-1002.1 | -275 | 8.1 | 709 | 1.280 | 0.078 | 0.077 | -270 | | -328 |
| KAS04/338 | 334-343 | -275 | 8 | 220 | 0.410 | 0.327 | 0.324 | -245 | | -328 |
| KAS04/460 | 440-481 | -280 | 8.1 | 407 | 0.600 | 0.259 | 0.256 | -247 | | -326 |
| KAV01/422 | 420-425 | -215 | 7.35 | 43 | 0.590 | | 1.600 | -208 | | -266 |
| KAV01/526 | 522-531 | -310 | 7 | 118 | 1.200 | | 2.230 | -189 | | -217 |
| KAV01/560 | 558-563 | -225 | 7.2 | 220 | 0.810 | 1.02 | 1.020 | -200 | | -228 |

$E_h$ (1) = $E_h$ as reported from borehole and/or surface Chemmac measurements.

$E_h^{(2)}$ = modelled $E_h$ for the $Fe^{3+}/Fe^{2+}$ couple using a $Fe^{3+}$ value calculated as the difference between $Fe_{tot}$ and $Fe^{2+}$.

$E_h^{(3)}$ = modelled $E_h$ for the $Fe(OH)_3/Fe^{2+}$ couple using the thermodynamic data for amorphous $Fe(OH)_3$ recommended by Grenthe et al. [34].

$pH^{(4)}$ = pH that was used in redox modelling: Chemmac downhole or surface values or mean of both measurements, or lab-measured pH (note that the 'adjusted' model pH values as shown in Table 1 above were not used for the modelled $E_h$ values shown here, but were used in a set of alternative models from which the results are shown in Figures 3 and 4).

$HS^{(5)}$ Recent studies have revealed that measured concentrations of $HS^-$ are sensitive to sampling procedure and to the prior history of perturbation by pumping etc. [35]

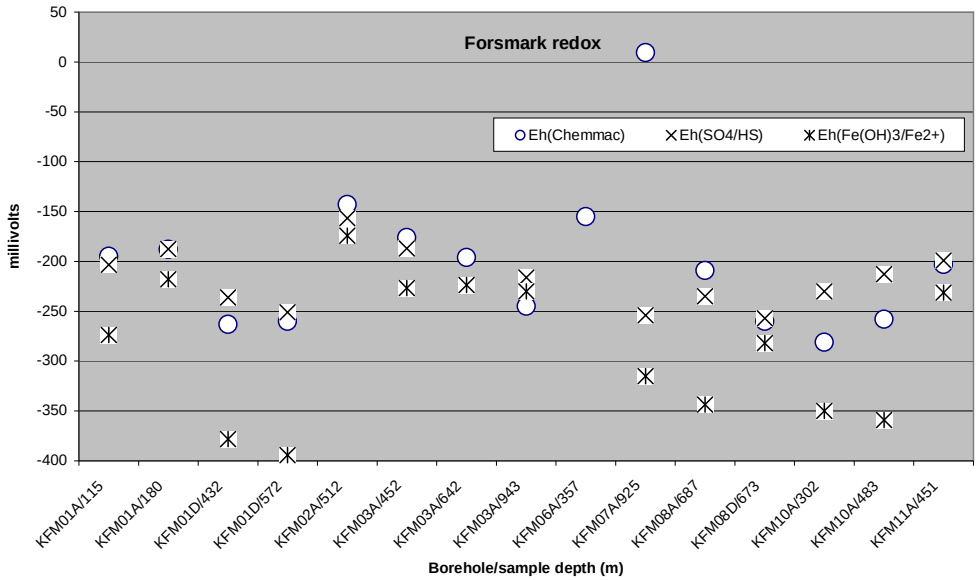


***Figure 1.*** *Compilation of calculated and measured $E_h$ data points from the selected set of hydrochemical data from Forsmark.*

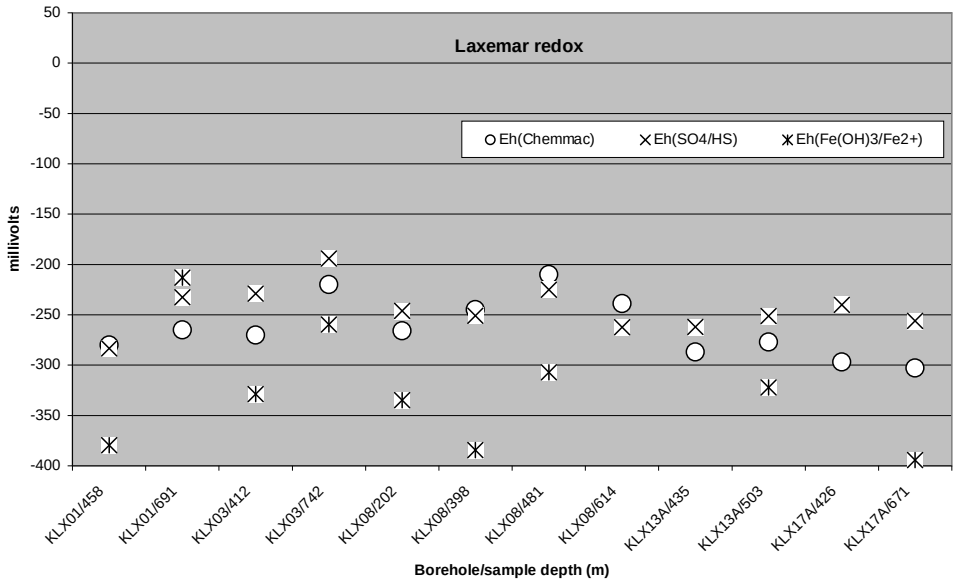


***Figure 2.*** *Compilation of calculated and measured $E_h$ data points from the selected set of hydrochemical data from Laxemar.*

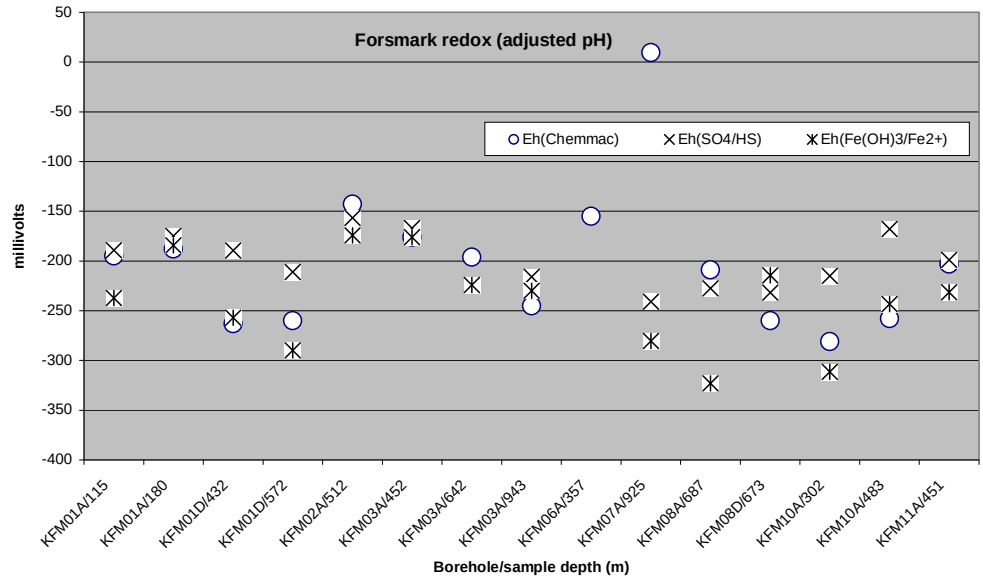


***Figure 3.*** *Compilation of calculated and measured $E_h$ data points from the selected set of hydrochemical data from Forsmark. $E_h$ values have been modelled using the pH values that have been adjusted for $CO_2$ outgassing (i.e. adjusted to give calcite saturation).*

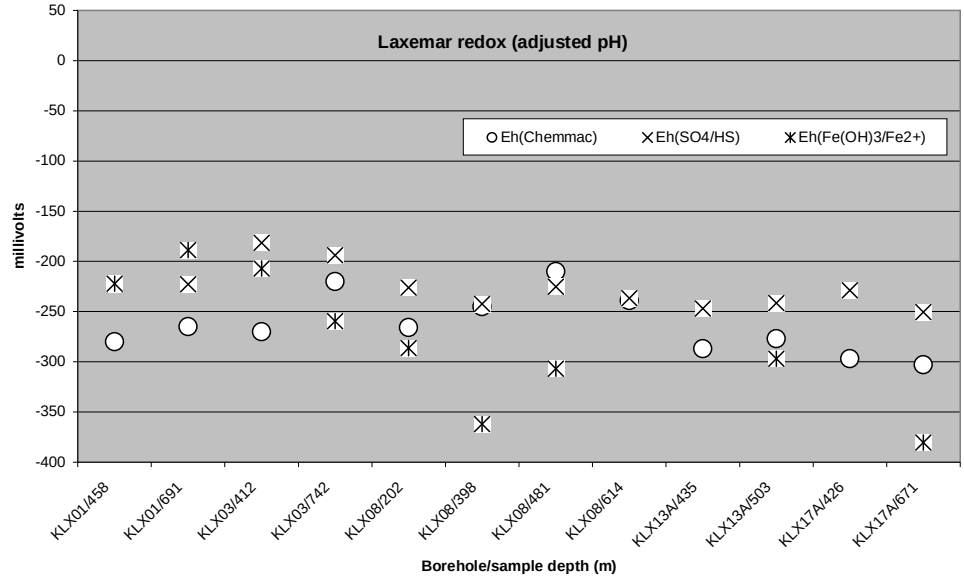


***Figure 4.*** *Compilation of calculated and measured $E_h$ data points from the selected set of hydrochemical data from Laxemar. $E_h$ values have been modelled using the pH values that have been adjusted for $CO_2$ outgassing (i.e. adjusted to give calcite saturation).*

Comparison of Figures 3 and 4 with Figures 1 and 2 indicates that using the adjusted pH values tends to give slightly higher, i.e. less negative, values of $E_h$ for the $SO_4^{2-}/HS^-$ and $Fe(OH)_3/Fe^{2+}$ couples, more so for the latter than the former. This has the effect of making the $E_h(Fe(OH)_3/Fe^{2+})$ values closer to the measured $E_h$. In other words, it is less clear-cut as to whether the measured $E_h$ is reflecting the $SO_4^{2-}/HS^-$ or $Fe(OH)_3/Fe^{2+}$ redox equilibria.

It has been inferred by SKB that pyrite ($FeS_2$) and siderite ($FeCO_3$) control redox in the bentonite buffer in which they occur as accessory minerals (see Section 6.1).

Concerning redox controls in groundwaters, calculations with PHREEQCI indicate that the reported compositions of water samples in Appendix B, specifically data for $Fe^{2+}$, $HS^-$, $HCO_3^-$ and pH, are:

- strongly oversaturated (between six and ten orders of magnitude) with respect to $FeS_2$,
- close to saturation (mostly ± 1 order of magnitude) with respect to FeS,
- slightly undersaturated (between zero and two orders of magnitude) with respect to $FeCO_3$,
- strongly oversaturated with respect to goethite (FeOOH) and hematite ($Fe_2O_3$) (six to eight and thirteen to seventeen orders of magnitude respectively) and slightly oversaturated (zero to two orders of magnitude) with respect to amorphous $Fe(OH)_3$.

This is compelling evidence that FeS and/or $FeCO_3$ equilibria are controlling dissolved $[Fe^{2+}]$ and probably also $[HS^-]$ in near-field groundwaters. This indicates that these solid phases and their biogeochemical equilibria may be the main long-term buffer for redox at repository depth. However the results of the comparisons of measured $E_h$ versus modelled $E_h$ in Figures 1 to 4 suggests that the $SO_4^{2-}/HS^-$ redox couple may be a stronger influence on measured $E_h$, i.e. on the electrochemical potential measured at the Chemmac electrodes, than the $Fe(OH)_3/Fe^{2+}$ couple. The $SO_4^{2-}/HS^-$ redox couple is a homogeneous equilibrium, i.e. both species are in solution and are evidently biogeochemically active, whereas the $Fe^{III}/Fe^{II}$ redox couple involves heterogeneous reactions between groundwater and $Fe^{II}$- and $Fe^{III}$-containing minerals. Therefore transient local redox behaviour at the measuring electrode being controlled by $SO_4^{2-}/HS^-$ is to be expected whilst long-term 'bulk' redox is controlled by $Fe^{III}/Fe^{II}$.

Siderite, $FeCO_3$, has not been reported as a common secondary mineral in fracture mineral assemblages at either Forsmark or Laxemar (Fe-containing carbonates are however reported to be in bentonite). This suggests that FeS is the dominant sink for $Fe^{2+}$, as well as for $HS^-$. The observation of pyrite, $FeS_2$, rather than amorphous FeS in fractures suggests that FeS transforms over time to more stable pyrite.

In the EBS, pyrite is an accessory mineral in bentonite and presumably is a significant buffer of redox due to irreversible reaction, for example consuming residual oxygen after emplacement as suggested in SR-Can [29]. If, as assumed by SR-Can, microorganisms are excluded from compacted bentonite then $HS^-$ production and FeS precipitation will be strongly diminished

in the buffer (see Section 6.3.2). However it can be noted that, if equilibrium with pyrite were to control the concentration of $Fe^{2+}$ at a very low level in the bentonite, $HS^-$ concentration could rise to a proportionately higher level before being limited by precipitation of FeS. The possibility of such a model, whereby $Fe^{2+}$ would be controlled by pyrite and maximum $HS^-$ by FeS equilibrium, should be considered when modelling pore water chemistry in the EBS.

## 6.3 Scenarios for redox-active species

### 6.3.1 Initial post-closure conditions

Biogeochemical conditions at the EBS-rock interface in the initial period after closure of a repository could be affected by higher temperatures (typically 40-60°C for 1000 years) and higher radiation. These transients will be precursors for the evolution of near-field conditions in the long term. Higher ambient temperatures will shift geochemical equilibria including those involving redox-active species, and will also increase microbiological effects on reaction kinetics. The natural biogeochemical regime in the near field will re-establish itself as the thermal and radiation perturbations diminish. More detailed considerations of these effects are outside the scope of this report. The impacts and potential variant scenarios of these early post-closure conditions should be fully considered in SR-Site.

### 6.3.2 Long-term changes in groundwater at repository depth

Interpretations and models of present-day conditions provide some insights into the possible sensitivity of the biogeochemical system to future changes of deep groundwater conditions.

The ways that long-term evolution of the groundwater system could change the chemical conditions at repository depth include:

- Increasing dominance of fresh (‘meteoric’) water recharge and circulation as land rise continues, relative sea level declines and the Baltic shoreline recedes, so that groundwater at repository depth will become more dilute. Drawdown during the excavation and operational phases of a repository will tend to accentuate this effect transiently.

- Increasing salinity if the hydraulic conditions change, so that the pressures in deep saline groundwater due to regional gradients increase relative to the pressure due to local recharge of fresh water. Salinity at repository depth might also increase transiently due to upconing during the excavation and operational periods when groundwater pressures are lowered.

- Sub-glacial enhanced recharge of fresh oxygenated melt waters, so that aerobic and oxidising conditions might persist to greater depths than under normal recharge conditions. This might also cause dilute water to penetrate to repository depth under steeper hydraulic gradients and

higher flow rates, potentially causing erosion and colloidal dispersion of bentonite buffer.

- Permafrost formation in overlying soils and rocks, causing salts to be excluded as fracture- and pore-filling ice forms and making the underlying residual groundwater more saline. Another potential process related to permafrost formation could be the trapping of methane ('geogas') as methane hydrate. This is discussed briefly below and more fully in Appendix C.

For increasing dominance of fresh water recharge, specific biogeochemical changes in deep groundwaters could be increasing or decreasing DOC concentrations, depending on soil conditions for biomass development and degradation, and associated changes of microbial populations. Increasing meteoric water infiltration would also increase dissolved oxygen input, though much or all of that would be attenuated by redox reaction with DOC in soils and shallow groundwaters and then by redox reactions with rock minerals, e.g. pyrite and $Fe^{II}$ minerals.

Future increases of flux of DOC to repository depth would probably increase activity of SRB and thus increase rate of $HS^-$ production in near-field groundwater. $HS^-$ production is limited by the availability of $SO_4^{2-}$. Thus the scenario for highest $HS^-$ production is probably a groundwater regime that supplies both DOC and $SO_4^{2-}$ at higher fluxes/concentrations into the near-field geosphere. A possible alternative source of DOC, apart from natural DOC derived from soils and transported to repository depth with infiltrating water, would be organic substances introduced to the repository as 'foreign materials'.

For the case of increasing salinity, one of the main changes with potential biogeochemical significance would be increasing or decreasing $SO_4^{2-}$ concentrations. The direction of change would depend on relative $SO_4^{2-}$ contents. At Forsmark, as at Olkiluoto in Finland, it is clear that $SO_4^{2-}$ has a maximum at an intermediate depth, typically 200-300 m, and then decreases to low concentrations in the deep saline groundwaters at and below repository depths. At Laxemar, $SO_4^{2-}$ increases progressively with increasing depth so that it reaches the maxima of observed concentrations in the deepest saline groundwaters. Thus increasing salinity at repository depth at Laxemar would be associated with increasing $SO_4^{2-}$, whereas increasing salinity at Forsmark would probably be associated with decreasing $SO_4^{2-}$. The $HS^-$ concentrations at both Forsmark and Laxemar do not seem to vary systematically with depth or salinity, and remain generally low, so $SO_4^{2-}$ changes would probably not correlate directly with $HS^-$ changes.

The specific question of whether fresh sub-glacial meltwaters retaining dissolved oxygen might reach repository depth has been considered in a previous report for SSM [2, 3]. Whether dissolved oxygen, if it were to reach repository depth according to the unlikely conditions described in [2, 3], could then come into contact with canisters and cause oxidative corrosion would depend on attenuation by the buffer. Thus a 'worst case' scenario would be conditions whereby infiltrating sub-glacial meltwaters could erode

buffer in addition to transporting DO without consumption by redox reactions in the intervening rocks. Whether sub-glacial infiltration will be always be oxidising or could be reducing remains uncertain – there is little if any direct observation of redox under ice sheets. Sub-glacial recharge might also cause fast transport to repository depth of anomalous quantities of e.g. DOC, microorganisms, $NH_4^+$ and other biosphere solutes and species, thus perturbing the biogeochemical system.

If permafrost were to cause significant salinity increase in underlying groundwater due to 'salt exclusion', the general effects at repository depth would be similar to those due to normal salinity changes as groundwater evolves. However one potentially significant difference is that $SO_4^{2-}$ would increase at both sites, whereas present deep saline groundwater at Forsmark has low $SO_4^{2-}$. The increase of $SO_4^{2-}$ could be markedly high at Forsmark because present groundwater at intermediate depth, i.e. 200-300 m, is already high. As in the case of glacial infiltration, the changes in hydrochemistry that would be associated with permafrost thaw are uncertain, e.g. possibly higher DOC and microorganism inputs especially from peat.

Trapping of $CH_4$ in permafrost as methane hydrate is mentioned as a hypothetical feature of the glacial stage of the normal long-tem evolution scenario in SR-Can. A related scenario is the trapping and accumulation of $CH_4$ below permafrost, both as methane hydrate and as $CH_4$ gas. Potential accumulation of methane hydrate over the duration of a permafrost period would depend on upwards $CH_4$ flux; theoretical considerations suggest that it could take on the order of hundreds of thousands to millions of years for substantial amounts of methane hydrate to accumulate, even in fairly porous rocks. No evidence has been found by the present authors for methane hydrate accumulating in permafrost in fractured crystalline rocks with low porosities, and a scoping calculation suggests that it would take a very long time to develop a significant accumulation (see Appendix C). However, if permafrost were to reach repository depth, it is conceivable that methane could accumulate and be trapped as hydrate in voids in the tunnels.

$CH_4$ concentrations and fluxes in deep groundwaters at around repository depth in crystalline rocks in the Fennoscandian Shield are apparently rather variable. In the deep boreholes at Forsmark and Laxemar, dissolved $CH_4$ concentrations are low: typically <1 mL/L (= 0.04 mmol/L) whilst at Olkiluoto they are significantly higher and close to or at saturation, up to 800 mL/L (= 36 mmol/L) below 800 m depth.

If this natural $CH_4$ flux were trapped as hydrate or in some other way during a period of permafrost, then $CH_4$ concentrations should be expected to rise transiently when the permafrost thaws. At the same time as $CH_4$ would be released, DOC and microbial activity might also increase in shallow groundwaters. Enhanced $CH_4$ concentrations could possibly promote $SO_4^{2-}$ reduction, as might be the case at present at Olkiluoto (see Section 5.2.1), but the production of $HS^-$ would be limited by $SO_4^{2-}$ concentration and the concentration of $HS^-$ would probably be limited by sulphide precipitation if $Fe^{2+}$ is sufficient. However, no evidence has been found to suggest that cou-

pled permafrost-$CH_4$-$HS^-$ biogeochemical processes have been significant during glacial cycles in the past.

Thus future concentrations of $HS^-$ in near-field groundwaters around deposition holes will depend on interplay of many biogeochemical properties and processes: influxes of $SO_4^{2-}$, DOC, $CH_4$, $Fe^{2+}$ and perhaps other redox-active solutes (including DO) in deep groundwater movements, quantities of locally 'introduced' organics and $SO_4^{2-}$ originating from the repository itself (including buffer and backfill materials), microorganism populations, and natural sources of $Fe^{II}$ and sulphide in local rock.

### 6.3.3 Biogeochemical model for sulphide in the EBS

The processes that constitute the conceptual model for the production and maximum concentration of corrodant $HS^-$ in pore water in the bentonite buffer adjacent to an emplaced copper canister are:

- Diffusion or advection of $SO_4^{2-}$, SRB, $H_2$, acetogens/acetate, DOC, $CH_4$ to a location where SRB are viable and reduction of $SO_4^{2-}$ is mediated;
- Reduction of $SO_4^{2-}$ to produce $HS^-$ outside the buffer, i.e. in near-field geosphere and in backfill;
- Diffusion of $HS^-$ through the buffer from the interface with rock or backfill towards the buffer-canister contact;
- Moderation of $HS^-$ concentration by precipitation of $FeS/FeS_2$ solid phase(s), in near-field geosphere, backfill and buffer, depending on the availability and rate of supply of $Fe^{2+}$. SR-Can [29] asserts that $HS^-$ concentrations would be controlled at low levels (e.g. $\leq 10^{-5}$ M) due to equilibration with iron sulphide (FeS) in the near-field geosphere and with pyrite ($FeS_2$) in the buffer.

This conceptual model makes the assumption that SRB are eliminated from the buffer due to the physical and biogeochemical conditions. This assumption is based mainly on experimental evidence that SRBs do not remain viable in the pores of bentonite buffer compacted to more than 1800 kg $m^{-3}$ [7, 31, 36, 37, 38, 39]. The experiments have been carried out with various bentonite mixtures, pure and sand mixtures, various compaction densities, various temperatures and in both laboratory and URL (Swedish and Canadian) conditions. They have shown that the rate of $HS^-$ production and, by inference, the population of active SRB declines as the swelling pressure and the density of compacted bentonite is increased. There is some remaining uncertainty about whether SRB numbers decline fully to zero and whether they could be reactivated if swelling pressure reduced. SKB have concluded that SRB probably cannot be active in the design conditions of intact compacted buffer in deposition holes, i.e. at density of 2000 kg $m^{-3}$. The thermodynamic activity of water, $\{H_2O\}$, in the bentonite pores at this compaction density is about 0.96 and it has been suggested that this might be a factor in the viability of microorganisms [39]. Experimental results have suggested that spores are rather more resilient but are eventually destroyed. Therefore it is assumed that all microbes and spores introduced in the bentonite and in

groundwater or added 'technical' water in deposition holes will be eliminated by the low initial water content, and eventual swelling pressure. However, Pedersen has stated that "….it is theoretically possible that sulphide producing microbes may be active inside a buffer, although the experiments so far have shown the opposite" [40]. So it is appropriate to be cautious about assumptions that microbes will inevitably be excluded and/or inactive in the buffer.

Transport of natural microbes and spores in groundwaters outside the deposition hole into the buffer has also been discounted, on the basis of experimental observations [7]. However the experiments showed that bacteria migrate 'at least 3 mm' into buffer over an experimental timescale of 28 weeks. A comment on these observations is that migration of 3 mm in 28 weeks does not seem to be sufficient evidence to totally discount diffusive migration over a much longer timescale. Therefore the buffer as a barrier to physical migration is not proven, per se, although of course the evidence that bacteria do not survive the high densities and low water activities of compacted rehydrated bentonite supports the microbial barrier concept.

In contrast, backfill is not expected to act as a microbial barrier. It would be expected to sustain a SRB population that would be capable of mediating the $SO_4^{2}$-$HS^-$ reduction, given a suitable electron donor such as DOC or $H_2$ [7].

SKB's model of EBS geochemistry as used in SR-Can has been described in [16, 41, 42]. This model represents ion exchange, protonation/deprotonation at smectite surfaces, and geochemical equilibria with solid phases including redox equilibria with pyrite/FeS and/or siderite. It assumes that microbes will not be viable in the buffer and therefore $SO_4^{2-}$ reduction to $HS^-$ is excluded from the model of the buffer.

A quantitative process model for biogeochemical conversion of $SO_4^{2-}$ to $HS^-$, for microbial mobility and viability, and for transport of $SO_4^{2-}$ and $HS^-$ in the EBS would represent the processes and limitations on microbial viability and transport as described above. The coupled transport-reaction models of Liu, Sidborn and Neretnieks [28, 43, 44] make progress towards this with the fundamental assumption that there will be no microbial activity within the buffer. There are scoping models with other assumptions and simplifications in how they represent biogeochemistry outside the buffer. The models are based on $SO_4^{2-}$ reduction taking place in a rock fracture that intersects the rim of a deposition hole. Produced $HS^-$ then partly diffuses into the buffer and migrates towards the canister and partly is advected away and does not enter the buffer. The $SO_4^{2-}$ reduction at the rock fracture-buffer interface is assumed to be kinetically fast due to microbial mediation by SRB, so that all supplied $SO_4^{2-}$ is transformed effectively to $HS^-$.

Neither of the models includes the moderation of $HS^-$ concentrations due to equilibrium with FeS or $FeS_2$, so that the modelled $HS^-$ source concentrations at the diffusive outer boundary are determined either by fluxes to that interface of either $SO_4^{2-}$ or the energy source for SRB which is DOC, acetate, $H_2$ or possibly $CH_4$.

The concentrations of $HS^-$ in groundwaters at and below repository depth are mostly $<2x10^{-6}$ M and $<3x10^{-7}$ M at Forsmark and Laxemar respectively (Table 2). Corresponding concentrations of $Fe^{2+}$ are mostly $<4x10^{-5}$ M and $<2x10^{-5}$ M respectively. If concentrations of $Fe^{2+}$ and/or $HS^-$ in either buffer pore water or near-field groundwater were to be controlled by equilibrium with $FeS_2$ then the values would be many orders of magnitude lower. As discussed above (Section 6.2), these concentrations are evidently controlled at the observed values by FeS equilibrium.

It is reasonable to expect that control of $HS^-$ by FeS equilibrium will continue in the long-term evolution of the near field, backfill and buffer. For the concentration of $HS^-$ in the near field to be kept low, the concentration of $Fe^{2+}$ must be maintained by release from dissolving minerals and by advection/diffusion in solution at about the same rate as $HS^-$ is being produced. Although it can be inferred from FeS equilibrium in groundwater compositions that these sources of $Fe^{2+}$ operate generally, there is evidence in localised high $HS^-$ concentrations (e.g. $5x10^{-6}$ M in KFM07A/925, $7x10^{-5}$ M in KLX01/691) that there are locations at repository depth where fluxes of $Fe^{2+}$ may be lower than elsewhere. Mineralogical and geochemical data that would give indications of the spatial variability of mineral sources and release rates of $Fe^{2+}$ are not available.

Pyrite is an accessory mineral in bentonite and presumably is a significant buffer of redox in the EBS as suggested in SR-Can [29]. If equilibrium with pyrite were to control the concentration of $Fe^{2+}$ at a very low level in the bentonite, then $HS^-$ concentration could in theory rise to a proportionately higher level before being limited by precipitation of FeS. However this hypothesis assumes that there would be no other limitations on $HS^-$, e.g. due to microbial inactivity inhibiting $SO_4^{2-}$ reduction.

Liu's and Sidborn's models do not constrain the rate of $SO_4^{2-}$ reduction according to the kinetics of the microbial mediation process, i.e. according to Monod kinetics or Michaelis-Menten formula (see Section 5.2.2). Monod kinetics might apply if the utilisation of DOC as energy source for SRB were directly the rate-determining process, whereas Michaelis-Menten kinetics might apply in the case where acetate, $H_2$ or $CH_4$, rather than DOC, is the electron donor. Alternatively, neither of these kinetic formulations would be appropriate if the rate of $SO_4^{2-}$ reduction is controlled by the numbers of active SRB, the population of SRB being sparse in this deep geosphere environment.

Liu's model [28, 43] assumes that $SO_4^{2-}$ reduction is instantaneous, whilst Sidborn's model [44] assumes a reduction rate of $10^{-6}$ $kmol^{-1}$ $m^{-2}$ $a^{-1}$ (where the $m^{-2}$ refers to rate per $m^2$ of a biofilm that is assumed to be the location of SRB activity at the rock-buffer interface). The latter also implies that $SO_4^{2-}$ reduction in the model is effectively instantaneous.

A worst case scenario conceptual model for activity of SRB and production of $HS^-$ corrodant at the interface between buffer and copper canister was proposed in Pedersen's review paper [7]. This scenario is contrary to the 'normal' model described above. It considers the possibility that SRB would

be viable at the buffer-canister interface with energy from DOC or acetate/$CH_4$ produced by action of methanogens on inorganic carbon (i.e. dissolved $HCO_3^-$ and $CO_2$). Microbial growth has the dual results of production of $HS^-$ and of a biofilm of metabolic by-products which would tend to enhance sulphide production in the most critical location, i.e. on the copper surface.

Another worst case scenario has emerged as a significant consideration in SR-Can [29, Sections 9.2.4 and 10.6]. It involves the possibility that buffer could be eroded if the frictional drag due to water flow were to exceed the cohesion between clay particles in the buffer, followed by mass loss of buffer and exposure of the canister directly to advective transport of corrodants such as $HS^-$. Buffer erosion is thought to be more likely in the operational and early post-closure stages when potential buffer piping could lead to erosion. However erosion might also be a hazard to buffer integrity during a future glaciation over the repository, if enhanced advection of fresh water to repository depth destabilised the buffer.

For these scenarios in which $SO_4^{2-}$ reduction is assumed to occur adjacent to canisters, the biogeochemical processes that should be added to the above list of processes for the normal conceptual model for maximum concentration of corrodant $HS^-$ are:

- Diffusion of $SO_4^{2-}$ through buffer, enhanced by internal mineral source of $SO_4^{2-}$ within buffer;

- Possibility of SRB not being eliminated in proximity of canister because of failure of buffer as designed, e.g. due to erosion, loss of swelling or colloidal dispersion/peptisation.

# 7. Implications for general corrosion of copper

The objective of this specific part of the work is to investigate potential impacts of changing corrodant and other geochemical conditions ($HS^-$, $Cl^-$, N species, $CH_4$, $H_2$, DO, DIC) on the stability of components in the EBS, particularly of copper, and to describe important qualitative aspects of near-field groundwater biogeochemistry that could, in any way, have an effect on corrosion.

The descriptive work focuses on chemical equilibria in subparts of the system Cu-Fe-Cl-N-S-C-H-O as described in accounted Pourbaix diagrams and the discussion on impacts on copper and iron corrosion of changing corrodant and other geochemical conditions in the repository has this information as a starting point.

## 7.1 Method

As a first step of work 'normal' corrosion processes that can be expected in a repository are outlined. Thereafter the 'normal' chemical environment is sketched. A selected set of Pourbaix diagrams is thereafter shown. Those are used as a background material in the subsequent discussion of the influence of changing corrodant conditions on EBS corrosion. The focus is here on copper corrosion.

Changes in corrodant concentrations have been discussed in previous works i.e. in [1-3] and relevant results from these are used here. Some other relevant works in this context are also accounted in [45-51]. Relevant descriptions and data from the mentioned references are partly excerpted and accounted here again to form a background to subsequent calculations. Data from [1-3] and [45-51] have been selected to cover the ranges of changed corrodant concentrations that could influence the stability of components in the EBS and particularly of copper but also of iron.

The thermodynamics of copper and iron, specifically in relation to sulphide and in saline environments, form an important part of the basis for this work. It gives the framework for subsequent modelling discussions and provides a convenient way to present calculated results as Pourbaix diagrams, each calculated for a specified set of conditions, which act as chemical maps and background to discussion of the potential impacts of changing corrodant and other geochemical conditions ($HS^-$, $Cl^-$, N species, $CH_4$, $H_2$, DO, DIC) on the stability of components in the EBS. Because of the complexity of the total chemical system, the calculations here are limited to parts of the chemical system Cu-Fe-Cl-N-S-C-H-O at 25 ºC. Calculations for the Pourbaix diagrams presented here have been done using Puigdomenech´s set of programs (MEDUSA) and also in part the related thermodynamic database (HYDRA)

[52]. Thermodynamic data in the MEDUSA database have been compared with thermodata used in other geochemical models, including PHREEQC, in Appendix 4 of [1].

Selected Pourbaix diagrams are presented in Section 7.4 and supplementary diagrams are in Appendices C and D.

## 7.2 Some introductory comments on EBS corrosion

### 7.2.1 Background

Copper can be exposed for both general and different kinds of localised corrosion in the repository. The complex mechanical, chemical and microbial environment with high pressures varying in time and location and with oxygen, chloride, sulphur and carbon-bearing compounds present will cause different types of attacks that are going to prevail during different time periods. The procedures of production, handling and treatment of the canister throughout the processes of filling, transportation and deposition could be crucial for its later, corrosion-related integrity throughout the storage period in the repository. There is also a risk that due to systematically induced faults, many canisters may have later corrosion related problems of the same kind.

There will certainly be an operational and initial post-closure period when the repository will have oxidising conditions due to residual $O_2$, after which reducing conditions are expected to establish as $O_2$ is consumed. As discussed elsewhere oxidising conditions might conceivably return at later stages, for example during glaciation events [3, 4, 29]. During a glaciation, complex pressure gradients could change the directions and rates of groundwater flow and cause sub-glacial intrusion of DO which, if not consumed by reaction with reducing minerals, could provide a driving force for the corrosion processes. An inhomogeneous environment with respect to pressure, heat and chemistry would promote corrosion.

Several potential corrosion mechanisms, principally due to $HS^-$, have to be considered for the long periods for which reducing conditions will be maintained in a repository. Preliminary findings from recent laboratory experiments have been interpreted to suggest that copper might experience $H_2$-evolving corrosion in anoxic pure water [53]. If these findings were confirmed, the view on copper thermodynamics and the models for copper corrosion would have to be revised. As the mentioned work [53] is as yet unverified by others, its consequences are not further treated here.

Different periods of the repository lifetime are going to be exposed to different driving forces for groundwater movement. This is valid both on a regional and a local scale. Groundwater flow controls the rates at which key corrodants could be transported towards the deposition holes. A few mechanisms for variable flow rates could be mentioned, but others are probably also possible. Groundwater flow during normal present-day conditions is a first. Changes of hydraulic gradients during glaciation periods is a second. Anthropogenically caused changes is a third. Gas evolution due to processes

in the repository or as a flow of geogas is a fourth possible mechanism for changing groundwater movements. A fifth is the presence of temperature gradients.

Alongside thermodynamic modelling, these transport limitations should be an important factor in a comprehensive assessment of corrosion rates. If thermodynamics indicates that copper is vulnerable in a particular solution environment, then the rate of corrosion and the overall degree of attack might be controlled by the rate at which the key corrodant can be transported to the copper surface and/or corrosion product can be transported away from the copper surface.

### 7.2.2 General corrosion

As already mentioned there are several chemical environments around and inside the canister that can be foreseen. During oxidising conditions in a concentrated $Cl^-$ solution, there will be general corrosion of copper. According to thermodynamic calculations copper is not stable in such an environment. Such a homogeneous attack is, however, not a major problem for copper integrity, as long as transportation rates of reacting matter are low.

The immunity $E_h$ limit, below which metallic copper is the stable phase, descends as a function of temperature at high $Cl^-$ concentrations. It is possible that copper could be neither noble (i.e. immune) nor passive at higher temperatures in a repository environment containing high concentrations of $Cl^-$. Thus, in such an environment, copper might be protected from serious general corrosion only by keeping fluxes to the copper surface of reacting species very low. High $Cl^-$ concentrations from upconing of highly saline groundwater combined with other factors such as rapid flow and solute transport plus buffer erosion would be detrimental for copper canister integrity.

In a 'normal' case $E_h$ has to go far above the values accounted in Figures 1 and 2, up to $E_h$ values about +250mV, before there is any risk for the canister to corrode. An increasing pH value will protect from this effect as CuO is stabilized. There is no essential problem for copper canister corrosion to be foreseen until $HS^-$ concentration reaches the same level as copper solubility at ambient temperature which could occur only at low $E_h$ values in strongly reducing conditions.

### 7.2.3 Microbially enhanced corrosion processes

It has been suggested [31, 36] that SRB will be absent from the interface between buffer and canister surface if buffer density exceeds 1800 kg $m^{-3}$ and thus pore water activity in the bentonite, $\{H_2O\}$ is <0.96 (see discussion in Section 6.3.3). If for any reason those conditions are not fulfilled in the buffer, SRB will be viable and could transform $SO_4^{2-}$ into $HS^-$. At a low enough $E_h$, the latter can react with copper in an anoxic environment to form copper sulphide with hydrogen evolution ($2Cu(s)+2H_2O+S^{2-} \rightarrow H_2+Cu_2S+2OH^-$).

### 7.2.4 Changing repository conditions

One objective of this work is to outline processes in the repository that could influence copper corrosion under changing conditions due to biogeochemical effects e.g. on the S, N and C systems. This can be assessed by using modelling of the thermodynamic limits for corrosion in the repository environment, but a comprehensive assessment would take account also of the microbiological kinetics and corrodant transport aspects that have been discussed in previous sections. A rough overview of the thermodynamics for important parts of the system Cu-Fe-Cl-N-S-C-H-O is therefore given to form a general background for the work. Data are normally accounted as Pourbaix diagrams that are valid at indicated conditions and, if not otherwise indicated, at 25 ºC.

There are many studies of canister corrosion accounted in literature. This work is, however, not intended as a literature survey and the reader is therefore urged to find such information directly in literature or in already existing surveys. However the mechanisms for corrosion can be expected to differ greatly for different situations, the general conclusion of the repository oriented literature data is that copper is a suitable canister material. It is foreseen to have a very long lifetime in the intended environment. There are, however, uncertainties in the estimation of the lifetime indicated in literature, especially at deviating conditions like those supposed to prevail at glaciation ($Cl^-$, DO, groundwater flow and solute transport patterns) and at the uncertain influences of agents like $HS^-$ and bacteria.

The effects of changes in those conditions (parameters) on copper (and iron) corrosion are the focus of this section.

## 7.3 Chemical environment at repository depth

### 7.3.1 General issues

SKB's data for the hydrochemical environment at repository depth were reviewed and evaluated in detail, especially with respect to redox and pH conditions and the related uncertainties, in a previous report for SKI [1]. An update of that approach, taking account of recent data reported since the 1.2 data freeze, is reported in Section 6 above. Those considerations provide the basis for the description of the chemical environment that is used in the following redox modelling.

The maxima of hydrostatic pressures at repository depth suggested in SR-Can [29] are 5 MPa (no glaciation, normal hydraulic conditions) and 30 MPa (glaciation, assuming that the load of the ice sheet is directly propagated into the groundwater column). There is an estimation of a probable maximum of 14 MPa. The pressure influences mechanical systems and groundwater flow and thereby solute transport patterns, but its influence on chemical equilibria that do not involve gaseous components is small and is therefore negligible for present purposes.

The temperature in the repository will roughly vary with time in a manner, which could give a maximum close to a canister of about 85°C a short time after repository sealing. Thereafter the temperature will decrease and will after some time adopt the surrounding rock temperature, about 10-15°C.

Lower temperatures could appear in connection with a prolonged glaciation. All calculations in this section of the report have been performed at 25°C as input data are normally given at that temperature. The difference to 15°C is judged to be negligible compared with other uncertainties.

As groundwater flows through the repository its composition can vary with time for different reasons, for example in connection with glaciation and as a function of other climate and environmental changes. The water contains chloride, carbonate and sulphide/sulphate in concentrations and relations that could vary. The ambient concentration of $Cl^-$ could rise to about 1.5 M.

Furthermore there will exist very low concentrations of reducible species, for example $Mn^{III, IV}$ and $Fe^{III}$, possibly bound as complexes together with e.g. chloride and organic complexing agents. In addition to low natural abundances, the latter species could be derived from introduced materials including organic material in the bentonite. Introduced substances are assumed to influence the prerequisites for corrosion.

At closure, the repository environment will be aerobic and therefore oxidising. The total amount of free $O_2$ in the aerated repository consists of $O_2$ left in pockets of air and as DO, for example in the bentonite pore water. The bentonite will also have open porosity partly filled with air. As an illustrative calculation, it is supposed that the bentonite pore water would be oxygen saturated (8 mg/L at normal pressure and temperature). Then the bentonite in a deposition hole (about 12 $m^3$ of bentonite) is going to contain about 28 g DO in water if the bentonite moisture content is about 28 vol. %. If this $O_2$ were consumed only in some mechanism(s) of attack on the canister, it would correspond to dissolution of about 200 g of copper metal.

Due to slow kinetics, reducible species might still be present in the masses of bentonite after the oxidising period. Those can serve as electron sinks in combination with other processes, for example formation of copper sulphide. The repository pH is assumed to be buffered by the bentonite, which implies a pH of about 7-9. Pyrite ($\approx FeS_2$) will occur and also residuals of organic materials.

The repository might be exposed to events which would involve penetration by water with high salt- and/or $O_2$ concentrations. There can also be events, which result in crack formation in or peptisation of the bentonite. Such events can, if they would happen, be supposed to strongly influence the chemical environment of the repository. Furthermore, it shall be pointed out that if the rock fracture system is not already biologically contaminated, the very opening and construction of the repository will imply a biological contamination. Therefore it is probable that microbes will exist in the repository after closure [19].

In summary it can be said that the global pH in the repository will be in the range of 7-9, buffered by the bentonite. The redox potential ($E_h$) will probably evolve through an initial period of oxidising conditions and gradually turn into a reducing after sealing. Redox conditions might fluctuate, especially during glaciation periods. An extreme fluctuation could conceivably

occur from reducing to oxidising potentials, although SR-Can [29] makes the case that reducing conditions will very probably be maintained even in the scenario that oxygenated sub-glacial water with DO at $3x10^{-4}$ M is recharged into groundwater with an enhanced downwards hydraulic gradient caused by ice-loading. The evidence and modelling in support of that case have been reviewed and the uncertainties have been examined for SKI in [2, 3].

The most important chemical entities related to copper corrosion in the repository would be:

*Metals*: Cu and Fe
*Simple anions*: $Cl^-$, $SO_4^{2-}$, $HCO_3^-$, $NO_3^-$, and $HS^-$
*Simple cations*: $Na^+$, $Ca^{2+}$, $Mg^{2+}$, $Cu^+$, $Cu^{2+}$, $Fe^{2+}$, and $Fe^{3+}$
*Complexes*: $CuCl_n^{1-n}$, $CuCl_n^{2-n}$, $FeCl_n^{2-n}$, $FeCl_n^{3-n}$, $Cu(OH)_n^{1-n}$, $Cu(OH)_n^{2-n}$, $Fe(OH)_n^{2-n}$, $Fe(OH)_n^{3-n}$, $Cu(CO_3)_n^{1-n}$, $Cu(CO_3)_n^{2-n}$, $Fe(CO_3)_n^{2-n}$, $Fe(CO_3)_n^{3-n}$, $Cu(HCO_3)_n^{1-n}$, $Cu(HCO_3)_n^{2-n}$, $Fe(HCO_3)_n^{2-n}$, and $Fe(HCO_3)_n^{3-n}$
*Solids*: CuO, $CuO_2$, $Fe_2O_3$, $Fe_3O_4$, $CuFe_2O_4$, $CuFeO_2$, $CuCl_2$:$3Cu(OH)_2$, $CuCO_3$, $Cu_2CO_3(OH)_2$, $Cu_2S$, $Cu_{1.75}S$, $Cu_{1.93}S$, CuS, and $\approx FeS_2$
*Colloids:* Dispersed bentonite, organic material
*Organic matter:* For example humic and fulvic acids
*Surfaces:* Bentonite, rock minerals and metals
*Gases:* Dissolved $O_2$, $N_2$ and other chemical components that at a proper pressure and other circumstances might generate gas (i.e. 'geogas' or methane).

After closure of the repository, groundwater will have access to the whole system and there will be a groundwater flow through the repository. The flow rate and composition of the water is determined by the outer (surface) conditions as well as by the repository conditions. Values for selected chemical and environmental isotopic parameters in water samples taken from the deep boreholes at the Forsmark and Laxemar sites are provided in Appendix B.

The composition of the bentonite to be used in the repository is important in many respects and is discussed e.g. in SR-Can [29]. The composition varies but the main components are clay minerals (>80 %), predominantly smectite (>70 %). The main chemical elements are Si and Al and lesser concentrations of Na, Mg, Fe, K and Ca. The concentration of sulphides and organic material should be below 200 mg/kg. The most common sulphide phase is pyrite, $FeS_2$.

A discussion of microbial influences can be found in the first part of this report and in [7]. A concern for the performance of copper canisters is that SRB may be present in the buffer and induce canister corrosion by production of reduced sulphur ($HS^-$). As discussed above, water activity has been suggested to be a strong limiting factor for activity of bacteria in compacted bentonite [31, 36]. $SO_4^{2-}$ reduction is an in situ process but the resulting $HS^-$ rich water can be transported to other locations. A more vigorous $SO_4^{2-}$ reduction takes place when DOC is high (>10 mg/l DOC), which is the case in sub-seabed sediments and groundwaters [54], and it is suggested above (Sec-

tion 5.2.1) that DOC concentrations may be the limiting factor for $SO_4^{2-}$ reduction in the groundwaters in crystalline rocks.

The chemical parameters in Table 3 are selected as the basis for the calculations of dissolved redox couples and related solid phase equilibria as shown in the following Pourbaix diagrams.

In order to evaluate the sensitivity of the corrosion processes on the main parameters pH/$E_h$, [$Cl^-$] and [$HS^-$], values for these and other parameters have been compiled from SKB reports (R- and P-series) and also from a recent data printout provided by SKB from their SICADA database. This compilation is in Appendix B. The pH and $E_h$ data for samples in which both parameters have been reported, and are believed to be reliable, are shown in Figure 5.

It can be seen that the spread in $E_h$ is around 150 mV, from about -140 to -350 mV, and the spread in pH is around 1.5 units, from about 6.9 to 8.7. The correlated variation of measured $E_h$ with pH is consistent with the theoretical dependence of $E_h$ on pH in the case of $E_h$ being controlled by the $SO_4^{2-}/HS^-$ redox couple, as shown by the calculated slope shown in Figure 5.

This work will consider broader intervals of pH and especially of $E_h$: $7<pH<10$ and $-500\ mV<E_h<+500\ mV$. The values of the main chemical parameters together with the concentration values of main species found in Table 3 are the 'reference' values used in the following calculations.

***Table 3.*** *Selected chemical parameter ranges from various sources. The ionic concentrations are selected from different sources to represent a groundwater on 500 m depth at a repository site.*

| Parameter | Units | Selected value | Minimum value | Maximum value |
|---|---|---|---|---|
| pH | | 8 | 7 | 10 |
| $E_h$ | V | -0.3 | -0.1 | -0.5 |
| $HCO_3^-$ | mg/l | 100 | 100 | 300 |
| $SO_4^{2-}$ | mg/l | 8 | 5 | 500 |
| $Cl^-$ | mg/l | 200 | 170 | 6500 (50000) |
| $HS^-$ | mg/l | 0.1 | | 0.5 |
| $Ca^{2+}$ | mg/l | 80 | 40 | 2000 |
| $Na^+$ | mg/l | 100 | 60 | 2000 |
| $Fe^{2+}$ | mg/l | 0.1 | | 1 |
| $K^+$ | mg/l | 5 | 5 | 20 |
| $Mg^{2+}$ | mg/l | 9 | 20 | 130 |
| $LogP_{O2}$ | bar | -2.8 | | -2.8 |
| $O_2$ | mg/l | | | 8 |

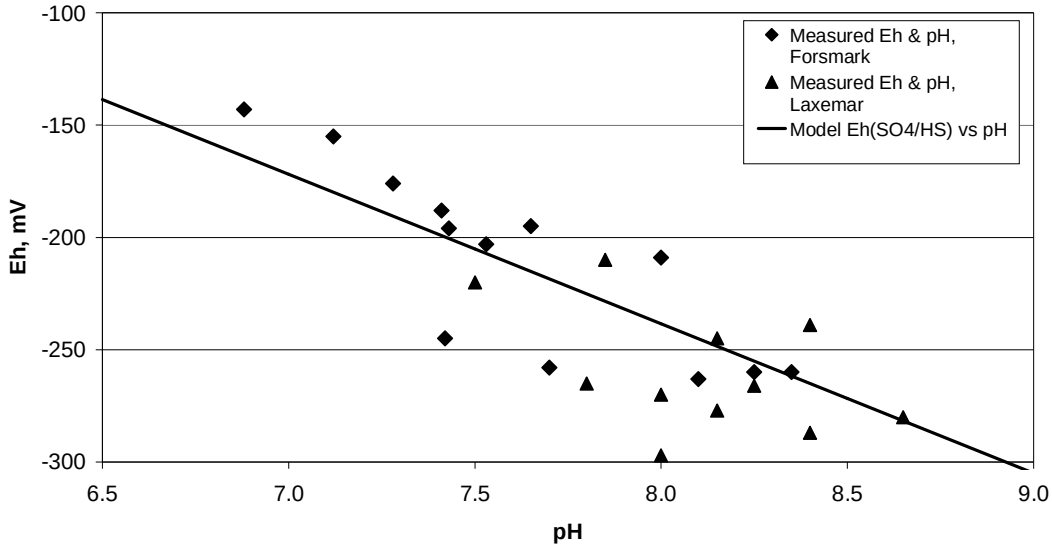


***Figure 5.*** *Compilation of pH/$E_h$ data points from the selected sets of groundwater data from Forsmark and Laxemar (see Appendix B). The line represents the redox equilibrium of the couple $SO_4^{2-}/HS^-$ at 10°C.*

### 7.3.2 Sulphide sources and equilibria in the Fe-S-O-H system

$HS^-$ has two main potential sources. One of them is sulphide coming from dissolution of sulphide minerals like pyrite, $FeS_2$. The other is from $SO_4^{2-}$ via the action of SRB (see Section 5.2). The stability of iron sulphides and oxides in the simple system Fe-S-O-H is shown at different conditions in Figures 6 and D1 to D5 (in Appendix D). 'Typical' concentrations noted for $Fe^{2+}$ and $HS^-$ in [1] for the near field have been used here for Pourbaix diagram calculations. A more detailed discussion of $Fe^{2+}$ and $HS^-$ concentrations and modelling of FeS and $FeS_2$ equilibria are given in Section 6.2.

### 7.3.3 Reduced nitrogen species

Copper and $NH_3$ form chemical complexes together and thus increase the solubility of copper. Other, simple nitrogen containing species like nitrate would have a negligible influence. As seen in following Pourbaix diagrams (Section 7.4.9 and Figure E8 in Appendix E), the limiting concentration for $[NH_3]$ influence is about 2 mM at a total copper concentration of 1 μM.

### 7.3.4 Chloride

Chloride has a strong influence on copper behaviour/solubility at higher concentrations, which has been outlined in [45] and can also be seen in the Pourbaix diagrams in the following sections. High $Cl^-$ concentrations could cause a complete loss of passivation ability of copper.

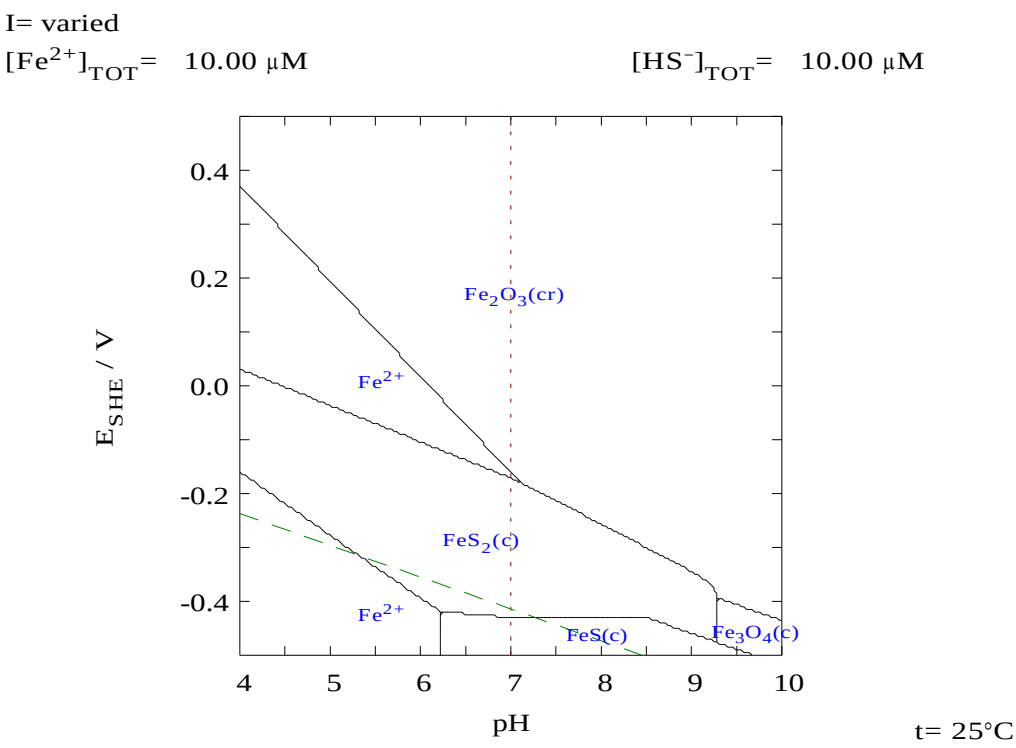


***Figure 6.*** *Stability of iron sulphides and oxides in the simple system Fe-S-O-H at shown conditions. This diagram shows the case in which [HS⁻] is at the upper end of the expected range (10 µM ≈ 0.35 mg/L) and [$Fe^{2+}$] is also typical (10 µM ≈ 0.56 mg/L).*

### 7.3.5 Carbonate alkalinity

Carbonate phases and hydroxycarbonates can be formed on copper at higher $E_h$ conditions. This has been outlined in [45] and can also be seen in the Pourbaix diagrams in the following sections. The influence on copper behaviour would be minor.

### 7.3.6 Dissolved oxygen and hydrogen

The Pourbaix type of diagrams used in this work inform about stability of species in a chemical system in the pH/$E_h$-plane at given total concentrations of components. There is, however, no information to be found directly about DO in a pH/$E_h$ point of such a diagram. $E_h$ is determined by pH and the predominating redox couple at that point, which in a specific case could be the $O_2/OH^-$ couple, but in a geological system is more likely to be $Fe^{II}/Fe^{III}$ or similar geochemical couples.

The chemical activity of $O_2$ can be calculated from Nernst's equation and the redox equilibrium data between oxygen and water. It is thus possible in theory to calculate equilibrium [$O_2$] for any 'background' $E_h$/pH point in the Pourbaix diagram. However it is not possible to specify DO 'threshold' concentrations for shifts in corrosion behaviour. Such considerations have to be expressed using corresponding $E_h$/pH values of which $E_h$ is determined by the dominant redox couple. For the same reason, $H_2$ concentrations are not either used in the discussion.

## 7.4 The chemical system Cu-Fe-Cl-N-S-C-H-O

### 7.4.1 Data and calculations

The material accounted in [55] tries to complete the picture from other investigations (as in [47, 56]) for the system Cu-Fe-Cl-N-S-C-H-O. This is done by including iron, $HS^-$ and $HCO_3^-$ as well as performing calculations for very high salinities. Calculations were also performed at an elevated temperature of 150 °C for the subsystem Cu-Cl-H-O in [56], but these are not accounted here. The calculations have been done using MEDUSA and the HYDRA thermodynamic database [52]. The calculations performed on the system Cu-Cl-H-O to higher salinities and temperatures (150 °C) were, however, partly done using data published in [47].

### 7.4.2 The sub-system Cu-Cl-H-O

In [47], three different total concentrations ($10^{-4}$, $10^{-6}$, and $10^{-8}$ molal) for dissolved copper were used for the calculations. It is stated in [47] that copper is a noble metal. However there are constraints to this immunity since copper corrodes with $H_2$ evolution at low pH above 125 °C with a copper concentration of $10^{-6}$ M and above 50 °C with a concentration of $10^{-8}$ M . The oxides ($Cu_2O$ (cr) and CuO (cr)) are stable at all temperatures and concentration levels $\geq 10^{-8}$ M, with the exception of $10^{-8}$ M at T ≥ 100 °C. The $Cu^{II}$ hydroxide, $Cu(OH)_2$(cr), is not thermodynamically stable in the interval investigated. $Cu^+$ predominates at T > 80 °C at all concentrations levels. CuOH (aq) appears in the Pourbaix diagrams only at the lowest concentrations and in the predominance diagram for dissolved species at 125 and 150 °C. $Cu(OH)_2^-$ predominates at all temperatures and concentrations investigated.

At acidic pH, an increasing temperature decreases the immunity area, and therefore the risk for corrosion of copper increases. At alkaline pH-values the risk for corrosion also increases with temperature due to decrease of both the passivity and immunity areas.

Examples of Pourbaix diagrams for the sub-system Cu-Cl-H-O that could be used in the present work are shown in Figures 7 to 9. They are calculated for 25 °C and $[Cl]_{tot}$= 0.001, 0.1 and 1.5 M, respectively.

Figures 8 and 9 indicate that in the simple system of Cu-Cl-H-O there is no protecting, passivating layer on copper in highly saline media in large $pH/E_h$ regions. This 'vulnerability' of copper develops rapidly as $[Cl^-]$ increases and is relevant to the impact of introduction of saline waters into the repository. If the diagram in Figure 7, which is calculated for 25°C, is compared with such for higher temperatures as presented in [47, 56], it can be seen that the immunity limit for copper also descends as a function of temperature at high $Cl^-$ concentrations. This means a possibility that copper could be neither noble (immune) nor passive at elevated temperatures in a repository environment with high concentrations of $Cl^-$. Higher reaction rates related to the increased temperature would also affect corrosion for conditions far from equilibrium.

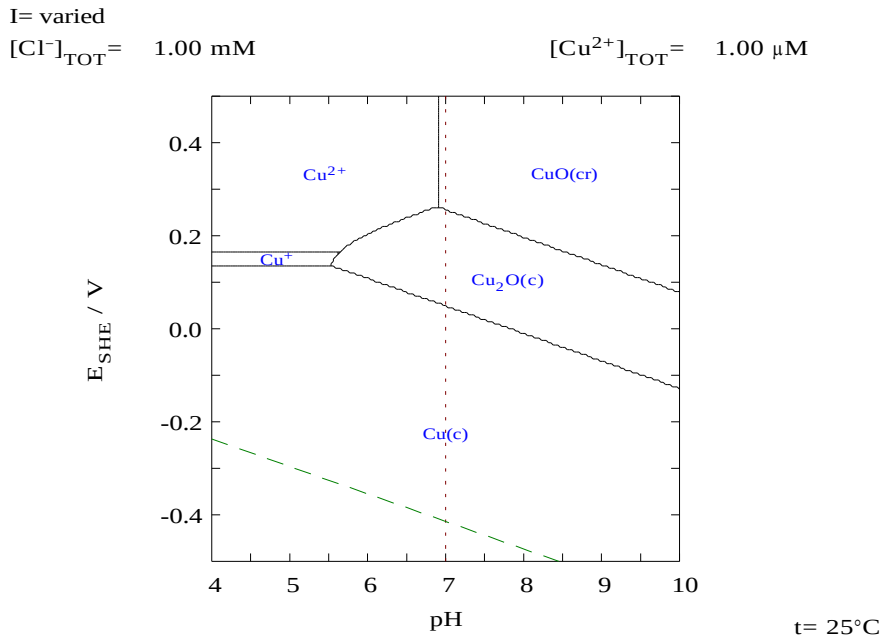


***Figure 7.*** *Pourbaix diagram for the system Cu-Cl-H-O at indicated conditions. This diagram shows the case in which [Cl⁻] is low, i.e. fresh water (1 mM ≈ 35 mg/L) and [$Cu^{2+}$] is much higher (1 µM ≈ 64 µg/L) than its likely range. Note: In this and following diagrams, [$Cu^{2+}$]$_{TOT}$ relates to total copper concentration, including solid phases containing Cu, and not just the dissolved ionic species.*

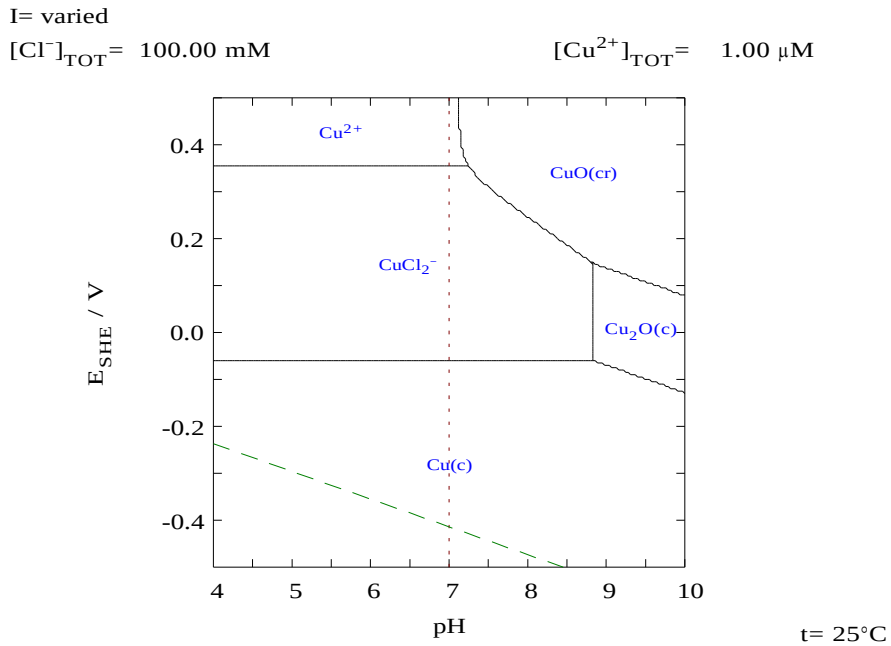


***Figure 8.*** *Pourbaix diagram for the system Cu-Cl-H-O at indicated conditions. This diagram shows the case in which [Cl⁻] is moderate, i.e. brackish water (100 mM ≈ 3500 mg/L) and [$Cu^{2+}$] is much higher (1 µM ≈ 64 µg/L) than its likely range.*

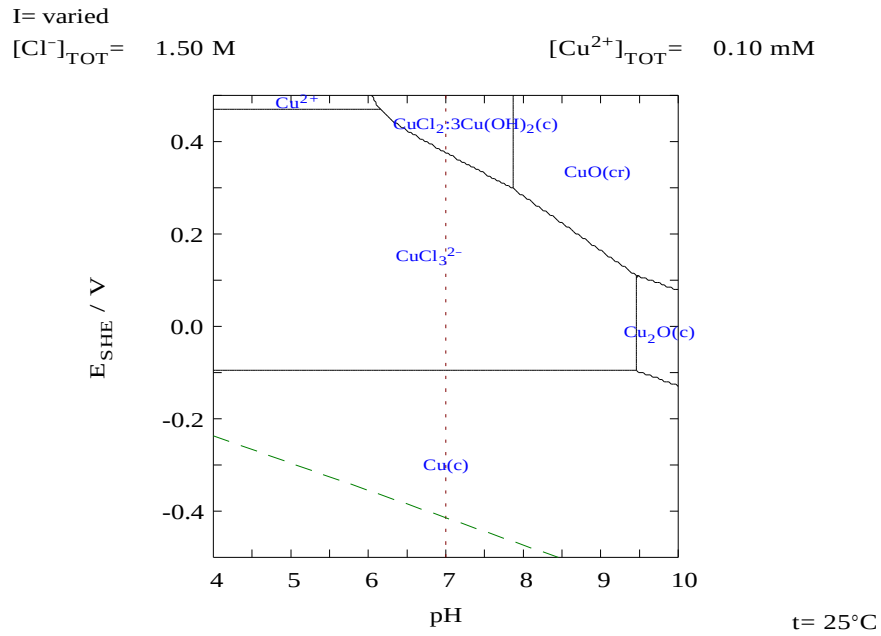


***Figure 9**. Pourbaix diagram for the system Cu-Cl-H-O at indicated conditions. This diagram shows the case in which [$Cl^-$] is high, i.e. very saline water (1.5 M ≈ 53000 mg/L) and [$Cu^{2+}$] is extremely high (0.1 mM ≈ 6.4 mg/L).*

### 7.4.3 The sub-system Cu-S-H-O

The selected set of diagrams shown in Figures 10 and 11 (also Figure E1 in Appendix E) were calculated at indicated conditions in order to be able to find critical concentrations for copper sulphide formation. A comparison of those and other diagrams not given here show that the corrosion behaviour of copper depends strongly on $HS^-$ and $Cl^-$ concentrations and the variation of the pH and $E_h$. The ionic strength itself, caused by generally high salinity, seems to have very little or no influence.

### 7.4.4 The sub-system Cu-Fe-S-H-O

Pourbaix diagrams for part of the system Cu-Fe-S-H-O were calculated and accounted in [56]. In certain types of environment $HS^-$ and also iron would have an influence on copper stability. $HS^-$ is important at low potentials. Iron is important for example if there would be a break through of the copper. Iron is also present “normally” in the repository environment.

Depending on conditions, two bi-metallic oxides can be found in the chemical system Cu-Fe-S-H-O beside the metals and simple oxides. The bi-metallic oxides are delafossite, $CuFeO_2$ and cuprospinel, $CuFe_2O_4$. However present evidence suggests that these phases only form at high temperatures, so they are probably not relevant to long-term evolution and corrosion in the EBS of a repository. There is also a bimetallic sulphide, $CuFeS_2$. Examples of Pourbaix diagrams for this sub-system are displayed in Figures 12a and 12b, showing copper containing species and iron containing species respectively.

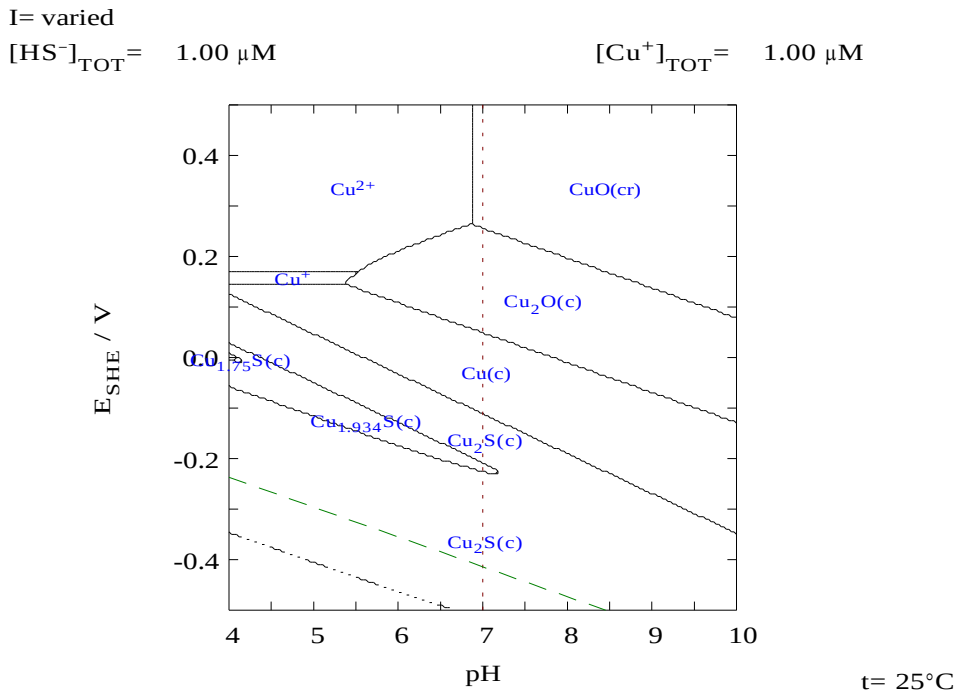


***Figure 10.*** *Pourbaix diagram for the system Cu-S-H-O at indicated conditions. This diagram shows the case in which [HS⁻] is lower (1 µM ≈ 35 µg/L) than typical values and [Cu²⁺] is much higher (1 µM ≈ 64 µg/L) than its likely range.*

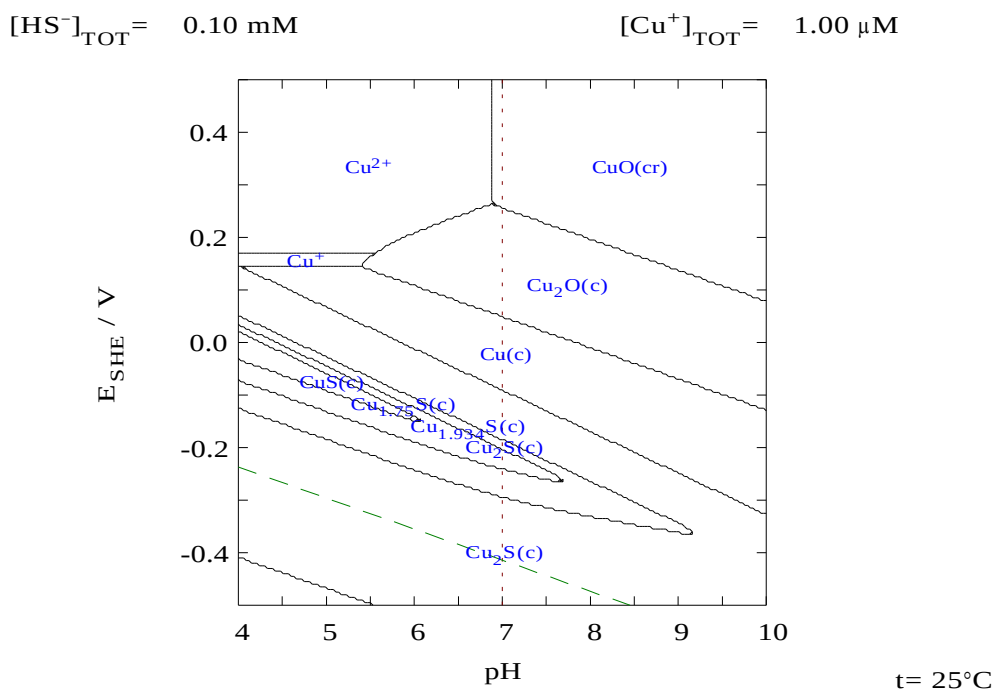


***Figure 11.*** *Pourbaix diagram for the system Cu-S-H-O at indicated conditions. This diagram shows the case in which [HS⁻] is at the high end (0.1 mM ≈ 3.5 mg/L) of the typical range and [Cu²⁺] is much higher (1 µM ≈ 64 µg/L) than its likely range.*

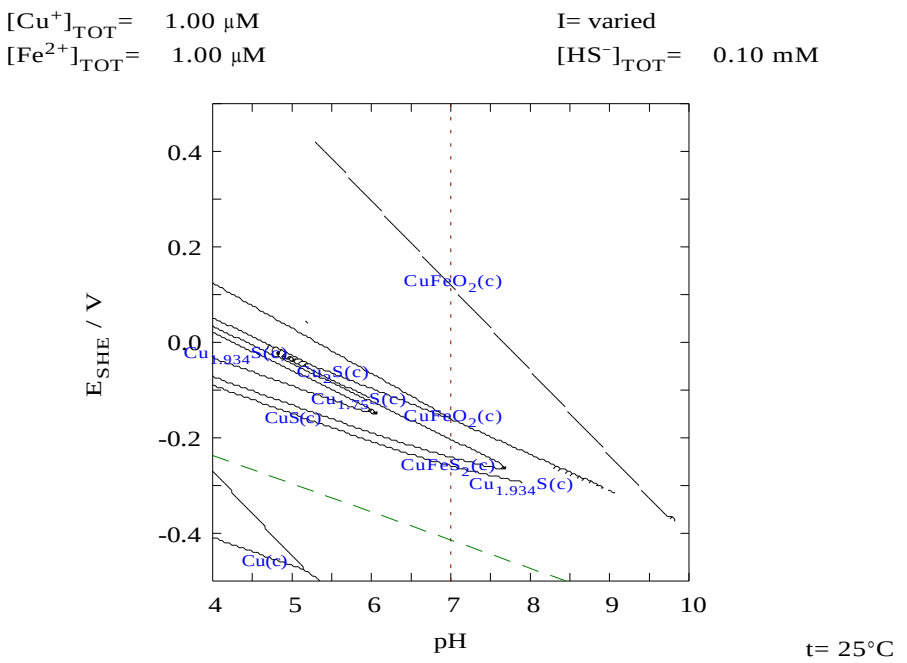


***Figure 12a.*** *Pourbaix diagram for the system Cu-Fe-S-H-O at indicated conditions. Copper containing species are shown. This diagram shows the case in which [HS⁻] is lower (35 µg/L) than typical values, [$Fe^{2+}$] is at the lower end (0.056 mg/L) of its range and [$Cu^{2+}$] is much higher (64 µg/L) than its likely range.*

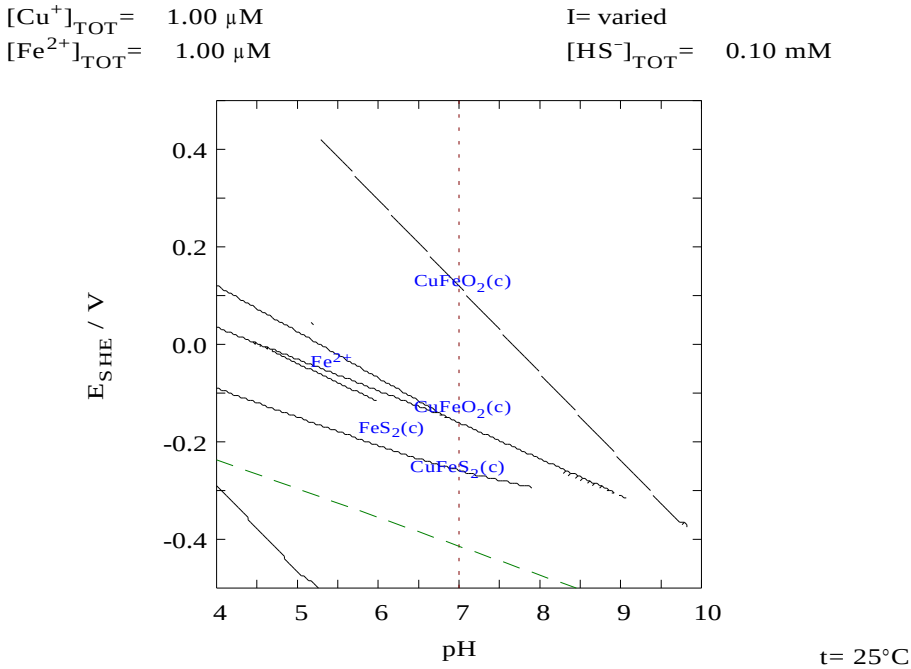


***Figure 12b.*** *Pourbaix diagram for the system Cu-Fe-S-H-O at indicated conditions. Iron containing species are shown. This diagram shows the case in which [HS⁻] is lower (35 µg/L) than typical values, [$Fe^{2+}$] is at the lower end (0.056 mg/L) of its range and [$Cu^{2+}$] is much higher (64 µg/L) than its likely range.*

It can be seen that $CuFeS_2$ and $Cu_2S$ both appear in the $pH/E_h$ area of interest with respect to repository conditions.

### 7.4.5 The sub-system Cu-Fe-S-Cl-H-O

An example of a Pourbaix diagram calculated for the system Cu-Fe-S-Cl-O-H at 25 °C and $[Cl]_{tot}$=1.5 is shown in Figure E2 in Appendix E.

One important feature that can be observed in Figure E2 is that the immunity limit of copper is further lowered in the S+Cl system compared with systems not containing sulphur. This could have consequences for copper corrosion in a reducing environment if a sulphide film had any significant passivating effect, but this is considered not to be the case.

### 7.4.6 The sub-system Cu-Cl-C-H-O

The system Cu-Cl-C-H-O is shown in Figure E3 for $Cl^-$ and $HCO_3^-$ concentrations at which copper species containing those components start to appear. It is found that the first chloride complex to appear is $CuCl_2^-$ at a $Cl^-$ concentration slightly above 1 mM. The first carbonate complex is $CuCO_3^0$, appearing at a total $HCO_3^-$ concentration of 0.5 mM.

The same system is also shown in Figure E4 at the solute concentrations chosen for the system model as shown in Table 3. It can be seen that at those concentrations of $Cl^-$ (2 mM) and $HCO_3^-$ (6 mM), $CuCl_2^-$ is still the predominating copper-chloride species. Among copper carbonates, malachite ($Cu_2CO_3(OH)_2$) appears beside the simple copper carbonate $CuCO_3$.

### 7.4.7 The sub-system Cu-Cl-S-C-H-O

In Figure E5 a diagram for the subsystem Cu-Cl-S-C-H-O is accounted for 25°C. It can be seen that sulphides and oxides predominate at low redox potentials, $Cl^-$ at intermediate and carbonates at high potentials. $HS^-$ decreases the immunity area of copper with only slight dependence on the total $HS^-$ concentration within the calculated range. An increased chloride concentration has little effect on the sulphide predominance.

### 7.4.8 The sub-system Cu-Fe-Cl-S-C-H-O

In Figure E6 a diagram for the system of Cu-Fe-Cl-S-C-H-O is accounted for 25°C at the conditions given in Table 3. In Figure E7 the same system is shown at a very high total $Cl^-$ concentration of 5 M, i.e. brine. Only copper-containing species are shown in the diagrams. These are the most generalised diagrams for the repository system when iron is also present. However, to calculate the diagrams it has been necessary to reduce the number of species participating in the calculation. The selection of species to be included in calculations depends on specific aims; the aim here has been to exclude species with a low probability of appearing within the 'envelope' of environmental conditions of the repository.

Figure E6, in the central parts of the diagram, demonstrates that copper sulphides dominate at low $Cl^-$ concentrations. There are also indications in the

diagram that the calculation program cannot properly select the predominating species at every point. The information should therefore be used with caution.

Figure E7 shows that copper sulphides still dominate in central parts of the diagram at high $Cl^-$ concentrations, but only at low potentials. At intermediate potentials $CuFeO_2$ predominates. The program had difficulties to converge in this calculation and the information should be used with the same caution as for that in Figure E6.

### 7.4.9 The sub-system Cu-Fe-N-S-H-O

In Figure E8 a diagram for the subsystem Cu-N-H-O is accounted for 25°C. At these concentrations ($[NH_3]$ = 2 mM) the complex $Cu(NH_3)_2^+$ starts to form and thus increases the solubility of copper dramatically. In Figure E9 a diagram for the subsystem Cu-N-S-H-O is accounted for 25°C. At the selected total concentrations (note that $[Cu^{2+}]_{TOT}$ relates to total copper concentration, including solid phase Cu, and not just the dissolved ionic species), the copper behaviour is similar as in the simple systems Cu-N-H-O (Figure E8) and Cu-S-H-O (Figure 10), respectively. It suggests that which of S or N will dominate copper behaviour is dependent on the $E_h$ value. Thus there seems to be no synergistic effects of the simultaneous presence of N and S in the system as they are active on copper at different $E_h$ values. S dominates the behaviour at low $E_h$ and N at high $E_h$ at pH values about 9 for indicated conditions. In Figure E10 a diagram for the entire subsystem Cu-Fe-N-S-H-O is accounted.

## 7.5 Changing corrodant conditions and influences on EBS corrosion

### 7.5.1 Summary of the main parameters that could change

The main parameters influencing the thermodynamics of copper (and iron) corrosion are temperature, pH, $E_h$, and concentrations of corrodants. Beyond thermodynamics, corrosion rates may also be effectively limited by the rates at which corrodants are transported in solution towards the copper surface and by the rates at which corrosion products are transported away from the surface.

The temperature in the repository will roughly vary with time and will after some time adopt the surrounding rock temperature, about 15°C. All calculations in this section of the report have been performed at 25°C as input data are normally given at that temperature. The difference between 25°C and 15°C is judged to be negligible.

Concerning chemical parameters, the envelope of pH/$E_h$ defined from Figure 5 can be written as the intervals $6.8<pH<8.7$ (main: $7.3<pH<8.4$) and $-300mV<E_h<-150mV$. This work will treat broader intervals: $7<pH<10$ and especially in $E_h$: $-0.5V<E_h<0.5V$.

Concentrations of $HS^-$, $Cl^-$, N species, DO, DIC (dissolved inorganic carbon) are considered to influence corrosion behaviour of copper in the EBS. Catalytic effects of microbes are also of importance, especially concerning $HS^-$ (see Section 5.2). The work therefore focuses on chemical equilibria in selected subparts of the chemical system Cu-Fe-Cl-N-S-C-H-O.

The $[HS^-]$ range in present groundwaters is mostly within $10^{-7}$ to $3x10^{-6}$ M and is controlled by FeS equilibrium (see Section 6.3.2). The higher end of this range has been selected as 'typical' for these calculations. $[HS^-]$ concentrations lower than $10^{-7}$ M could conceivably occur if more oxidising groundwaters penetrated to repository depth, for example due to inflow of oxygenated sub-glacial meltwater. $[HS^-]$ concentrations higher than $3x10^{-6}$ M might occur in near-field groundwaters in certain conditions where SRB promoted rapid reduction of $SO_4^{2-}$ and the availability of $Fe^{2+}$ were inadequate to maintain buffering of $HS^-$ by FeS equilibrium (as discussed in Section 6.3.2).

The ambient concentrations of dissolved $Cl^-$ in present groundwaters at repository depth range from fresh water, i.e. close to 0 M, to around 1.5 M, ~ 50000 mg/L.

The most important nitrogen containing species influencing copper is $NH_3$. According to Figure E8 there is likely to be an influence only at high redox potential and a total concentration of $>2x10^{-4}$ M to see an influence. $[NH_4^+]$ in present-day groundwaters varies from 0.01 to 3 mg/L, i.e. $5x10^{-7}$ to $2x10^{-4}$ M. Higher $NH_3$ concentrations could conceivably derive from anthropogenic substances that could be introduced during construction and operation of a repository, i.e. affecting near-field chemistry during operation and the initial post-closure stage.

DIC is mainly $HCO_3^-$ and much smaller concentrations of $CO_3^{2-}$ anions, which start to influence copper corrosion at a total concentration of >0.5 mM and at higher potentials at neutral pH, see Figure E3. $[HCO_3^-]$ in present groundwaters at repository depth varies from 5 to 400 mg/L, i.e. $8x10^{-5}$ to $6x10^{-3}$ M, and is generally inversely correlated with salinity so that the more saline groundwaters have the lower $[HCO_3^-]$.

### 7.5.2 Sulphide and SRB

$[HS^-]$ in present-day groundwaters at repository depth is mostly between $10^{-7}$ and $3x10^{-6}$ M and is controlled by FeS equilibrium (Section 6.3.2). $FeS_2$ present in the bentonite is expected to control total reduced sulphur concentrations at $\leq 10^{-5}$ M [29]. Already in this range there could be sulphide phases on copper, see Figures 10 and D3.

If for any reason conditions in the buffer allow microorganisms to be viable at the buffer-canister interface, SRB could transform $SO_4^{2-}$ into $HS^-$ adding to the amount of $HS^-$ available for copper sulphide formation. If all $SO_4^{2-}$ indicated in Table 3 were converted by SRB to $HS^-$, the latter concentration would increase to the range $5x10^{-5}$ to $5x10^{-3}$ M. This would increase the stability areas of both $FeS_2$ and of copper sulphides with respect to pH and $E_h$. The probability of sulphide formation would thus increase in a broader

range of pH/$E_h$. At high [$HS^-$] concentrations and low $E_h$, copper can react with $H_2$ evolution to form copper sulphide. See for example Figure 10.

$$2Cu(s)+2H_2O+S^{2-} \rightarrow H_2+Cu_2S+2OH^-$$

A systematic summary of the above can be made by reference to the Pourbaix diagrams already accounted above. Starting from the 'typical' chemical environment as defined above, the following evolution will be possible:

- Lowering $E_h$ further would cause evolution of $H_2$. This would, however, be the stopping point for any further $E_h$ drop in a undisturbed repository long after time of closure.

- If [reduced S]$_{tot}$ decreases $<10^{-6}$ M, copper sulphides would disappear in favour of metallic copper stability. See Figures 10 and E1. As a result, corrosion influenced by $HS^-$ would tend to decrease. This would perhaps also be the case in a closed and undisturbed repository with a gradient of decreasing $HS^-$ concentrations towards the canisters.

- Increasing $E_h$ at [reduced S]$_{tot}$ = $10^{-6}$ M will also cause copper sulphides to be replaced first by metallic copper at about $E_h$ = -0.1 V and thereafter by $Cu_2O$ at about $E_h$ = +0.1 V. See Figure 11. As a result, corrosion influenced by sulphide would tend to decrease. This would be the case if more oxidising water were to penetrate to repository depth, for example due to penetration of oxygenated sub-glacial meltwater.

- Lowering pH at [reduced S]$_{tot}$ = $10^{-6}$ M would not cause any substantial change. The already existing copper sulphides would stay. See Figure 10.

- Increasing pH at [reduced S]$_{tot}$ = $10^{-6}$ M would cause copper sulphides to disappear at about pH=9 and be replaced by metallic copper. See Figure 10. As a result, corrosion influenced by $HS^-$ would have a tendency to decrease.

- Increasing [reduced S]$_{tot}$ above $10^{-6}$ M, for example due to SRB activity and other conditions discussed above, will further increase the $E_h$/pH region of copper sulphide stability. Compare Figures 10, 11 and E1. As a result, corrosion influenced by $HS^-$ would tend to increase.

It should be noted that the presence of iron could cause the formation of bimetallic sulphides (and possibly also oxides) that would increase the passivation of copper. Instead of immune metallic copper, passivating films of bimetallic sulphide would appear. The overall influence on corrosion behaviour is still uncertain.

### 7.5.3 Chloride

$Cl^-$ has a strong influence on copper behaviour/solubility at higher concentrations, i.e. >0.1 M $Cl^-$, which has been outlined in [45] and can also be seen in the Pourbaix diagrams. Very high $Cl^-$ concentrations could cause a complete loss of passivation ability of copper. The global concentrations of dis-

solved $Cl^-$ in the repository could rise from fresh water, ~0 M, to roughly 1.5 M. The typical value would be about $6x10^{-3}$ M (Table 3), at which $Cl^-$ does not have any influence. See Figure 7.

Increasing $[Cl^-]$ will cause corrosion due to formation of copper-chloride complexes. See Figures 7, 8 and 9. This situation could develop with upconing of high salinity water.

If $HS^-$ is present at $[HS] > 10^{-6}$ M, copper sulphide formation will dominate over $Cl^-$ complex formation when all other parameters are as in Table 3. See Figures E2, E5, E6 and E7.

Beside the direct influence by changing $[Cl^-]$ as discussed above, a simultaneous decrease in pH and increase in $E_h$ would increase the influence by $Cl^-$ on copper corrosion.

### 7.5.4 Nitrogen species

Copper and $NH_3$ form chemical complexes and thus increase the solubility of copper. As seen in the Pourbaix diagrams, the limiting total concentration for $[NH_3]$ influence is about $2x10^{-3}$ M at a total copper concentration of $10^{-6}$ M. See Figure E8. pH has to exceed 8 and $E_h$ exceed about 0 V to get an influence.

If $HS^-$ is present at concentrations previously discussed, $HS^-$ and $NH_3$ will influence corrosion at different combinations of $E_h$/pH. There will thus be no synergism between the two in attacking the copper.

Increasing $[NH_3]$ over $2x10^{-3}$ M will increase the stability of $NH_4^+$ complexes and thus also increase ammonia-influenced corrosion. Copper sulphide formation is likely to dominate aver ammonia-copper species formation in most conditions.

### 7.5.5 Carbonate (DIC)

Carbonates and hydroxycarbonates can be formed on copper at higher $E_h$ conditions. This has been outlined in [45] and can also be seen partly in Figures E3, E4 and E5. The influence on copper behaviour at present groundwater conditions and within the range of possible changes would be minor. $E_h$ has to be increased above + 0.2 V for an influence to occur at $[DIC]_{tot} < 2x10^{-3}$M. This would be seen only at the time of construction and shortly thereafter.

It should be noted, however, that other carbon containing compounds (mostly organic compounds) could act as complexing agents, increasing the corrosion on copper. The origin for such compounds could for example be as anthropogenic substances introduced during the construction and operation phases.

### 7.5.6 Summary

The main parameters influencing copper (and iron) corrosion are temperature, pH, $E_h$, and concentrations of corrodants.

Changes of concentrations of $HS^-$, $Cl^-$, N species and carbonate (DIC) have been considered in relation to external changes (glaciation, anthropogenic actions, etc) that could give rise to deviations from presently observed groundwater conditions at repository depth. The influences on corrosion behaviour of copper in the EBS have been discussed.

The result is that beside redox potential $E_h$ and pH, $HS^-$ is likely to be the dominant agent influencing copper corrosion behaviour in most if not all likely conditions, with $Cl^-$, $NH_3$ and $HCO_3^-$ having subsidiary effects.

$E_h$ changes as results of residual $O_2$ in the initial phase after closure, penetration of oxidising water for example during a glaciation, or changes in the controlling near-field biogeochemical systems would affect corrosion in two ways: the speciation and stability of corrodants, mainly $HS^-$, and the stability of the corrosion products.

# 8. Natural system studies of native copper

## 8.1 Introduction

The objectives of this specific part of the work are:

- to review literature and other information about the occurrence and geochemical stability/alteration of native copper, particularly with respect to ambient biogeochemical conditions including redox species, salinity and microbial populations;
- to review electrochemical basis of natural analogues of native copper and to evaluate experimental and theoretical evidence for copper stability/instability under natural aqueous conditions, oxic or anaerobic.

## 8.2 Method

The approach used here has involved:

- search for literature describing native copper occurrences and physicochemical conditions for stability/alteration;
- definition of thermodynamic conditions under which native copper is stable;
- evaluation of experimental and theoretical evidence for copper stability/instability under natural aqueous conditions, oxic or anaerobic.

## 8.3 Native copper

### 8.3.1 Occurrences and their formation conditions

This is not intended to be a comprehensive geological/mineralogical description of the formation in nature of native (metallic) copper. Reviews of that already exist and the reader is referred to those for such information [e.g. 57, 58].

There are four main types of copper occurrences in nature: porphyry copper ores, sedimentary copper ores, massive sulphide copper ores and copper/gold ores. Native copper can be found in conjunction with all of those principal ores and it was the first metal to be used by man some 10,000 years ago due to its relatively easy, natural availability and easy handling to produce tools and weapons.

However, deposits of native copper are normally very small in volume. The principal 'bulk' copper-containing mineral is chalcopyrite ($CuFeS_2$) in porphyry-type ores and native copper specimens are today seen more as inter-

esting souvenirs. Among other principal minerals of copper than chalcopyrite there are deposits of copper sulphides as ~$Cu_2S$ (constituting a family of minerals) and copper oxides mainly as cuprite ($Cu_2O$) and tenorite (CuO). Among carbonates, azurite ($Cu_3(CO_3)_2(OH)_2$) and malachite ($Cu_2CO_3(OH)_2$) could be mentioned as examples.

A generalized map of copper mining areas (all types of findings, sometimes including small amounts of native copper) around the world and valid for 2002, can be seen in Figure 13 [58].

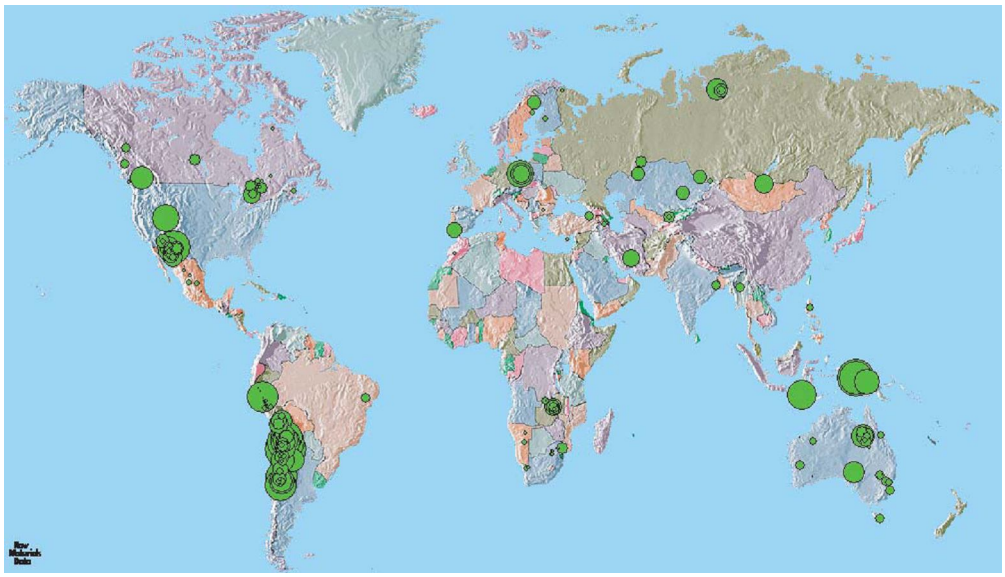

***Figure 13*** *Copper mines in operation 2002 [58].*

In Table 4 some examples of places are accounted where native copper has been or still is found. Native copper has been mined for centuries and is still found in limited quantities in some of the once-active native copper mining regions. However, these finds are today valuable only as mineralogical specimens and natural analogues of copper preservation. There are also some data on formation and preserving environment. The expected, theoretical stability of natural copper at some given chemical conditions is evaluated in the later sections and compared with the conditions in Table 4.

Major copper producing nations include Australia, USA, Canada, Chile, China, Mexico, Russia, Peru, and Indonesia. Of the copper ore mined today in the United States, the majority is produced in three western states: Arizona, Utah, and New Mexico, though up to the 1960s the Keweenaw province in Michigan was a prime producer. Many ore deposits have native copper as one of the copper-containing minerals beside sulphides, oxides and carbonates. The native copper part of the total deposit is, however, as a rule very minor.

***Table 4.*** *A couple of examples of finding-places for native copper*

| Finding-place/ Ref. | Coordinates | Native copper form | Age/type of formation | Geochemical environment |
|---|---|---|---|---|
| Keweenaw [59, 60] | Michigan, USA | Big lumps/plates (up to 10 m). | Precambrian sandstone, conglomerates, ash and basalt, | Reducing hydro-thermal low-sulphur fluids with late supergene alteration |
| Yunnan [61, 62] | Yunnan province, China | | Permian basalts and bituminous sediments | Reducing hydro-thermal fluids |
| Darhand [63] | Iran | Round or ellipsoidal grains (up to 2 cm) | Tertiary basalts overlain by limestones | |
| Littleham Cove/GB/[64, 65, 66] | Devon, SW GB | Small plates (up to 160 mm long and 1-4 mm thick). | Permian clay shale, mud- and sand-stone | Reducing early diagenetic pore waters and later alteration by $Cl^-$ $CO_3^{2-}$ |
| Hyrkkölä [67] | Southwest Finland | Microscopic grains | Pegmatite veins in Precambrian crystalline rock | |

The Keweenaw deposit is an exception from this rule; about 5 million tons of refined copper was recovered from 380 million tons of ore, however most of it is not as native copper. It is famous for large, metre-scale masses of native copper: the largest piece of native copper ever reported was discovered there in 1857. Its estimated mass was over 500 tonnes and the piece was 14 m long, 5.6 m wide and roughly 2.5 m thick. Other large pieces of native copper have been found in the Keweenaw district, one of which was recovered from the bottom in a shallow part of Lake Superior (Figure 14). It occurred in a vein within basalt that was exposed through a veneer of organic-rich lake sediments. In Figures 15 and 16 are shown a couple of souvenir-sized pieces from the Keweenaw district. A lightly polished example is shown in Figure 15 and an un-polished example in Figure 16.

The general theory for the formation of native copper deposits in the Keweenaw-type setting is that it precipitated from chemically-reducing copper-enriched hydrothermal fluids, depleted in sulphur possibly due to outgassing [59, 60].

Similar deposits of native copper, but less massive in nature, have been found in Yunnan province in China [61, 62]. It is thought to have an epigenetic hydrothermal origin, copper having been leached from basalt into the fluids and then deposited when the fluid entered the fissured interface between basalt and overlying bituminous clay-rich sediments. At Darhand in Iran, native copper occurs as small (2 cm) round or ellipsoidal grains in Tertiary-age basalts which have been epigenetically altered by hydrothermal

fluids, and in this case are overlain by limestone [63]. In all these cases, sulphide-poor reducing conditions are believed to be a central factor in native copper formation.

***Figure 14*** *Bob Barron and the 17-ton copper plate he found diving in Lake Superior along Michigan's Keweenaw Peninsula.*

***Figure 15*** *Native copper nugget (6 cm) from Keweenaw Peninsula, Michigan, USA. Souvenir piece, lightly polished to remove surface deposits.*


***Figure 16*** *Native copper nugget (5 cm) from Keweenaw Peninsula, Michigan, USA. Unpolished.*

The Littleham cove occurrences of native copper in southwest Devon (UK) have been specially investigated by SKB as a natural analogue [64, 65, 66]. It is especially important as a natural analogue as native copper sheets (cm-scale) are found in clay shale, mudstone and sandstone of Permian age (Figure 17). The copper sheets are associated with complex uranium-vanadium concretions and they are altered to oxides, arsenides and sulphide with some nickel content (though reinterpretation considers the arsenides and sulphides to be superimposed rather than alteration products [66]). Deposition of the copper and most alteration are interpreted to have taken place at an early stage of sediment diagenesis before compaction. The sedimentary burial environment was reducing, having green reduction spots where pyrite occurs instead of hematite and chlorite instead of smectite. The copper occurs in micro-fractures parallel to sediment bedding and is thought to have precipitated from low-sulphide diagenetic pore fluids that leached copper from the Permian sediments. Late-stage weathering, after erosion and exposure of the sediments to chloride and carbonate in groundwaters, has resulted in some surficial alteration.

***Figure 17*** *A 176 million years old copper (mm scale at the bottom) plate found embedded in clay in Littleham Cove, Devonshire, GB (from a presentation 2007-12-05 by L. Werme, SKB).*

Those examples and the fact that native copper can be found in many more places in nature than those indicated here, show that copper is stable as a metal in a variety of natural conditions.

The Hyrkkölä U-Cu mineralization contains native copper in an open fracture zone in crystalline rocks at about 8.3 m depth [67]. The native copper is associated with uranium mineralization in granite pegmatite veins 0.05 – 0.5 m thick. Unusually, copper sulphides also occur but these are thought to result from alteration by groundwater.

### 8.3.2 Environments of preservation and alteration

The Keweenaw copper, and most if not all of the other more minor native copper deposits are now found to have surface alteration that results in deposits or staining that is coloured green, brown and blue. Alteration of the large copper slab that was recovered from the lake bottom would be interesting with respect to corrosion. It is likely that the vein in which the copper was located would have been exposed to supergene alteration by groundwaters and lake water after glacial erosion of the Palaeozoic cover rocks during Pleistocene glaciation, i.e. within the last 2-10 million years [59, 60]. Products of this alteration are thin coatings of oxide, carbonate and chloride minerals. Supergene alteration has been detected in the host rocks here to about 300 m depth. Lake water that interacted with the large slab is of course fresh and aerobic.

Early diagenetic alteration of native copper in Permian mudstones at Littleham was dominantly to oxides such as cuprite [66]. The subsequent pore water environment during and after burial would have remained reducing until erosion exposed the beds in cliff faces and landslips. Sulphide mineralisation is thought to have occurred at a relatively late stage and is to some extent intergrown with native copper so that it can be said that some degree of sulphide corrosion has occurred at that stage. It is reported that 30-80% of the original thickness of copper sheets (typically 1-2 mm and up to 4 mm thick) has been preserved. Subsequent exposure to oxidising groundwaters seems to have converted some of the sulphide to sulphate and there are also copper oxide and carbonate products. More information about the likely timescales and hydrochemical conditions of oxidative corrosion and prior reductive alteration would help to understand more about the context of 20-70% of original native copper having been judged to have been lost, but it is unlikely that much more firm interpretation is possible because these and other variables are not well constrained.

## 8.4 Conditions for native copper stability

### 8.4.1 Important parameters

The stability of native copper is dependant on the ability of copper to either stay immune or be effectively passivated in the physical and chemical environment. This is influenced by the presence or absence of chemical species that could act as corrodants. The transport of corrodants to and from the copper surface is also likely to be important.

The parameters that would be potentially significant for the stability of native copper in a natural geochemical environment have already been discussed in relation to corrosion of copper canisters in the EBS of a repository. These are T, $E_h$/pH, [reduced S]$_{tot}$, [$Cl^-$], [$NH_3$]$_{tot}$, [$CO_3^{2-}$]$_{tot}$ and combinations of them, which have been discussed in Section 7.5 and also in e.g. [45-51]. There are additional factors governing transport of these reactants, i.e. advection or diffusion of reactants and reaction products to and away from the surface of copper metal, which apply equally to native copper as well as to emplaced copper canisters.

### 8.4.2 Native copper stability

In earlier reports for SKN and SKI on the stability of copper in the KBS-3 disposal concept, evidence from Cu and Cu-Fe sulphide minerals in natural conditions was used to construct conceptual models for how metallic copper might corrode in oxidising and reducing groundwater conditions [57, 68, 69]. The conditions under which native copper has been deposited are also described in these reports, but there is no information relating directly to the nature and extent of alteration of native copper in oxidising and reducing geochemical environments. Potential alteration of copper metal in geochemical environments is inferred only indirectly by interpretation of the relative stabilities of Cu and Cu-Fe minerals. Three types of geochemical alteration environments in ore deposits corresponding to different corrosion situations were discussed:

1. Under oxidizing and low $Cl^-$ conditions, passivating oxide type of layers form on the copper surface.
2. Under oxidizing and high $Cl^-$ conditions, the species formed may all be dissolved.
3. Under reducing conditions, non-passivating sulphide type layers form on the copper surface.

Amcoff [57, 68, 69] concluded that mineral formation and mineral transitions on the surface of copper canisters in the geochemical environment of a repository will be governed by reaction kinetics and transient formation of metastable sulphide phases rather than by thermodynamic stability relations alone. This suggests that the conclusions reached on the basis of thermodynamic calculations in Section 7 of this report are insufficient if not combined with available kinetic information. It was inferred that the dominating kinetic control on copper alteration by $HS^-$ in reducing geochemical conditions would probably be the transport of reactants, i.e. $HS^-$, to the surface of copper canisters, especially when surrounded by bentonite as a diffusing medium. Another kinetic factor determining which sulphide phases might form would be the diffusion of copper ions through the surface layer of existing copper sulphides.

Thus it is not possible to formulate a general model for the stability and alteration of native metallic copper. Some values or limits of important single parameters have been used to calculate the Pourbaix diagram in Figure 18. The meaning of ‘limiting’ in this respect is that an attack on copper by that component can be found at and above the ‘limiting’ concentration. In Figure

19, the Pourbaix diagram for the pure system Cu-H-O is shown for comparison.

If the concentration of a component as shown in Figure 18 is decreased below the 'limiting' value, that type of attack will disappear, but on the other hand it will probably increase if concentrations are increased. Exactly how is not evaluated here but can be partly found elsewhere [e.g. 51]. $HS^-$ starts to attack at low $E_h$ values at virtually all pH (see Section 7.5.2). $Cl^-$ starts at low $E_h$ and low pH, $NH_3$ at intermediate $E_h$ and slightly elevated pH and $HCO_3^-$ and phosphate at neutral pH and elevated $E_h$. It should also be noted that there seems to be no synergistic effects between the corrosive agents. Their corrosive effects could thus within limits be discussed independently of each other.

Native copper should be preserved when copper in its environment is either immune to attack, passivated by a protecting stable oxide or otherwise protected by a very low transportation rate of corrodants or by high temperature (virtually no water present) or at freezing temperatures. Within the water stability area of Figures 18 and 19, copper immunity (copper metal stable) is marked with orange and passive areas (passivating and protecting oxides stable) with orange lines ($Cu_2O$) and black (CuO) respectively.

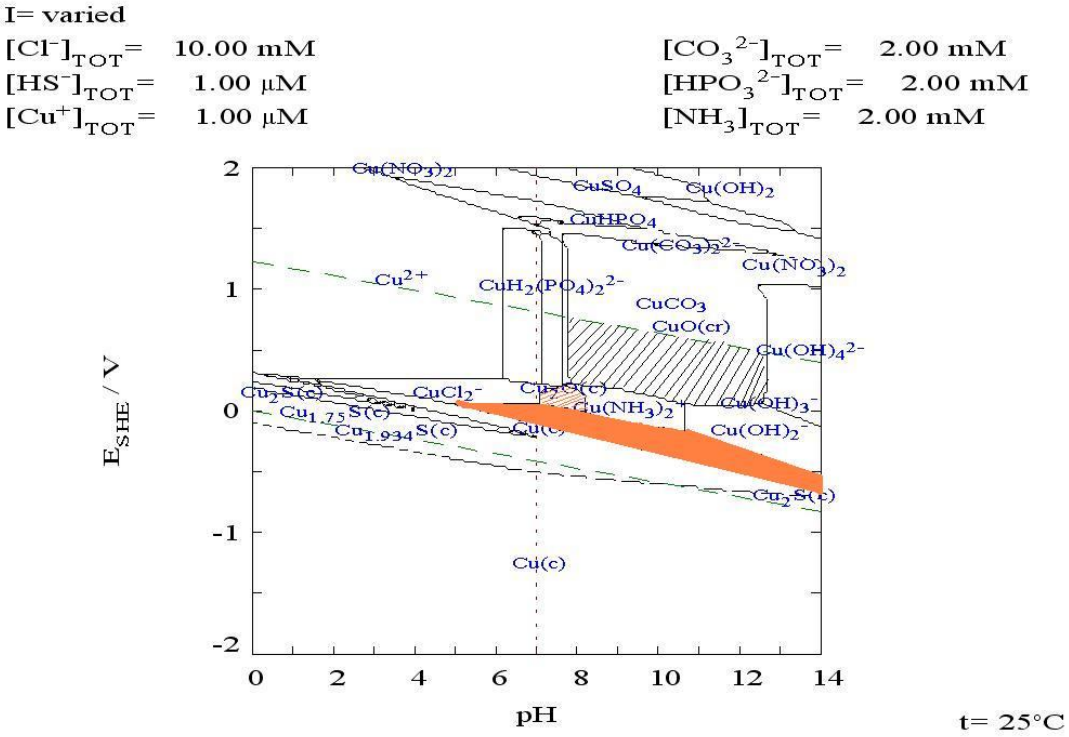


***Figure 18*** *Pourbaix diagram for the system Cu-S-Cl-N-C-P-H-O at indicated (limiting) conditions. Within the water stability area copper immunity (copper metal stable) is marked with orange and passive areas (passivating and protecting oxides stable) with orange lines ($Cu_2O$) and black lines (CuO) respectively.*

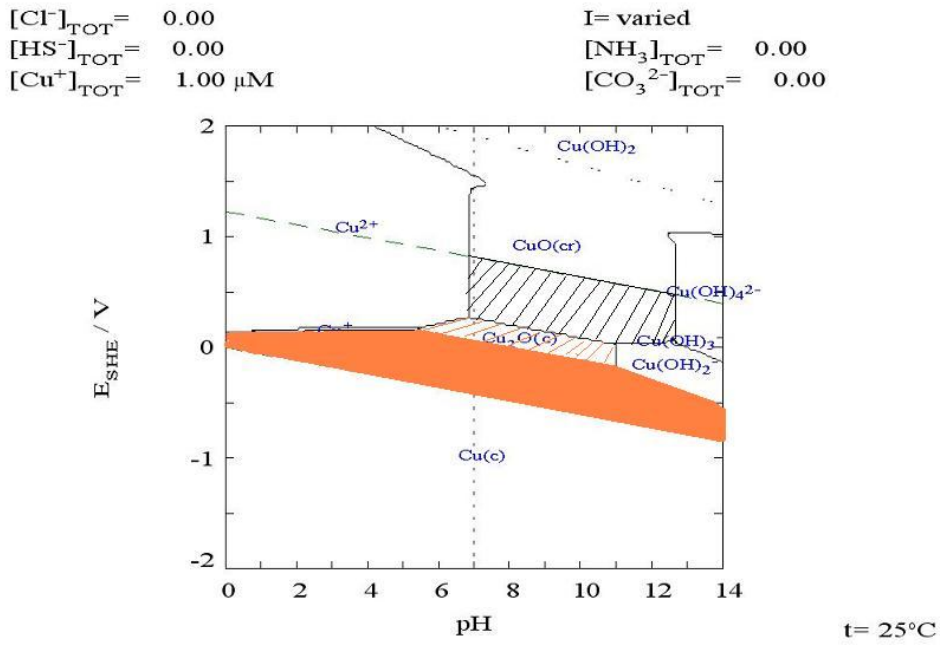


***Figure 19*** *Pourbaix diagram for the system Cu-H-O at indicated conditions. The same marking code is used as in Figure 18.*

It could be summarized from Figures 18 and 19 that in a pollution-free, slightly alkaline environment without $NH_3$, native copper would survive for a long time even if $HS^-$ and $Cl^-$ are present to some extent.

If also iron is present the situation could be summarized as in Figure 20 in which a Pourbaix diagram for the system Cu-Fe-S-Cl-N-C-P-H-O is shown at indicated (limiting) conditions. Due to calculational approximations, there are large uncertainties in this diagram. However, if the information in Figure 20 is compared with that found in Figures 18 and 19, some comments can be made:

- Copper is never immune at conditions in Figure 20.
- $HS^-$ takes away the immunity of copper at low potentials all the way to pH 10 when iron is present. However, the extension of the sulphide area is not as large as in the absence of iron (Figure 18).
- Mixed copper-iron oxides seem to supply an impressively large area of passivity on copper when iron is present. $CuFeO_2$ is the main "passivator" over large areas of $pH/E_h$ within the water stability area, also for extended pH ranges. At high $E_h$ conditions this function is over-taken by $CuFe_2O_4$.
- In presence of iron, the area of total passivity is much larger than supplied by the simple copper oxides (Figure 19).
- As a consequence of the extended areas of passivity that the mixed copper-iron oxides provide, the problematic influences on copper stability

of $Cl^-$, phosphate, $HCO_3^-$ also seems to be much less or virtually abolished. $HS^-$ influences remain but are diminished.

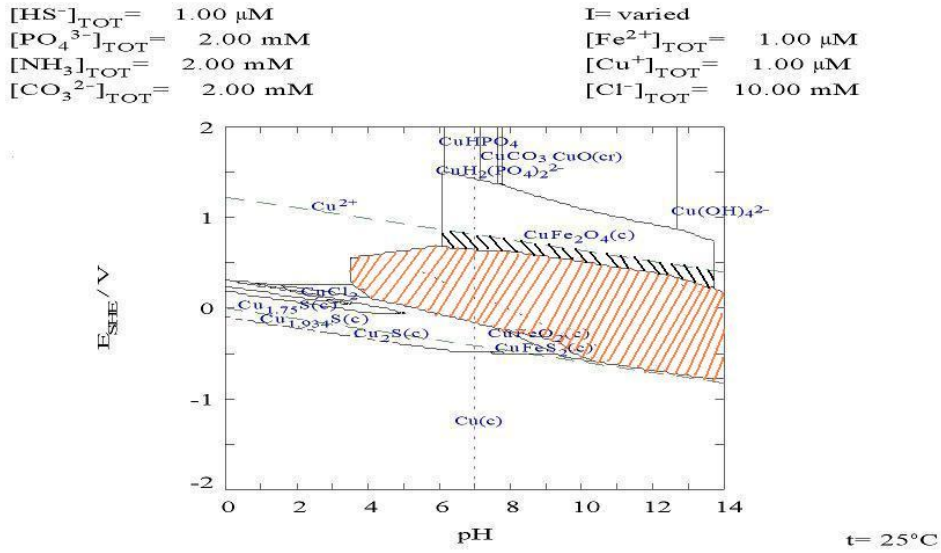


***Figure 20*** *Pourbaix diagram for the system Cu-Fe-S-Cl-N-C-P-H-O at indicated (limiting) conditions. Within the water stability area copper immunity (copper metal stable) is marked with orange and passive areas (passivating and protecting oxides stable) with orange lines ($CuFeO_2$) and black ($CuFe_3O_4$) respectively. Due to calculational approximations the validity of this diagram could be questioned.*

## 8.5 Discussion and conclusions

Many copper ore deposits have native copper in their mineral assemblages along with sulphides, oxides and carbonates. The native copper part of the ore is generally very minor. The Keweenaw occurrence in the US is an exception, in which native copper appears on a large scale from microscopic beads up to chunks weighing over 500 tonnes, being 14 m long, 5 m wide and 2 m thick. In most cases, native copper has been preserved in situ, in its mode of deposit, for long periods of geological time. For example, an occurrence in Permian mudstones in the UK is more than 200 million years old.

As native copper can be found in many different types of places in nature it can be inferred that it is stable as a metal at a variety of natural conditions, where it either stays immune or is effectively passivated or reactions are otherwise inhibited in the physical and chemical environment. Immunity and passivation are strongly influenced by the presence or absence of chemical species that could act as corrodants. Transport of corrodants to and from the copper surface is also important. A slow or hindered transport mechanism would slow down an otherwise active corrosion process.

The parameters T, $E_h$/pH, [reduced S]$_{tot}$, $[Cl^-]$, $[NH_3]_{tot}$ and $[CO_3^{2-}]_{tot}$ and combinations of them as well as corrodant transport factors are all important for the stability of native copper. If iron is also present together with relevant corrodants copper is never immune, but passivated over large areas of pH/$E_h$.

The extended areas of passivity that the mixed copper-iron oxides provide would decrease the negative influences on copper stability of $Cl^-$ and $HCO_3^-$, though there is doubt whether these phases would form at low temperatures due to kinetic factors. $HS^-$ influences remain but are diminished when iron is present. It could thus be summarized that in a transport-limited, slightly alkaline environment unperturbed by external contaminants especially ammonia, with dissolved iron being buffered by iron minerals and typical natural concentrations of $HS^-$ and $Cl^-$, native copper survives for a long time.

# 9. Summary and conclusions

## 9.1 Issues to be considered in review of SR-Site

- SKB have carried out state-of-art biogeochemical characterisation (sampling and analyses) at both sites. Data can be compared with similar data from Olkiluoto. There are also background data and experimentation carried out at Äspö HRL. In general, the interpretations of abundances and distributions of microorganism populations and of correlations between populations and water chemistry are not conclusive because of the densities and variabilities of data. However some compelling interpretative concepts and models about biogeochemistry have resulted from SKB's investigations and these are significant inputs to SR-Site.

- Numbers of microorganisms in deep groundwater samples from Forsmark and Laxemar are low relative to shallow environments. All major types are present (SRB, IRB, MRB, acetogens, methanogens). Distributions are heterogeneous, with a tendency to IRB being dominant at shallow depths and SRB being dominant at repository depth and below.

- In general, SRB are higher in locations with lower $E_h$, i.e. more reducing. Higher SRB also correlate with lower $SO_4^{2-}$ at Forsmark. Correlation of higher SRB with $HS^-$ at Laxemar is inconclusive because data are sparse. There are no clear patterns for acetogens and methanogens except that populations of acetogens are greater than those of methanogens and SRB.

- DOC and $CH_4$ concentrations in water samples are low, mostly <5mg/L and <0.1 mL/L respectively. These potentially are the energy sources for microbial respiration, so low abundances would account for low microbial populations. Acetate is an intermediate product in respiration pathways utilising either DOC or DIC, but there are no data for its concentrations in these groundwaters. $CH_4$ at Forsmark and Laxemar contrasts with much higher concentrations of $CH_4$ at Olkiluoto, >100 mL/L below 500m depth where $SO_4^{2-}$ concentrations are very low. $CH_4$ may be linked with $SO_4^{2-}$ reduction at Olkiluoto where anaerobic $CH_4$ oxidation (AOM) has been suggested. $CH_4$ is probably too low at Forsmark and Laxemar for AOM to be a major cause of $HS^-$ production at present. DOC is probably the dominant energy source for microbial respiration.

- The implication of these interpretations of present-day biogeochemistry is that $SO_4^{2-}$ reduction is dependent on many variables in the microbial and geochemical conditions. Future changes of any of these variables would very probably affect the rate at which $SO_4^{2-}$ is reduced and $HS^-$ is produced in groundwaters at repository depth. The maximum $HS^-$ con-

centration could theoretically equal $SO_4^{2-}$ concentration in inflowing groundwater, but supply of DOC or $CH_4$ would probably be the limiting factor in $SO_4^{2-}$ reduction.

- Maximum $HS^-$ concentration would also be attenuated by precipitation of iron sulphide. Geochemical modelling indicates that FeS solubility is the effective limit in present-day groundwaters at repository depth, resulting in $HS^-$<0.1 mg/L (<$3x10^{-3}$ mM). That control is likely to persist into the future if $Fe^{2+}$ buffering by water-rock reaction with mineral sources of $Fe^{II}$ continue and pH conditions remain stable. With data for reactive $Fe^{II}$ available in the rock surrounding the deposition holes, it would be possible to estimate the amount of $SO_4^{2-}$, supplied by groundwaters and then reduced to $HS^-$, that could exhaust the $Fe^{II}$ supply and therefore increase the possibility that at some time in the future $HS^-$ concentrations might cease to be kept low due to FeS precipitation.

- Whilst $FeS_2$ equilibrium is not indicated for near-field groundwaters, pyrite is an accessory mineral in bentonite and presumably is a significant buffer of redox in the EBS as suggested in SR-Can [29]. If equilibrium with pyrite were to control the concentration of $Fe^{2+}$ at a very low level in the bentonite, then $HS^-$ concentration could in theory rise to a proportionately higher level before being limited by precipitation of FeS (though empirical evidence suggests that production of $HS^-$ in situ would be inhibited because microbes are not viable in highly compacted bentonite). The possibility of such a model, whereby $Fe^{2+}$ would be minimised because of its pyrite source and $HS^-$ would be controlled at a relatively higher concentration by FeS equilibrium, should be considered when modelling pore water chemistry in the EBS.

- A small amount of experimental work in Äspö HRL has confirmed that $SO_4$ reduction to HS does take place in *in situ* conditions at typical repository depth range. It also suggested that biofilms may be effective hosts for promoting SRB activity.

- SKB's mass budget calculation of $SO_4^{2-}$ reduction limited by DOC supply indicates that the concentration of $HS^-$ adjacent to a deposition hole would be 0.06 mg/L. This is inferred to be equivalent to a total of 10 moles of $HS^-$ per deposition hole. The assumptions and reasoning in this scoping calculation should be checked. SKB's calculation of this limit on sulphide corrosion assumes that present-day biogeochemical conditions persist.

- Review of literature on $SO_4^{2-}$ reduction rates in marine sediments, where SRB population and DOC are not such limiting parameters, indicates $SO_4^{2-}$ reduction rates over a wide range of $10^{-3}$ to $10^2$ mM $yr^{-1}$. $SO_4^{2-}$ reduction rate by AOM would be about $10^{-1}$ mM $yr^{-1}$, with very large uncertainty, for an environment with low SRB populations. Overall, reduction rate of $SO_4^{2-}$ is likely to be relatively rapid so that $HS^-$ production will be controlled by microbe populations, DOC/$CH_4$, and $SO_4^{2-}$, as discussed above.

- Geochemical modelling of hydrochemical data for redox-active couples shows that the measured $E_h$ values are most usually closer to the electrochemical potential calculated for the $SO_4^{2-}/HS^-$ couple. The potential for the $Fe(OH)_3/Fe^{2+}$ couple is usually lower, i.e. more negative $E_h$ values. This provides further evidence that $SO_4^{2-}$ reduction is active, presumably because of mediation by SRB. Other lines of interpretation, and the fact that $Fe^{2+}$ is much more abundant in the total system than $SO_4^{2-}$ or $HS^-$ because of the $Fe^{II}$ reservoir in minerals, suggest that long-term stability of reducing conditions is likely to depend on $Fe^{2+}$ redox reactions. It is also possible that $CH_4$, though present only at low abundance, might also influence redox because of its relatively strongly reducing character – that would depend on biogeochemical reactivity with methanotrophic bacteria (i.e. microbes utilising $CH_4$ as energy source).

- Biogeochemical conditions at the deposition holes in the initial period after closure of a repository could be affected by higher temperatures (typically 40-60°C for 1000 years) and higher radiation. These transients will be precursors for the evolution of near-field conditions in the long term. Higher ambient temperatures will shift geochemical equilibria including those involving redox-active species, and will also increase microbiological effects on reaction kinetics. The natural biogeochemical regime in the near field will re-establish itself as the thermal and radiation perturbations diminish. More detailed considerations of these effects are outside the scope of this report. The impacts and potential variant scenarios of these early post-closure conditions should be fully considered by SKB in SR-Site.

- The quantity and reproducibility of SKB's data for the microbial and hydrochemical parameters justify these provisional conclusions, but the variability of microbial data is quite high and the data are sparse, considering the complexity of the system. There are many uncertainties and potential alternatives in the interpretations because of the various aspects of biogeochemical interdependence. There are also data gaps with varying significance, for example in concentrations and variability of DOC, $CH_4$, $H_2$; there are no data for acetate. The uncertainties and alternative models for these biogeochemical conditions and scenarios should be taken fully into account in the near-field and EBS models for SR-Site.

- A consideration in review of SR-Site will be the possibilities for substantial variations of biogeochemical conditions away from those presently observed, and the potential impact of those changes on production of corrodants that could challenge the integrity of the engineered barrier system (EBS) of a repository and ultimately impact long-term safety. Corrodants could, in theory, be produced in the EBS itself or be produced in the near-field geosphere and migrate through the EBS buffer to the canisters. Concerning the latter scenario, the most significant changes would probably be either greater penetration of fresh water recharge carrying greater amounts of DOC and possibly also increasing microbial numbers and activity, or increasing salinity and influx of greater amounts of $SO_4^{2-}$ to the near field. In principle, both possibilities could increase $HS^-$ production outside the EBS which would cause more a greater diffu-

sive flux of $HS^-$ towards the canisters. There is a strong argument that $HS^-$ will, however, be limited by precipitation of FeS so that $HS^-$ concentration is unlikely to exceed 0.1 to 1 mg/L unless the availability of reactive $Fe^{2+}$ buffered by mineral $Fe^{II}$ is exhausted. FeS will gradually transform to $FeS_2$, pyrite, and will accumulate in fractures and matrix pores. SR-Site should consider whether there is any scenario that could remobilise that sulphide as a 'pulse' of $HS^-$; acidic conditions could cause that but are thought not to be a significant possibility.

- The stability of copper metal in terms of $HS^-$ concentration and other ambient hydrochemical parameters can be examined by thermodynamic analysis and displayed in $E_h$-pH space in Pourbaix diagrams. These are indications of chemical equilibria but do not give any indication of reaction kinetics or of other factors, e.g. passivation and/or transport limitations for corrodants and products, that might inhibit equilibrium being achieved or corrosion continuing to occur. Corrosion of copper by $HS^-$, whether general corrosion or localised corrosion, could form rather complex products. Passivation would be variable depending on those products.

- A Pourbaix diagram for the Fe-S-O-H system with typical $HS^-$ and $Fe^{2+}$ concentrations shows $FeS_2$ (pyrite) to be the thermodynamically stable solid phase at equilibrium, rather than crystalline FeS. Geochemical modelling with PHREEQC suggests that the amorphous FeS in that model's thermodynamic database is the more likely equilibrium solid.

- Pourbaix modelling of the Cu-Cl-H-O system shows that there is no passivating layer on copper in highly saline (e.g. 1.5 M $Cl^-$) solutions at $E_h$ more oxidising than about -100 mV. This illustrates the increasing vulnerability of copper as salinity increases. This vulnerability is also increased as temperature increases. The $E_h$-pH space over which copper is immune to corrosion also decreases as the pH decreases, so stability of pH in the EBS is another factor to be considered. $E_h$ of -100 mV is slightly above the $E_h$ range that has been measured in groundwaters at repository depth.

- Pourbaix modelling of the Cu-S-H-O system shows that a range of complex sulphide phases account for copper corrosion at reducing $E_h$ values. Temperature, $Cl^-$ concentrations, and pH are the main variables that affect the immune area for copper metal. Comparable Pourbaix diagrams constructed for more complex chemical systems, e.g. with Fe, $Cl^-$, N and $CO_3^{2-}$ added, illustrate greater complexity in what controls the immune areas and solid equilibria that influence corrosion. It is worth noting that the Cu-N-H-O system with $NH_3$ would affect copper corrosion significantly, but only at relatively high $NH_3$ concentrations, typically 2 mM, which are much greater than observed in present groundwaters at repository depth. Perturbations that could increase $NH_3$ significantly should be considered, but are thought to be unlikely, though it can be noted that the source of the presently observed concentrations of $NH_3$ at mg/L levels, apparently in the brackish Littorina water component, is not fully explained.

- The long-term stability of copper metal in certain geosphere conditions is evidenced by a rather small number of native copper occurrences in ore deposits and in more minor occurrences. With such special and rare phenomena, the possibility should be considered that there might be other environments where native copper could have existed originally but has since been corroded away by the particular groundwater conditions. However the occurrences of native copper represent the preservation (immunity) of metallic copper against corrosion in varying geological and geochemical settings. In most if not all cases, geological conditions have probably protected the copper against external changes of geochemical conditions for much of their geological ages.

- Exposure of native copper to active open-system biogeochemical fluctuations and processes has happened for rather shorter periods of time, but nevertheless substantial periods in terms of analogue interest. In most cases, that exposure period has been initiated by erosion, e.g. glacial erosion in the case of Keweenaw copper in Lake Superior and cliff erosion in the case of Littleham Cove. In most or all native copper occurrences, the copper has surface alteration or corrosion deposits. These are thin coatings of oxides, carbonates and chlorides. Copper sulphide phases also occur in the Littleham Cove occurrences. It is not possible to make any firm conclusions about the relationship of these alteration products to either specific environmental conditions (e.g. groundwater compositions) or timescales.

- Stability fields of copper metal in natural conditions, plus the areas in $E_h$-pH space where passivating oxides are stable, have been examined with Pourbaix diagrams for complex geochemical systems. It is observed in these diagrams that the possibility for formation of mixed copper-iron oxides would increase significantly the area of passivity and thus diminish the $E_h$-pH spaces in which $Cl^-$, phosphate and $HCO_3^-$ would enhance corrosion. However it is thought that these Cu-Fe oxides form only at high temperatures, so are probably not relevant for these scenarios. Previous work by Amcoff and others for SKN and SKI on alteration of copper in natural conditions concluded that reaction kinetics and transient metastable copper sulphide phases, in addition to thermodynamic relationships, will govern corrosion of copper canisters under KBS-3 conditions.

- In conclusion, this report has found that SKB's data and models for biogeochemistry of redox at repository depth provide a reasonably coherent understanding of how concentrations of corrodant solutes would be controlled in the near field, assuming that the present natural biogeochemical conditions persist. Data for *in situ* conditions are rather sparse and are judged to be only just adequate to underpin the interpretations. There are data gaps or large uncertainties in some of the more 'difficult' biogeochemical parameters, e.g. acetate and $H_2$. Relationships and spatial variabilities of parameters are not clear cut, therefore interpretations are tentative. The central theme of the biogeochemical model is that microbial mediation causes redox reactions to achieve equilibrium much faster

than they would otherwise. Therefore the system will be reactive to external changes, e.g. increase of $CH_4$ concentrations, and also will be internally buffered by water-rock reactions, e.g. reactions with mineral sources of $Fe^{II}$. The models provide a basis for prognosis of the biogeochemical effects in scenarios for evolution of the system at repository depth. SKB's long-term safety case in SR-Site should be evaluated in terms of its robustness to those scenarios on the basis of redox equilibria, outside the EBS and probably also inside the EBS, being reached relatively quickly and also on the basis of fluxes and mass budgets of chemical and microbial species.

# 10. References


[1] Bath, A. and Hermansson, H-P. (2007) Variability and Uncertainties of Key Hydrochemical Parameters for SKB Sites. SKI Report 2007:03

[2] INSITE/OVERSITE (2008) International expert review of SR-Can: Site investigation aspects. External review contribution in support of SKI's and SSI's review of SR-Can. SKI Report 2008:09, SSI Report 2008:11.

[3] Bath, A. and Hermansson, H-P. (2008) Impacts of future glaciations on geochemical conditions at repository depth: Review of SKB's approach. Chapter 8 in 'Review of SKB's Safety Assessment SR-Can: Contributions in Support of SKI's and SSI's Review by External Consultants', SKI Report 2008:16, SSI Report 2008:06.

[4] Glynn, P. (2008) Future intrusion of oxygenated glacial meltwaters into the Fennoscandian shield: a possibility to consider in performance assessments for nuclear-waste disposal sites? Chapter 6 in 'Review of SKB's Safety Assessment SR-Can: Contributions in Support of SKI's and SSI's Review by External Consultants', SKI Report 2008:16, SSI Report 2008:06

[5] Haveman, S.V. and Pedersen, K. (2002a) Distribution of culturable microorganisms in Fennoscandian Shield groundwater. FEMS Microbiology Ecology, 39, 2, 129-137.

[6] Haveman, S.A., Pedersen, K. and Ruotsalainen, P. (1999) Distribution and metabolic diversity of microorganisms in deep igneous rock aquifers of Finland. Geomicrobiology Journal, 16, 4, 277-294.

[7] Pedersen, K. (2000) Microbial processes in radioactive waste disposal. SKB Report TR-00-04.

[8] Hallbeck, L. and Pedersen, K. (2008) Characterization of microbial processes in deep aquifers of the Fennoscandian Shield. Applied Geochemistry, 23.7, 1796-1819.

[9] Puigdomenech, I., Ambrosi, J-P., Eisenlohr, L., Lartigue, J-E., Banwart, S.A., Bateman, K., Milodowski, A.E., West, J.M., Griffault, L., Gustafsson, E., Hama, K., Yoshida, H., Kotelnikova, S., Pedersen, K., Michaud, V., Trotignon, L., Rivas Perez, J. and Tullborg, E-L. (2000) $O_2$ depletion in granitic media. The REX project. SKB Report TR-01-05.

[10] Banwart, S., Tullborg, E-L., Pedersen, K., Gustafsson, E., Laaksoharju, M., Nilsson, A-C., Wallin, B. and Wikberg, P. (1996) Organic carbon oxidation induced by large-scale shallow water intrusion into a

vertical fracture zone at the Äspö Hard Rock Laboratory (Sweden). J. Contaminant Hydrology, 21, 1-4, 115-125.

[11] Kotelnikova, S. and Pedersen, K. (1999) The Microbe-REX project. Microbial $O_2$ consumption in the Äspö tunnel. SKB Report TR-99-17.

[12] Samper, J., Molinero, J., Yang, C. and Zhang, G. (2003) Redox Zone II. Coupled modelling of groundwater flow, solute transport, chemical reactions and microbial processes in the Äspö island. SKB Report TR-03-16.

[13] Pedersen, K. and Ekendahl, S. (1992) Assimilation of $CO_2$ and introduced organic compounds by bacterial communities in groundwater from southeastern Sweden deep crystalline bedrock. Microb. Ecol., 23, 1-14.

[14] Grandia, F., Domènech, C., Arcos, D. and Duro, L. (2006) Assessment of the oxygen consumption in the backfill. Geochemical modelling in a saturated backfill. Report R-06-106, Swedish Nuclear Fuel and Waste Management Company (SKB), Stockholm.

[15] Auqué, L. F., Gimeno, M. J., Gómez, J. B., Puigdomenech, I., Smellie, J., Tullborg, E-L. and Wallin, B. (2006) Modelling of groundwater chemistry over a glacial cycle. Background data for SR-Can. SKB Report TR-06-31.

[16] Bruno, J., Arcos, D. and Duro, L. (1999) Processes and features affecting the near field hydrochemistry. Groundwater-bentonite interaction. SKB Report TR 99-29.

[17] Guimerà, J., Duro, L., Jordana, S. and Bruno, J. (1999) Effects of ice melting and redox front migration in fractured rocks of low permeability. SKB Report TR-99-19.

[18] Guimerà, J., Duro, L. and Delos, A. (2006) Changes in groundwater composition as a consequence of deglaciation. Implications for performance assessment. SKB Report R-06-105.

[19] Hallbeck, L., Vegrandis, V., Grivé, M., Gaona, X., Duro, L. and Bruno, J. (2006) Main organic materials in a repository for high level radioactive waste. SKB Report R-06-104.

[20] Hunter, K.S., Wang, Y. and van Cappellen, P. (1998) Kinetic modeling of microbially-driven redox chemistry of subsurface environments: coupling of transport, microbial metabolism and geochemistry. Journal of Hydrology, 209, 1-4, 53-80.

[21] van Cappellen, P. and Wang, Y. (1996) Cycling of iron and manganese in surface sediments: a general theory for the coupled transport and reaction of carbon, oxygen, nitrogen, sulfur, iron, and manganese. American Journal of Science, 296, 197-243.

[22] Moosa, S., Nemati, M. and Harrison, S.T.L. (2002) A kinetic study on anaerobic reduction of sulphate, Part 1: Effect of sulphate concentration. Chemical Engineering Science, 57, 14, 2773-2780.

[23] Lovley, D.R. and Klug, M.J. (1983) Sulfate reducers can outcompete methanogens at freshwater sulfate concentrations. Applied and Environmental Microbiology, 45, 1, 187-192.

[24] Lovley, D.R., Dwyer, D.F. and Klug, M.J. (1982) Kinetic analysis of competition between sulfate reducers and methanogens for hydrogen in sediments. Applied and Environmental Microbiology, 43, 6, 1373-1379.

[25] Boetius, A., Ravensclag, K., Schubert, C.J., Rickert, D., Widdel, F., Gieseke, A., Amann, R., Jørgensen, B.B., Witte, U. and Pfannkuche, O. (2000) A marine microbial consortium apparently mediating anaerobic oxidation of methane. Nature, 407, 623-626.

[26] Nauhaus, K., Boetius, A., Krüger, M. and Widdel, F. (2002) *In vitro* demonstration of anaerobic oxidation of methane coupled to sulphate reduction in sediment from a marine gas hydrate area. Environmental microbiology, 4, 5, 296-305.

[27] Hallam, S.J., Putnam, N., Preston, C.M., Detter, J.C., Rokhsar, D., Richardson, P.M. and DeLong, E.F. (2004) Reverse methanogenesis: testing the hypothesis with environmental genomics. Science, 305, 5689, 1457-1462.

[28] Liu, J. (2006) Coupled transport/reaction modelling of copper canister corrosion aided by microbial processes. SKI Report 2006:07, Swedish Nuclear Safety Inspectorate (SKI), Stockholm

[29] SKB (2006) Long-term safety for KBS-3 repositories at Forsmark and Laxemar – a first evaluation. Main Report of the SR-Can project. SKB Report TR-06-09.

[30] Arcos, D., Grandia, F. and Domènech, C. (2006) Geochemical evolution of the near field of a KBS-3 repository. SKB Technical Report TR-06-16.

[31] SKB (2006) Buffer and backfill process report for the safety assessment SR-Can. SKB Technical Report TR-06-18.

[32] Savage, D., Bennett, D., Apted, M., Sällfors, G., Saario, T. and Segle, P. (2008) International Expert Review of SR-Can: Engineered Barrier Issues. External review contribution in support of SKI's and SSI's review of SR-Can. SKI Report 2008:10.

[33] Parkhurst, D.L. and Appelo, C.A.J. (1999) User's guide to PHREEQC (Version 2). A computer program for speciation, batch-reaction, one-

dimensional transport, and inverse geochemical calculations, U.S. Geological Survey Water-Resources Investigations Report 99-4259 (1999).

[34] Grenthe, I., Stumm, W., Laaksoharju, M., Nilsson, A.-C. and Wikberg, P. (1992) Redox potentials and redox reactions in deep groundwater systems. Chemical Geology, 98, 131-150.

[35] Hallbeck, L. and Pedersen, K. (2008) Explorative analysis of microbes, colloids and gases. SDM-Site Forsmark. Report R-08-85, Swedish Nuclear Fuel and Waste Management Company (SKB), Stockholm.

[36] Pedersen, K., Motamedi, M. and Karnland, O. (1995) Survival of bacteria in nuclear waste buffer materials. The influence of nutrients, temperature and water activity. Technical Report 95-27, Swedish Nuclear Fuel and Waste Management Company (SKB), Stockholm.

[37] Motamedi, M., Karland, O. and Pedersen, K. (1996) Survival of sulfate reducing bacteria at different water activities in compacted bentonite. FEMS Microbiology Letters, 141.1, 83-87.

[38] Pedersen, K., Motamedi, M., Karnland, O. and Sandén, T. (2000a) Cultivability of microorganisms introduced into a compacted bentonite clay buffer under high-level radioactive waste repository conditions. Engineering Geology, 58, 2, 149-161.

[39] Pedersen, K., Motamedi, M., Karnland, O. and Sandén, T. (2000b) Mixing and sulphate-reducing activity of bacteria in swelling, compacted bentonite clay under high-level radioactive waste repository conditions. Journal of Applied Microbiology, 89, 6, 1038-1047.

[40] Pedersen, K. (1999) Subterranean microorganisms and radioactive waste disposal in Sweden. Engineering Geology, 52, 3-4, 163-176.

[41] Arcos, D., Grandia, F. and Domènech, C. (2006) Geochemical evolution of the near field of a KBS-3 repository. SKB Technical Report TR-06-16.

[42] SKB (2006) Buffer and backfill process report for the safety assessment SR-Can. SKB Technical Report TR-06-18.

[43] Liu, J. and Neretnieks, I. (2004) Coupled transport/reaction modelling of copper canister corrosion aided by microbial processes. Radiochimica Acta, 92, 9-11, 849-854.

[44] Sidborn, M. and Neretnieks, I. (2006) Corrosion of copper canisters through microbially mediated sulphate reduction. Sci. Basis for Nuclear Waste Management XXIX (Ed. P van Iseghem), Mat. Res. Soc. Symp., Sept. 2005, Volume 932, Paper 109. Materials Research Society.

[45] Hermansson H-P and Eriksson S. (1999) Corrosion of the copper canister in the repository environment. SKI-R-99:52.

[46] Hermansson H-P and Gillén P. (2004) Whiskers and Localized Corrosion on Copper in Repository Environment, SKI-R-04:56.

[47] Beverskog B and Puigdomenech I. (1995) SITE-94. Revised Pourbaix diagrams for copper at 5-150 C. SKI-R-95:73.

[48] Hermansson H-P. (1997) Theoretical evaluation of the stability of steam generator sludge containing copper and magnetite. STUDSVIK/M-97/6.

[49] Eriksson S and Hermansson H-P. (1997) Pitting Corrosion of Copper in Nuclear Waste Disposal Environments. SKI-R-98:02.

[50] Hermansson H-P. (1995) SITE-94. Some Properties of Copper and Selected Heavy Metal Sulfides. A limited Literature Review. SKI-R-95:29.

[51] Engman U and Hermansson H-P. (1994) SITE-94. Korrosion av kopparmaterial för inkapsling av radioaktivt avfall – En litteraturstudie. SKI-R-94:06.

[52] Puigdomenech, I., MEDUSA program for creating speciation and predominance diagrams; HYDRA thermodynamic database of logK data. Royal Institute of Technology, Stockholm. http://web.telia.com/~u15651596/

[53] Szakálos P, Hultquist G and Wikmark G. (2007) Corrosion of Copper by Water. Electrochemical and Solid-State Letters, 10-11, C63-C67.

[54] King , F. et.al. (2001) Copper corrosion under expected conditions in a deep geological repository. SKB Report TR-01-23.

[55] SKB FUD-PROGRAM 92 (1992) Kärnavfallets behandling och slutförvaring. SKB, Stockholm, September.

[56] SKI SITE-94. (1997) Deep Repository Performance Assessment Project. Summary. SKI, Stockholm (Sweden).

[57] Amcoff, Ö. (1998) Mineral Formation on Metallic Copper in a 'Future Repository Site Environment': Textural Considerations Based on Natural Analogs. SKI Report 98:7, SKI Stockholm.

[58] SGU Mineralmarknaden (2002) PerPub 2003:5

[59] Bornhorst, T.J. (2002) Precambrian supergene alteration of native copper deposits in the Keweenaw Peninsula, Michigan. Abstracts, Paper No 163-5, GSA Annual Meeting, Denver.

[60] Bornhorst, T.J. (2005) Copper deposits of the midcontinent rift in Michigan. GSA Abstracts with programs, 37, 5, 74.

[61] Bingquan, Z. et al. (2007) Geochemistry and geochronology of native copper mineralization related to the Emeishan flood basalts, Yunnan province, China. Ore Geology Reviews, 32, 1-2, 366-380.

[62] Bingquan, Z., Yaoguo, H., Zhengwei, Z. and Xiangyang, C. (2003) Discovery of the copper deposits with features of the Keweenawan type in the border area of Yunnan and Guizhou provinces. Science in China (Series D), Vol 46 Supp, 60-72.

[63] Nezafati, N., Momenzadeh, M. and Pernicka, E. (2005) Darhand copper occurrence: an example of Michigan-type native copper deposits in central Iran. Mineral Deposits Research: Meeting the Global Challenge (eds. J. Mao and F.P. Blerlein). pp 165-166. Springer.

[64] Milodowski, A E., Styles, M.T. and Hards, V.L. (2000) A natural analogue for copper waste canisters: The copper uranium mineralised concretions in the Permian mudrocks of south Devon, UK. SKB Technical Report TR-00-11.

[65] Milodowski, A.E., Styles, M.T., Werme, L. and Oversby, V.M. (2001) Native copper in Permian mudstones from south Devon: A natural analogue of copper canisters for high-level radioactive waste. Proceedings MRS Spring Meeting, April 2001. Also published in SKB (2001) Nuclear Waste Containment Materials, Papers related to the SKB waste disposal programme, SKB Technical Report TR-01-25, pp 5-10.

[66] Milodowski, A.E., Styles, M.T., Horstwood, M.S.A. and Kemp, S.J. (2002) Alteration of uransiferous and native copper concretions in the Permian mudrocks of south Devon, UK. SKB Technical Report TR-02-09.

[67] Marcos Perea, N. (1997) The Hyrkkölä native copper mineralization: a natural analogue for copper canisters. Mat. Res. Soc. Symp. Proc. Vol. 465, pp 1153-1160.

[68] Amcoff, Ö and Holényi, K. (1992) Stability of metallic copper in the near surface environment. SKN Report 57, SKN Stockholm.

[69] Amcoff, Ö and Holényi, K. (1996) Mineral formation on metallic copper in a “future repository site environment”. SKI Report 96:38, SKI Stockholm.

[70] SKB (2005) Hydrogeochemical evaluation. Preliminary site description, Forsmark area – version 1.2. Report R-05-17, Swedish Nuclear Fuel and Waste Management Company (SKB), Stockholm.

[71] SKB (2006) Site descriptive modeling, Forsmark stage 2.1. Feedback for completion of the site investigation including input from safety assessment and repository engineering. Report R-06-38, Swedish Nuclear Fuel and Waste Management Company (SKB), Stockholm.

[72] SKB (2006) Hydrogeochemical evaluation of the Forsmark site, modelling stage 2.1 – Issue report. Report R-06-69, Swedish Nuclear Fuel and Waste Management Company (SKB), Stockholm.

[73] SKB (2006) Hydrogeochemical evaluation. Preliminary site description, Laxemar area – version 1.2. Report R-06-12, Swedish Nuclear Fuel and Waste Management Company (SKB), Stockholm.

[74] Pedersen, K. (2005) Numbers and metabolic diversity of microorganisms in borehole KLX03. Results from sections 193.0-198.0 m, 408.0-415.3 m, 735.5-748.0 m and 964.5-975.2 m. Oskarshamn site investigation. Report P-05-182, Swedish Nuclear Fuel and Waste Management Company (SKB), Stockholm.

[75] SKB (2006) Hydrogeochemical evaluation. Preliminary site description Laxemar subarea – version 2.1. Report R-06-70, Swedish Nuclear Fuel and Waste Management Company (SKB), Stockholm.

[76] Hallbeck, L. and Pedersen, K. (2008) Explorative analysis of microbes, colloids and gases together with microbial modelling. Site description model SDM-Site Laxemar. Report R-08-109, Swedish Nuclear Fuel and Waste Management Company (SKB), Stockholm.

[77] Kotelnikova, S.V. and Pedersen, K. (1998) Distribution and activity of methanogens and homoacetogens in deep granitic aquifers at Äspö Hard Rock Laboratory, Sweden. FEMS Microbiology Ecology, 26, 121-134.

[78] Pedersen, K. (2005) Äspö Hard Rock Laboratory. MICROBE. Analysis of microorganisms and gases in MICROBE groundwater over time during MINICAN drainage of the MICROBE water conducting zone. IPR 05-29. Swedish Nuclear Fuel and Waste Management Company (SKB), Stockholm.

[79] Pedersen, K. (2006) Microbiology of transitional groundwater of the porous overburden and underlying shallow fractured bedrock aquifers in Olkiluoto 2005, Finland. Working Report WR 2006-09, Posiva Oy, Olkiluoto, Finland.

[80] Pedersen, K. (2008) Microbiology of Olkiluoto groundwater 2004-2006. Report Posiva 2008-02, Posiva Oy, Olkiluoto, Finland.

[81] Haveman, S. and Pedersen, K. (2002b) Microbially mediated redox processes in natural analogues for radioactive waste. Journal of Contaminant Hydrology, 55, 1-2, 161-174.

[82] Kvenvolden, K.A. (1998) A primer on the geological occurrence of gas hydrate. In: Henriet, J-P & Mienert, J (eds) Gas Hydrates: Relevance to World Margin Stability and Climate Change. Geological Society, London, Special Publications, 137, 9-30.

[83] Rempel, A. W. and Buffett, B.A. (1998) Mathematical models of gas hydrate accumulation. In: Henriet, J-P & Mienert, J (eds) Gas Hydrates: Relevance to World Margin Stability and Climate Change. Geological Society, London, Special Publications, 137, 63-74.

[84] Ruskeeniemi, T., Paananen, M., Ahonen, L., Kaija, J., Kuivamäki, A., Frape, S., Moren, L. and Degnan, P. (2002) Permafrost at Lupin, Report of Phase I. Report YST-112, Geological Survey of Finland (GTK), Espoo.

[85] Ruskeeniemi, T., Ahonen, L., Paananen, M., Frape, S., Stotler, R., Hobbs, M., Kaija, J., Degnan, P., Blomqvist, R., Jensen, M., Lehto, K., Moren, L., Puigdomuenech, I. and Snellman, M. (2004) Permafrost at Lupin, Report of Phase II. Report YST-119, Geological Survey of Finland (GTK), Espoo.

[86] Pitkanen, P. and Partamies, S. (2007) Origin and implications of dissolved gases in groundwater at Olkiluoto. Report Posiva 2007-04, Posiva Oy, Helsinki.

# Appendix A. Biogeochemical data

## A.1 Data for groundwaters at Forsmark

Data for the identities and abundances of microorganisms in water samples taken from deep boreholes at Forsmark have been reported by SKB in the Site Descriptive Models (SDM) versions 1.2 and 2.1 [70, 71, 72]. Data for each metabolic group of microorganisms and discusses the microbial model for Forsmark groundwaters in an overview report for SDM-Site [35]. These data for Forsmark, plus some data from Laxemar and from underground boreholes at the Äspö HRL, are also published and discussed in an overview paper by Hallbeck and Pedersen [8].

Data for six water samples in three deep boreholes (i.e. KFM samples) were reported in SDM v1.2; data for a further four water samples were reported in SDM v2.1, though at that time only MPN ('most probable number' of cultivable microbes) data were available. These microbiological data plus relevant chemical data are presented in Table A1 and are summarised below:

- Total numbers of cells in water samples were all $<10^5$ $mL^{-1}$, of which the proportion of cultivable anaerobic cells was <1% except at KFM01A/115m and KFM03A/943m.

- Microbial populations in shallowest groundwaters are dominated by iron-reducing bacteria (IRB) and manganese-reducing bacteria (MRB); these groundwaters also have relatively higher redox potentials. IRB numbers decrease with depth from 4000 $mL^{-1}$ in KFM01A/115m to <10 $mL^{-1}$ in KFM03A/943m and /990m.

- SRB numbers are low, <2 $mL^{-1}$, in samples down to repository depth and higher at >600 m with a maximum of 5000 $mL^{-1}$ in KFM03A/943m. SRB and $SO_4^{2-}$ generally have an inverse correlation, with the deeper water samples having low $SO_4^{2-}$ and higher SRB.

- At repository depth range, numbers of methanogens and acetogens are variable over several orders of magnitude with no clear dominance or patterns; in KFM02A/512m, methanogens were the dominant anaerobe.

- In KFM03A/943m, both acetogens (23900 $mL^{-1}$) and SRB (5000 $mL^{-1}$) had relatively very high abundances suggesting a microbial respiration system whereby SRB use acetate to reduce $SO_4^{2-}$ to $HS^-$. This water also had the lowest $E_h$ value. In contrast, KFM07A/925 has very low MPN values for all four anaerobe types, and also has an anomalously high $E_h$ value. Otherwise, there is no obvious relation between microbe populations and redox potential.

***Table A1.*** *Microbiological and related hydrochemical data for water samples taken from deep boreholes at Forsmark (up to SDM 2.1 data freeze). MPN = 'most probable number' of cultivable microorganisms; A&H = total of autotrophic and heterotrophic cells. Where '~' values for microorganisms are shown, these values have been estimated from data points in graphical illustrations in SDM reports.*

| | Total no of cells $mL^{-1}$ | IRB MPN $mL^{-1}$ | SRB MPN $mL^{-1}$ | Methan-ogens A&H MPN $mL^{-1}$ | Acet-ogens A&H MPN $mL^{-1}$ | $E_h$ mV | $SO_4^{2-}$ $mgL^{-1}$ | $HS^-$ $mgL^{-1}$ | $Fe^{2+}$ $mgL^{-1}$ | $Fe_{tot}$ $mgL^{-1}$ | DOC $mgL^{-1}$ | $CH_4$ $mL\ L^{-1}$ | $H_2$ $\mu L\ L^{-1}$ | Drill water |
|---|---|---|---|---|---|---|---|---|---|---|---|---|---|---|
| KFM01A 115.4m | 58000 | 4000 | 1.2 | | 1.2 | -175 | 316 | <0.03 | 0.95 | 1.00 | 1.5 | - | - | 0.7% |
| KFM01A 180.4m | 39000 | 4 | 0.2 | | 1.7 | -170 | 547 | <0.03 | 0.48 | 0.54 | 2.3 | - | - | 4.8% |
| KFM02A ??142m* | | ~10 | ~1 | ~10 | ~100 | - | - | - | - | - | - | - | - | - |
| KFM02A 512.5m^ | 59000 | 11 | 1.4 | 160 | 0.8-1 | -140 | 498 | 0.01 | 1.84 | 1.85 | 2.1 | 0.04 | 199 | 6.7% |
| KFM03A 450.5m | | ~10 | ~20 | ~100 | ~1 | - | 472 | <0.03 | 0.92 | 0.92 | 1.2 | - | - | 0.25% |
| KFM03A 642.6m | 21000 | 22 | 30 | 1.7 | 28 | -200 | 197 | | 0.23 | 0.23 | 1.6 | - | - | 4.3% |
| KFM03A 943m | 61000 | <0.2 | 5000 | 17 | 23900 | -245 | 74 | 0.06 | 0.21 | 0.22 | - | - | - | 8.8% |
| KFM03A 990m | 58000 | <0.2 | 24 | 5 | 32 | (-150) | 46.7 | 0.03 | 0.026 | 0.033 | 1.4 | 0.05 | <3.8 | 3.8% |
| KFM06A 357m/a* | 72000 | 30 | 0.8 | 0.2 | 54 | -155 | 157 | - | - | - | - | 0.03 | 370 | 7.10% |
| KFM06A 357m/b* | 52000 | 23 | 0.4 | 0.6 | 48 | -155 | 157 | - | - | - | - | 0.03 | 370 | 7.10% |
| KFM06A 771m* | 17000 | 2.3 | 0.2 | <0.2 | 8.8 | (-200) | 36 | 0.02 | - | - | - | 0.09 | <3.2 | 1.60% |
| KFM07A 925m* | 60000 | <0.2 | <0.2 | 0.2 | 0.7 | +9 | 99 | 0.17 | 0.16 | 0.19 | <1 | 0.04 | <4.8 | 0.35% |

Notes: * Microbiological data in SDM 2.1 only; ^ Microbiological data in SDM 1.2 only.

- Overall, this compilation of microbiological and geochemical data does not offer a clear picture of the biogeochemical processes and relationships at repository depth at Forsmark.

## A.2 Data for groundwaters at Laxemar

Data for the identities and abundances of microorganisms in water samples taken from deep boreholes at Laxemar have been reported by SKB in the Site Descriptive Models (SDM) versions 1.2 and 2.1 [73, 74, 75]. There is an overview report for SDM-Site that evaluates data for each metabolic group of microorganisms and discusses the microbial model for Laxemar groundwaters [76]. These data for Laxemar, plus data from Forsmark and from underground boreholes at the Äspö HRL, are also presented and discussed in an overview paper [8].

Data for three water samples from different intervals in deep borehole KSH01A at Simpevarp, plus sparse pre-existing microbial data from historical boreholes at Laxemar, Äspö and Ävrö, were reported in SDM v1.2. Data, mostly total number of microorganisms only, had been obtained for water samples from nine points in boreholes KLX01 and KLX02 at Laxemar (samplings in 1990 and 2000 respectively), four points in borehole KAV01 at Ävrö, and eight points in boreholes KAS02, 03 and 04 at Äspö. Data for four water samples from intervals in borehole KLX03 were reported in SDM v2.1. Microbiological data plus relevant chemical data are presented in Table A2 and are summarised below:

- Variations of SRB populations in one sample from KLX01 and two samples from KAS04 correlate broadly with concentrations of $HS^-$, but overall SRB and $HS^-$ data are too sparse to justify interpreting such a comparison. $HS^-$ data are missing from samples from KSH01A. $SO_4^{2-}$ increases regularly with depth to a maximum of about 1000 mg/L in KLX02 but there is no depth trend of $HS^-$.

- Methanogens and acetogens were analysed in two samples from KSH01A and in four samples from KLX03A. Populations of acetogens were consistently higher, mostly by 1-2 orders of magnitude, than populations of both methanogens and SRB. The maximum population of acetogens was 2500 cells $mL^{-1}$ at 412m depth. Although no methanogen or acetogen data were reported for the KAS borehole samples, high numbers of methanogens were measured in samples from Äspö HRL [77, 78].

## A.3 Groundwaters at Olkiluoto (Finland)

Similar biogeochemical investigations have been carried out by Posiva in deep boreholes at the Olkiluoto/ONKALO site in Finland [79, 80]. The main observations are summarised as follows:

- Total numbers of microorganisms in shallow groundwaters (0-20 m depth) were $8 \times 10^3$ to $2.5 \times 10^6$ $mL^{-1}$ and in deeper groundwaters (20-500 m) were up to $1.5 \times 10^5$ $mL^{-1}$ with an average of $5.7 \times 10^4$ $mL^{-1}$. Up to 14% of these totals, i.e. $10^0$ to $10^5$ $mL^{-1}$, are cultivable using MPN methods. Numbers of cultivable heterotrophic aerobic bacteria are typically $3 \times 10^3$ $mL^{-1}$ and do not vary much with depth.

***Table A2.*** *Microbiological and related hydrochemical data for water samples taken from deep boreholes at Simpevarp-Laxemar (up to SDM 2.1 data freeze). MPN = 'most probable number' of cultivable microorganisms; A&H = total of autotrophic and heterotrophic cells. Where '~' values for micro-organisms are shown, these values have been estimated from data points in graphical illustrations in SDM reports.*

| | Total no of cells $mL^{-1}$ | IRB MPN $mL^{-1}$ | SRB MPN $mL^{-1}$ | Methan-ogens A&H MPN $mL^{-1}$ | Acet-ogens A&H MPN $mL^{-1}$ | $E_h$ mV | $SO_4^{2-}$ $mgL^{-1}$ | $HS^-$ $mgL^{-1}$ | $Fe^{2+}$ $mgL^{-1}$ | $Fe_{tot}$ $mgL^{-1}$ | DOC $mgL^{-1}$ | $CH_4$ $mL\ L^{-1}$ | $H_2$ $\mu L\ L^{-1}$ | Drill water |
|---|---|---|---|---|---|---|---|---|---|---|---|---|---|---|
| KLX01 274.5m | ~200000 | | | | | - | 48 | 0.53 | 0.129 | 0.129 | 1.5 | 0.11 | - | 4.6% |
| KLX01 466m | ~300000 | | | | | - | 106 | 0.46 | 0.04 | 0.041 | 1.4 | - | - | 13% |
| KLX01 691.1m | ~300000 | | 56000 | | | - | 351 | 2.5 | 0.029 | 0.032 | 1.2 | 0.22 | - | 2.6% |
| KLX01 835.5m | ~10000 | | | | | - | 670 | 0.07 | 0.214 | 0.219 | - | 0.025 | - | 0.1% |
| KLX01 915.5m | ~20000 | | | | | - | 770 | 0.32 | 0.051 | 0.052 | - | 0.027 | - | 0.8% |
| KLX01 1038.5m | ~60000 | | | | | - | 695 | 0.18 | 0.356 | 0.364 | - | - | - | 1.8% |
| KLX02 1160m | ~500000 | 330 | | | | - | 265 | <0.01 | 1.43 | 1.44 | 11.5 | - | - | - |
| KLX02 1350m | ~400000 | 0 | | | | - | 1020 | 0.03 | 0.56 | 0.58 | 90 | - | - | - |
| KLX02 1388.5m | ~3000000 | 0 | | | | - | 1205 | 0.05 | 3.45 | 3.44 | - | - | - | - |
| KLX03 196m* | 84000 | 3.4 | <0.2 | 10.3 | 1100 | -275 | - | - | 0.25 | - | 20 | 0.87 | <1.9 | - |
| KLX03 412m* | - | 2.3 | 220 | 530 | 2500 | -270 | 127 | 0.01 | 0.43 | 0.44 | 13 | 0.62 | 110 | 1.88% |
| KLX03 742m* | 10000 | 50 | 17 | 6.3 | 800 | -220 | 398 | 0.01 | 0.90 | 0.92 | 4 | 0.21 | 190 | 10.8% |
| KLX03 | 20000 | <0.2 | <0.2 | 2.3 | 60 | - | 758 | 0.09 | <0.01 | <0.01 | 1.4 | 0.059 | <2.3 | 0.04% |

| | Total no of cells $mL^{-1}$ | IRB MPN $mL^{-1}$ | SRB MPN $mL^{-1}$ | Methan-ogens A&H MPN $mL^{-1}$ | Acet-ogens A&H MPN $mL^{-1}$ | $E_h$ mV | $SO_4^{2-}$ $mgL^{-1}$ | $HS^-$ $mgL^{-1}$ | $Fe^{2+}$ $mgL^{-1}$ | $Fe_{tot}$ $mgL^{-1}$ | DOC $mgL^{-1}$ | $CH_4$ $mL\ L^{-1}$ | $H_2$ $\mu L\ L^{-1}$ | Drill water |
|---|---|---|---|---|---|---|---|---|---|---|---|---|---|---|
| 970m* | | | | | | | | | | | | | | |
| KSH01A 161.8m | 140000 | 2.1 | 160 | - | - | -220 | 31.7 | - | 1.40 | 1.41 | 0.9 | 0.06 | <3.4 | 2.4% |
| KSH01A 253.2m | 100000 | 2.1 | 22 | 700 | 900 | -210 | 51.1 | - | 1.30 | 1.32 | <1 | - | - | 8.0% |
| KSH01A 556.5m | 72000 | 3.3 | 35 | 2.6 | 47 | -230 | 230.5 | - | 0.51 | 0.52 | <1 | 0.04 | 81 | 10% |
| KSH02 ~400m* | | | | | | | | | | | | | | |
| KSH02 ~550m* | | | | | | | | | | | | | | |
| KAS02 208.5m | ~200000 | | | | | -257 | 106 | 0.5 | 0.48 | 0.50 | 6 | 0.03 | - | 0.81 |
| KAS02 316.5m | ~100000 | | | | | -350 | 270 | 0.01 | 0.788 | 0.794 | 2.4 | - | - | 0.62 |
| KAS02 326m | | | | | | - | 291 | 0.15 | 0.624 | 0.719 | 2 | - | - | 0.71 |
| KAS02 465.5m | ~300000 | | | | | - | 290 | 0.13 | 0.941 | 0.964 | 3 | - | - | 0.38 |
| KAS02 532.5m | | | | | | -300 | 550 | 0.18 | 0.24 | 0.244 | 1 | - | - | 0.28 |
| KAS02 863m | | | | | | -150 | 522 | 0.01 | 0.023 | 0.027 | 0.5 | - | - | 0.22 |
| KAS02 892m | | | | | | -150 | 519 | 0.72 | 0.049 | 0.051 | <0.5 | 0.034 | - | 0.22 |
| KAS03 131.5m | ~200000 | | | | | -275 | 31.1 | 0.71 | 0.123 | 0.125 | 2 | 0.016 | - | 0.06 |
| KAS03 | | | | | | - | 39 | 0.15 | 0.283 | 0.289 | <0.5 | - | - | 1.04 |

| | Total no of cells $mL^{-1}$ | IRB MPN $mL^{-1}$ | SRB MPN $mL^{-1}$ | Methan-ogens A&H MPN $mL^{-1}$ | Acet-ogens A&H MPN $mL^{-1}$ | $E_h$ mV | $SO_4^{2-}$ $mgL^{-1}$ | $HS^-$ $mgL^{-1}$ | $Fe^{2+}$ $mgL^{-1}$ | $Fe_{tot}$ $mgL^{-1}$ | DOC $mgL^{-1}$ | $CH_4$ $mL\ L^{-1}$ | $H_2$ $\mu L\ L^{-1}$ | Drill water |
|---|---|---|---|---|---|---|---|---|---|---|---|---|---|---|
| 249.5m | | | | | | | | | | | | | | |
| KAS03 466.5m | | | | | | - | 300 | 0.11 | 0.194 | 0.196 | <0.5 | - | - | 2.13 |
| KAS03 616m | | | | | | - | 470 | 0.05 | 0.068 | 0.072 | 1.1 | - | - | 2.23 |
| KAS03 846m | | | | | | - | 680 | 0.11 | 0.047 | 0.053 | <0.5 | - | - | 2.57 |
| KAS03 931m | ~200000 | | | | | -275 | 709 | 1.28 | 0.077 | 0.078 | <0.5 | 0.037 | - | 0.13 |
| KAS04 230.5m | ~600000 | | 1600 | | | -300 | 180 | 1.1 | 0.04 | 0.041 | 6.9 | - | - | 0.16 |
| KAS04 338.5m | ~300000 | | <100 | | | -275 | 220 | 0.41 | 0.324 | 0.327 | 5.3 | 0.028 | - | 0.52 |
| KAS04 460.5m | ~100000 | | | | | -280 | 407 | 0.6 | 0.256 | 0.259 | 1.3 | 0.004 | - | 0.08 |
| KAV01 420m | ~2000000 | | | | | -215 | 43 | 0.63 | 1.68 | 1.69 | 9.6 | - | - | 9 |
| KAV01 522m | ~400000 | | | | | - | 118 | 1.2 | 2.23 | 2.23 | 6.4 | - | - | 10 |
| KAV01 558m | ~400000 | | | | | -225 | 220 | 0.81 | 1.02 | 1.02 | 3.9 | - | - | 15.3 |
| KAV01 635m | ~200000 | | | | | - | 390 | <0.01 | 0.43 | 0.438 | <0.5 | - | - | 0.5 |

Notes:
* Microbiological data in SDM 2.1 only

- IRB range from >$10^2$ to ~0 $mL^{-1}$. IRB predominate in groundwaters at the Palmottu natural analogue site and correlate with iron oxide abundance [81].

- SRB range from ~$10^3$ to ~0 $mL^{-1}$ and do not show a clear depth trend. Dissolved $HS^-$ is low, <0.1 mg/L, down to ~200 m depth and then is higher between 200-300 m reaching a maximum of ~10 mg/L, whilst $SO_4^{2-}$ peaks to ~500 mg/L between 100-300 m depth and is very low below 500 m.

- Methanogens range from >10 to ~0 cells $mL^{-1}$ and acetogens range from $10^3$ to ~0 $mL^{-1}$. Methane-oxidising bacteria vary from >$10^3$ to ~0 $mL^{-1}$; the greater abundance relative to methanogens is probably related to the high methane concentrations which increase regularly with depth to a maximum of $10^2$-$10^3$ $mL_{STP}$/L below 500 m depth.

Thus there are no clear differences apparent between microbiological populations at Olkiluoto and at Forsmark and Laxemar-Simpevarp. There is a substantial contrast in methane concentrations between Olkiluoto and the Swedish areas, and there might be a corresponding contrast in numbers of methane-oxidising bacteria but there are no data in this respect for the Swedish areas.

Anaerobic oxidation of methane (AOM) coupled with sulphate reduction is suspected to be a significant, perhaps major, process of Olkiluoto [80]. The peak of dissolved $HS^-$ at around 300 m depth corresponds to a step increase of $CH_4$ (10-100 mL/L), a locally higher population of SRB (up to 100 cells $mL^{-1}$), and slightly higher populations of methanogens (up to 40 cells $mL^{-1}$). It is thought that SRB and methanogens are able to cooperate to oxidise $CH_4$ to produce $H_2$ and then use this $H_2$ to reduce $SO_4^{2-}$ to $HS^-$ [80]. The property of Olkiluoto deep groundwaters that may trigger this process is the higher concentration of $CH_4$ relative to the deep groundwaters at Äspö, Forsmark and Laxemar. If AOM does operate here then the rate of $HS^-$ production from $SO_4^{2-}$ at <300m depth is possibly limited by the $CH_4$ flux. Below 300m depth, AOM is possibly limited by decreasing $SO_4^{2-}$ concentrations. This would then suggest that $HS^-$ production by AOM could be accelerated at repository depth if excavation of ONKALO were to cause drawdown of $SO_4^{2-}$-containing groundwaters to mix with groundwaters with higher $CH_4$. However evidence that microbial populations are capable of mediating AOM has not yet been confirmed here. On the evidence of biogeochemical data considered in this review, there is no convincing basis for interpreting that AOM occurs at Olkiluoto.

# Appendix B. Hydrochemical spreadsheet

| Sample | SKB No | Depth range | Drill water | Temp Chem-mac | pH Chem mac* | pH surf* | pH lab* | pH mod* | Eh Chem mac | pe | Na | K | Ca | Mg | $HCO_3$ | Cl | $SO_4$ | $S^{2-}$ | Fe(tot) | $Fe^{2+}$ | $Fe^{3+}$ calc | $NH_4$ | Charge bal | Data sources |
|---|---|---|---|---|---|---|---|---|---|---|---|---|---|---|---|---|---|---|---|---|---|---|---|---|
| | | m bgl | % | °C | | | | | mV | | mg/L | | | | | | | | | | | | % | |
| **FORSMARK** | | | | | | | | | | | | | | | | | | | | | | | | |
| KFM01A/115 | 4538 | 110.1-120.77 | 0.76 | 6.91 | 7.68 | 7.62 | 7.47 | 7.65 | -195 | -3.48 | 1740 | 25.6 | 874 | 142 | 61 | 4563 | 316 | <0.03 | 1.00 | 0.95 | 0.04 | 1.07 | -1.65 | P-03-94, R-05-17, R-05-18 |
| KFM01A/180 | 4724 | 176.8-183.9 | 4.80 | 7.60 | 7.41 | 7.41 | 7.60 | 7.41 | -188 | -3.36 | 2000 | 29.2 | 934 | 204 | 99 | 5330 | 547 | <0.03 | 0.54 | 0.48 | 0.06 | 1.01 | -3.80 | P-03-94, R-05-17, R-05-18 & SICADA 28-03-08 |
| KFM01D/432 | 12326 | 428.5-435.6 | 6.30 | 9.65 | 8.10 | 8.10 | 7.55 | 8.10 | -263 | -4.70 | 1550 | 9.0 | 1430 | 20 | 36 | 4940 | 125 | 0.01 | 2.08 | 2.04 | | 0.20 | -0.6 | SICADA 28-03-08 |
| KFM01D/572 | 12354 | 568.0-575.1 | 0.90 | 10.75 | 8.40 | 8.10 | 7.40 | 8.25 | -260 | -4.64 | 1770 | 7.7 | 1830 | 15 | 20 | 5800 | 38 | 0.01 | 1.24 | 1.23 | | 0.12 | 1.6 | P-06-227 |
| KFM02A/512 | 8016 | 509-516.08 | 6.77 | 11.40 | 6.83 | 6.93 | 7.18 | 6.88 | -143 | -2.55 | 2040 | 34.2 | 934 | 226 | 125 | 5410 | 498 | 0.01 | 1.85 | 1.84 | 0.01 | 2.30 | -3.11 | P-04-70, R-05-17, R-05-18 |
| KFM03A/452 | 8284 | 448.5-456.6 | 0.40 | 10.70 | 7.29 | 7.27 | 7.42 | 7.28 | -176 | -3.14 | 2180 | 27.5 | 1070 | 216 | 93 | 5330 | 511 | 0.05 | 1.10 | 1.11 | | | 1.4 | P-04-108 & SICADA 28-03-08 |
| KFM03A/642 | 8273 | 639-646.12 | 4.35 | 13.10 | 7.38 | 7.48 | 7.55 | 7.43 | -196 | -3.50 | 1660 | 14.3 | 1440 | 53 | 22 | 5430 | 197 | | 0.23 | 0.23 | 0.00 | 0.16 | -2.79 | P-04-108, R-05-17, R-05-18 & SICADA 28-03-08 |
| KFM03A/943 | 8281 | 939.5-946.6 | 8.80 | 17.20 | 7.32 | 7.53 | 7.78 | 7.42 | -245 | -4.38 | 1890 | 10.4 | 3100 | 18 | 9 | 8560 | 74 | 0.06 | 0.22 | 0.21 | 0.01 | | -0.815 | P-04-108, R-06-38 & SICADA 28-03-08 |
| KFM06A/357 | 8838 | 353.5-360.6 | 7.10 | 8.94 | 6.91 | 7.33 | 7.41 | 7.12 | -155 | -2.77 | 1470 | 13.4 | 1280 | 74 | 48 | 4850 | 157 | | | | | | -2.30 | P-05-178, R-06-38 |
| KFM07A/925 | 8879 | 848-1001.6 | 0.35 | 14.20 | 8.04 | 8.05 | 8.00 | 8.04 | 9 | 0.17 | 2850 | 13.7 | 5840 | 20 | 6 | 14800 | 99 | 0.17 | 0.19 | 0.16 | | 0.02 | -0.14 | P-05-170, R-06-38 |
| KFM08A/687 | 12000 | 683.5-690.64 | 5.05 | 11.90 | 8.00 | 8.00 | 7.79 | 8.00 | -209 | -3.73 | 1560 | 10.6 | 2090 | 14 | 10 | 6100 | 92 | 0.01 | 0.72 | 0.73 | | 0.09 | 0.0 | SICADA 28-03-08 |
| KFM08D/673 | 12818 | 669.7-676.8 | 5.40 | 11.70 | 8.40 | 8.30 | 8.14 | 8.35 | -260 | -4.64 | 1900 | 5.4 | 2740 | 5 | 7 | 7460 | 101 | <0.006 | <0.006 | <0.006 | | 0.04 | 1.8 | P-07-190 |
| KFM10A/302 | 12552 | 298-305.1 | 4.50 | 8.56 | 8.10 | 8.20 | | | -281 | -5.02 | 1350 | 6.6 | 1130 | 30 | 21 | 4050 | 215 | 0.03 | 1.45 | 1.43 | | | -0.5 | P-07-42 & SICADA 28-03-08 |
| KFM10A/483 | 12517 | 478-487.5 | 3.60 | 9.46 | 7.70 | 7.70 | 7.13 | 7.70 | -258 | -4.61 | 1410 | 29.1 | 731 | 151 | 169 | 3690 | 400 | 0.07 | 15.30 | 15.40 | | | -1.8 | P-07-42 & SICADA 28-03-08 |
| KFM11A/451 | 12727 | 447.5-454.64 | 5.88 | 9.71 | 7.53 | 7.54 | 7.58 | 7.53 | -203 | -3.63 | 1250 | 5.9 | 1280 | 38 | 24 | 4210 | 264 | 0.01 | 0.25 | 0.24 | | 0.05 | -1.2 | SICADA 28-03-08 |
| **LAXEMAR** | | | | | | | | | | | | | | | | | | | | | | | | |
| KLX01/458 | 1528 | 456-461 | 13.70 | | 8.60 | 8.70 | 8.20 | 8.65 | -280 | -5.00 | 860 | 6.10 | 223 | 18.0 | 78 | 1700 | 106 | 0.46 | 0.04 | 0.04 | 0.00 | 0.06 | -1.18 | TR-02-19 (p 246), TR-98-03, R-04-74, R-05-08, R-06-12, R-06-70 (App3 Ta |
| KLX01/691 | 1516 | 680-702.11 | 2.60 | | 7.80 | | 8.10 | 7.80 | -265 | -4.73 | 1680 | 7.10 | 1400 | 23.0 | 24 | 4870 | 351 | 2.50 | 0.03 | 0.03 | 0.00 | 0.00 | 0.08 | R-06-10 (p 376), TR-98-03, R-04-74, R-05-08, R-06-12, R-06-70 (App3 Tab |
| KLX03/412 | 10091 | 408-415.3 | 1.88 | | 8 | | 7.89 | 8.00 | -270 | -4.82 | 791 | 5.5 | 234 | 11 | 189 | 1390 | 127 | 0.01 | 0.44 | 0.43 | | 0.028 | 2.4 | R-06-70 (App3 Tabs 1-1 & 4-1a) & SICADA 28-03-08 |
| KLX03/742 | 10242 | 735.5-748.04 | 10.80 | | 7.5 | | 7.41 | 7.50 | -220 | -3.93 | 1450 | 10.9 | 1090 | 13 | 34 | 3940 | 398 | 0.01 | 0.92 | 0.90 | | 0.012 | -0.4 | R-06-70 (App3 Tabs 1-1 & 4-1a) |
| KLX08/202 | 10649 | 197-206.65 | 1.29 | 8.7 | 8.1 | 8.4 | 8.29 | 8.25 | -266 | -4.75 | 98 | 3.4 | 19 | 4 | 296 | 13 | 13 | 0.00 | 0.12 | 0.11 | | 0.094 | 1.3 | SICADA 28-03-08 |
| KLX08/398 | 10747 | 396-400.87 | 1.15 | 11.5 | 8 | 8.3 | 8.32 | 8.15 | -245 | -4.38 | 103 | 2.4 | 15 | 2 | 290 | 15 | 14 | 0.04 | 1.02 | 1.02 | | 0.057 | 0.2 | SICADA 28-03-08 |
| KLX08/481 | 11183 | 476-485.62 | 5.89 | 12.85 | 7.6 | 8.1 | 7.87 | 7.85 | -210 | -3.75 | 799 | 3.9 | 294 | 7 | 32 | 1600 | 132 | 0.01 | 0.28 | 0.28 | | 0.028 | 1.8 | SICADA 28-03-08 |
| KLX08/614 | 11228 | 609-618.51 | 10.70 | 13.49 | 8.4 | 8.4 | 8.19 | 8.40 | -239 | -4.27 | 947 | 5.9 | 367 | 8 | 21 | 2030 | 145 | 0.01 | <0.005 | <0.005 | | 0.036 | -0.2 | SICADA 28-03-08 |
| KLX13A/435 | 11609 | 432-439.16 | 10.40 | 13.8 | 8.5 | 8.3 | 8.33 | 8.40 | -287 | -5.13 | 449 | 1.8 | 51 | 3 | 75 | 728 | 37 | 0.00 | 0.01 | <0.006 | | 0.011 | -0.3 | SICADA 28-03-08 |
| KLX13A/503 | 11544 | 499.5-506.66 | 15.90 | 14.8 | 8.2 | 8.1 | 8.10 | 8.15 | -277 | -4.95 | 459 | 2.1 | 60 | 4 | 87 | 740 | 46 | <0.006 | 0.05 | 0.04 | | 0.039 | 0.3 | SICADA 28-03-08 |
| KLX17A/426 | 11810 | 416-437.51 | 1.71 | 12.2 | 8 | 8 | 7.92 | 8.00 | -297 | -5.30 | 329 | 4.0 | 68 | 10 | 118 | 576 | 24 | 0.02 | 0.89 | | | 0.056 | -0.2 | SICADA 28-03-08 |
| KLX17A/671 | 11692 | 642-701.08 | 0.21 | | | 8.3 | 8.36 | 8.3 | -303 | -5.41 | 88 | 1.3 | 12 | 2 | 238 | 17 | 6 | <0.006 | 0.69 | 0.68 | | 0.028 | 1.2 | SICADA 28-03-08 |
| **SIMPEVARP, ÄSPÖ, ÄVRÖ** | | | | | | | | | | | | | | | | | | | | | | | | |
| KSH01A/161 | 5263 | 156.5-167 | 2.39 | 6.3 | | 8.17 | 7.36 | 8.17 | -257 | -4.59 | 2280 | 14.7 | 960 | 71 | 25 | 5590 | 32 | 0 | 1.413 | 1.397 | 0.02 | 0.095 | -1.669 | P-04-12, R-04-74, R-05-08, R-06-70 Tab 4-1a in Appendix 3 |
| KSH01A/253 | 5268 | 245-261.5 | 8.02 | | | 8.08 | 7.34 | 8.08 | -160 | -2.86 | 2430 | 13.2 | 1180 | 65 | 17 | 6298 | 51 | 0 | 1.318 | 1.296 | 0.02 | 0.079 | -2.401 | P-04-12, R-04-74, R-05-08, R-06-70 Tab 4-1a in Appendix 3 |
| KSH01A/556 | 5288 | 548-565 | 10.74 | 3 | | 8.15 | 7.63 | 8.15 | -173 | -3.09 | 3500 | 77.0 | 1900 | 47 | 11 | 8876 | 230 | | 0.523 | 0.511 | 0.01 | 0.048 | -0.392 | P-04-12, R-04-74, R-05-08, R-06-70 Tab 4-1a in Appendix 3 |
| KAS02/208 | 1548 | 202-214.5 | | | | 7.5 | 7.4 | 7.5 | -257 | -4.59 | 1300 | 6.6 | 990 | 65 | 71 | 3820 | 106 | 0.5 | 0.502 | 0.483 | 0.02 | 0.4 | 0.2528 | TR-92-31; TR-98-03, R-04-74, R-05-08 |
| KAS02/532 | 1433 | 530-535 | | 15.3 | | 7.73 | 8 | 7.73 | -308 | -5.50 | 2200 | | 1890 | | 10 | 6330 | 550 | 0.18 | 0.244 | 0.24 | 0.00 | 0.03 | 0.0579 | TR-92-31; TR-98-03, R-04-74, R-05-08 |
| KAS03/131 | 1569 | 129-134 | | 10.2 | | 8 | 8 | 8 | -275 | -4.91 | 613 | 2.4 | 162 | 21 | 61 | 1220 | 31 | 0.71 | 0.125 | 0.123 | 0.00 | 0.04 | 0.7275 | TR-92-31; TR-98-03, R-04-74, R-05-08; R-06-70 Table 1-1 in Appendix 3 |
| KAS03/931 | 1582 | 860-1002.06 | | 20.5 | | 8 | 8.1 | 8.1 | -275 | -4.91 | 3020 | 7.3 | 4380 | 50 | 11 | 12300 | 709 | 1.28 | 0.078 | 0.077 | 0.00 | 0.005 | -0.959 | TR-92-31; TR-98-03, R-04-74, R-05-08 |
| KAS04/338 | 1603 | 334-343 | | 12.15 | | | 8 | 8 | -275 | -4.91 | 1180 | 6.1 | 740 | 30 | 69 | 3030 | 220 | 0.41 | 0.327 | 0.324 | 0.00 | 0.09 | -0.075 | TR-92-31; TR-98-03, R-04-74, R-05-08 |
| KAS04/460 | 1588 | 440-480.98 | | | | 8.1 | 8.1 | 8.1 | -280 | -5.00 | 1890 | 7.8 | 1660 | 61 | 21 | 5840 | 407 | 0.6 | 0.259 | 0.256 | 0.00 | 0.05 | -0.854 | TR-92-31; TR-98-03, R-04-74, R-05-08, R-06-70 Table 4-1a in Appendix 3 |
| KAV01/422 | 1390 | 420-425 | | 12.9 | | 6.9 | 7.35 | 7.35 | -215 | -3.84 | 255 | 4.7 | 156 | 21 | 186 | 575 | 43 | 0.59 | | 1.60 | | | 1.5 | R-04-74; R-06-70 Tabs 1-1 & 4-1a in Appendix 3 |
| KAV01/526 | 1383 | 522-531 | | 14.9 | | 7 | | 7 | -310 | -5.54 | 750 | 7.4 | 440 | 42 | 81 | 1970 | 118 | 1.20 | | 2.23 | | | -0.9 | R-04-74; R-06-70 Tabs 1-1 & 4-1a in Appendix 3 |
| KAV01/560 | 1374 | 558-563 | | 15 | | 7.2 | | 7.2 | -225 | -4.02 | 1500 | 6.0 | 1100 | 60 | 42 | 4300 | 220 | 0.81 | 1.02 | 1.02 | 0.00 | 0.08 | -0.433 | R-04-74, R-05-08; R-06-70 Tabs 1-1 & 4-1a in Appendix 3 |

* pH Chemmac = pH measured by downhole Chemmac module; pH surf = pH measured by surface Chemmac module; pH lab = pH measured in static sample in laboratory; pH mod = pH value selected for $CO_2$-loss modelling

Data reported as most reliable in SKB reports

Reported data but 'not representative' or 'to be used with caution'

# Appendix C. Potential impact of methane hydrate ice

## C.1 Introduction

Trapping of methane in permafrost as methane hydrate is mentioned as a hypothetical feature of the glacial stage of the normal long-tem evolution scenario in SR-Can. Natural methane hydrate is known to occur world-wide at the present day in polar regions, usually associated with permafrost or seabed sediments on the outer parts of continental shelves. The amount of methane in hydrate worldwide has been estimated to be in the order of 103 to 106 gigatons (which is believed to be comparable with the amount of carbon locked up in fossil fuel deposits) – this is based on occurrence in oceanic sediments and with a fairly low estimate of average porosities, 2 to 4 %, occupied by the hydrate [82]. In general, only a fraction of the high porosity of oceanic sediments is occupied by methane hydrate. The amount that is estimated to be in permafrost in continental sedimentary rocks in the north American Arctic has been estimated to be around 400 gigatons [82]. There has been no estimate of the possible amount in non-sedimentary rocks in these environments, the inference being that it is considered to be negligible due to low porosities and non-existent sources of methane.

A related scenario is the trapping and accumulation of methane below permafrost, both as methane hydrate and as methane gas, i.e. that permafrost and hydrate might act as an impermeable seal or 'cap' under which methane accumulates initially as an enhancement of dissolved methane and eventually as a distinct gas phase. This scenario requires there to be a deep source of methane, migrating with a flux that is greater than can be dissipated around the permafrost seal.

Although no direct impact on long-term safety has been attributed to methane hydrate, it is clear that the hypothesis of methane accumulating in the vicinity of a repository at some time in the future suggests some scenarios. These scenarios need to be considered with the background of the probability of methane hydrate actually forming, the potential abundances of hydrate and the potential fate and impacts of methane hydrate as climate continues to change.

## C.2 Science of methane hydrate in ice

Methane hydrate is a solid state 'clathrate' structure in which water molecules enclose methane (and possibly minor amounts of other gases). In an ideal methane-saturated hydrate, the molar ratio $CH_4$:$H_2O$ is 1:6 which is equivalent to a volumetric ratio of 164:1, i.e. 1 $m^3$ of solid hydrate can potentially contain methane that would occupy up to 164 $m^3$ as free gas (at Standard Temperature and Pressure of 0 ºC and 0.1 MPa). The amount of methane that can be trapped is therefore limited by the amount of water. This

is an important consideration in relation to the amount of methane that could be trapped in permafrost above a deep repository in fractured crystalline rock that has low porosity (noting also the possibility of permafrost acting as a 'cap' on an underlying accumulation of methane).

Formation of methane hydrate involves transfer of dissolved or gaseous methane from pore spaces in the rock to the ice lattice. This transfer and incorporation of methane into hydrate involves release of latent heat which then has to be dissipated, otherwise the hydrate would be destabilised. Therefore hydrate stabilisation depends on interplay between ice formation, gas migration into the ice lattice, and advective or diffusive transport of heat away from the hydrate [83].

Rempel and Buffett's mathematical model for hydrate formation and growth in a porous medium [83] indicates that the hydrate volume fraction, i.e. the fraction of porosity occupied by hydrate, is likely to be low, even as low as <1 %, in systems with low methane abundance, because of the high methane storage capacity of hydrate and the low thermal diffusivity for latent heat dissipation. Rempel and Buffett note that advective flow in fractures might locally change this condition, i.e. greater advective inwards transport of methane and greater advective dissipation of latent heat. This mathematical model also indicates that it might take many tens or hundreds of thousands of years for significant methane hydrate to accumulate in a system with very low fluid velocity; the model suggests about a million years for hydrate to accumulate to occupy 10 % of pore space. In other words, stable thermal and pressure conditions, as well as constant methane production or inwards flux, are required over a long period to produce a high occupancy of hydrate.

The thermodynamics of both methane hydrate and water ice are illustrated in Figure C1 which shows the stability fields of methane hydrate and ice in terms of temperature and pressure (represented as depth).

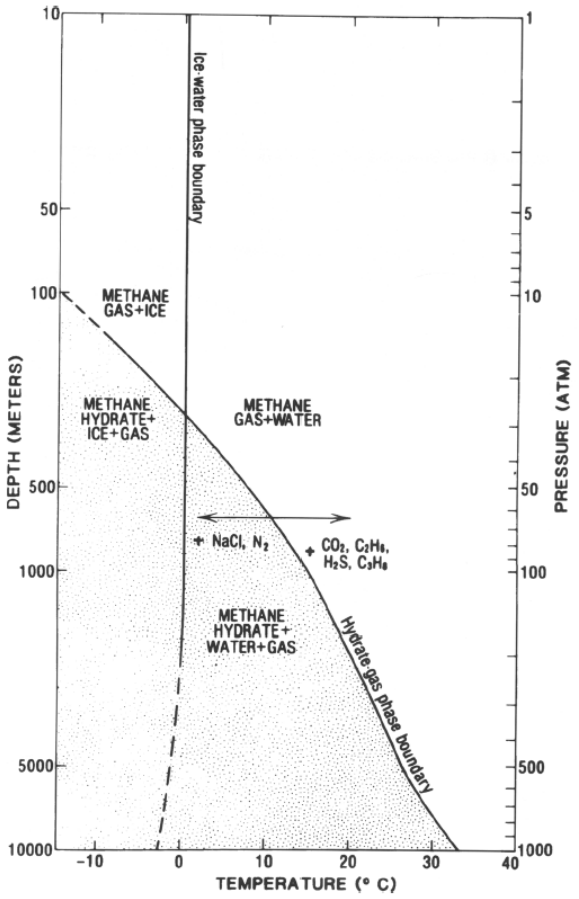


***Figure C1.*** *Phase diagram showing stability fields of methane hydrate and water ice in temperature-depth space [82). 'Depth' represents hydrostatic pressure gradient. The zones of stability of methane hydrate in particular environmental conditions, i.e. oceanic sediments or permafrost in continental sediments, depends on the hydrothermal and geothermal gradients existing in the specific locations. The horizontal arrow shows the effects on hydrate stability of increasing water salinity (phase boundary moves to the left) and of other gases mixing into methane (phase boundary moves to the right).*

## C.3 Occurrence in permafrost

Methane hydrate occurrence, both in oceanic sediments on continental shelves and in permafrosted onshore regions, is patchy, presumably related to both the existence of conditions that are favourable for its stability and the distribution of sources of methane.

Methane hydrate is more widely distributed in oceanic sediments than in permafrost, probably because of the greater abundance of sources of organic carbon from which methane can be derived in oceanic sediments. Organic geochemical and isotopic evidence indicates in general that methane in subseabed hydrate occurrences has been derived from microbial breakdown of organic material, either in situ or in an adjacent location from which it has migrated into the zone of permafrost formation.

Methane hydrate has been found in permafrost regions of Siberia, Kamchatka, Alaska, northern Canada and the Sverdrup basin in the Arctic.

Available evidence suggests that methane hydrate and permafrost usually occur together in sedimentary rocks that have higher porosities. For example, methane hydrate in the Beaufort-Mackenzie region of northern Canada is mainly associated with coarse-grained and other predominantly sandy deltaic sedimentary rocks that have high porosities. Many of the hydrate occurrences in these permafrosted sedimentary rocks have underlying conventional hydrocarbons as the source of methane.

No published reports have been found describing methane hydrate in the permafrosted fractures of crystalline rocks, so it appears that this mode of occurrence is rare or non-existent. Anomalously high concentrations of methane were not recorded in water samples taken from within (250 m depth) and below (880 and 1130 m depth) the permafrost zone intersected by the Kinross Lupin gold mine in Nunavut Territories, northern Canada [84, 85].

In permafrost, methane hydrate can exist at depths where the temperature is low enough and the hydrostatic/lithostatic pressure is high enough to stabilise it. The broad range of stability is from ~200 to ~1100 metres depth, defined by the upper pressure regime at which the hydrate is stabilised at a temperature of -10 °C and the lower geothermal regime at which the hydrate is destabilised despite increasing pressure (Figure C2). An important observation from the phase diagram of methane hydrate stability is that the hydrate is stable below the depth at which permafrost, i.e. water ice, is stable – in Figure C2 this zone of hydrate occurrence beneath permafrost ice is from 600 to ~1100 metres. In other words, it is conceivable that, even in a glacial condition where permafrost would not reach to repository depth, methane hydrate would be theoretically stable through the design depth range of a repository.

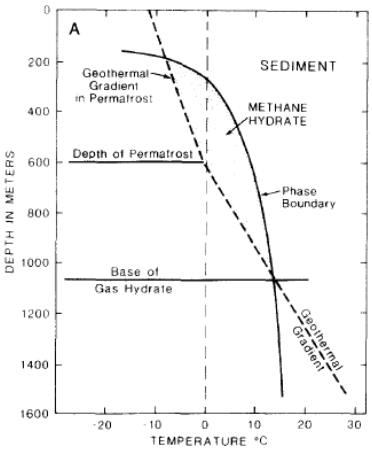


***Figure C2.*** *Phase diagram showing stability field of methane hydrate in relation to temperature and depth [82]. The depth range of permafrost formation is shown as 0 to 600 metres and the field of stability of methane hydrate extends from about 200 to ~1100 metres depth.*

## C.4 Sources and fluxes of methane

The amount of methane that could accumulate by this process cannot be quantified the absence of data for methane fluxes, though low dissolved methane concentrations suggest that flux is also low.

Potential accumulation of methane hydrate over the duration of a permafrost period would depend on upwards methane flux, minus the flux that is lost out of the ground to atmosphere and via groundwater pathways that remain active (e.g. discharges at taliks). The theoretical considerations in the model of Rempel and Buffett [83] suggest that it could take on the order of hundreds of thousands to millions of years for substantial amounts of methane hydrate to accumulate, even in fairly porous rocks.

Methane concentrations and fluxes in deep groundwaters at around repository depth in crystalline rocks in the Fennoscandian Shield are apparently rather variable. In the deep boreholes at Forsmark and Laxemar, dissolved $CH_4$ concentrations are low – typically <1 mL/L (= 0.04 mmol/L) whilst at Olkiluoto they are significantly higher and close to or at saturation, up to 800 mL/L (= 36 mmol/L) below 800 m depth.

Isotopic and other evidence indicates that dissolved methane in these crystalline rock environments tends to be biogenic at shallow depths where the abundances are very low and is increasingly thermogenic (presumed to be thermogenic in the sense of being derived from abiogenic equilibria between C-containing fluids, primarily $CO_2$ and $CH_4$, in the deep crust) with increasing depth.

Based on evidence of groundwater ages and other hydrodynamic considerations, Pitkänen and Partamies [86] deduce that the timescale for methane build-up in deep saline groundwaters at Olkiluoto has been of the order of millions of years, implying that the methane flux from the deep thermogenic source is very low, and was not enhanced by the impacts at depth of glaciations during that period.

## C.5 Evidence about permafrost in the past

At present there is rather large uncertainty in these hypothetical and speculative scenarios connected with permafrost. There is no evidence that the coupled permafrost-methane-sulphide processes have been significant during glacial cycles in the past. Positive confirmation that this is the case should be sought.

## C.6 Scenarios for the impacts of methane hydrate

The theoretical background to methane hydrate described above suggests that hydrate would be stable over a significant depth range beneath permafrost, i.e. over the depth range in which a repository would be located.

Therefore the potential impacts of methane hydrate should include (a) the effect of the hydrate itself on a repository, and (b) the effect on a repository of locally high concentrations of methane, dissolved and gaseous, should hydrate become destabilised at some time in the future.

These potential impacts of methane hydrate would be minimised by low porosities in rocks down to and below repository depth. Equally or more important would be minimising void spaces within the repository so that the probability of methane hydrate formation or accumulation of methane gas would be kept low.

Methane would participate in redox reactions, notably the reduction of sulphate to sulphide ($HS^-$). $HS^-$ is corrosive with respect to copper. SR-Can [29] asserts that $HS^-$ concentrations would anyway be controlled at low levels (e.g. $\leq 10^{-5}$ M) due to equilibration with iron sulphide (FeS). It is possible that a release of methane, e.g. when permafrost and methane hydrate thaw, could cause transient high concentrations of methane and sulphide due to redox reactions being mediated by enhanced microbial activity. However the local accumulation of $HS^-$ would be limited by the supply of sulphate.

It is problematic to derive a scoping calculation that provides reasonable and robust bounds on the probability of substantial hydrate formation in a low porosity fractured crystalline rock. The following is suggested as one approach to bounding the issue. It neglects the possibility that hydrate formation in a fractured rock may be less probable because of the lower distribution of pathways for methane migration and the lower diffusivity that would control latent heat dissipation. In other words, the scoping calculation is based simply on the conceptual model of a very low porosity porous medium:

- Assume fracture porosity = 1 %, of which void space hydrate forms in 10 %, i.e. hydrate occupies 0.1 % of total rock volume;
- Estimate methane flux from below on basis of Olkiluoto interpretation that it takes $\geq 10^6$ years to accumulate dissolved methane to 36 mmol/L; for porosity of 1 %, this suggests upwards flux of ~0.36 mmol/$m^2$ in $10^6$ years, neglecting methane losses by upwards and lateral advection and diffusion, i.e. methane flux in bedrock is ~3.6 x $10^{-10}$ mol/$m^2$/a;
- Hydrate contains 164 $m^3$ STP $CH_4$ for each 1 $m^3$ of fracture water, i.e. each 1 $m^3$ of rock would contain 0.164 $m^3$ STP $CH_4$ = 7.3 mols $CH_4$;
- If hydrate layer is 500 metres thick, i.e. occupying the rock column between 600 and 1100 metres depth, then that contains 500 x 7.3 mols = 3650 mols $CH_4$ per $m^2$ of cross-section;
- Time taken for that amount of methane to accumulate by upwards migration = 3650 / 3.6 x $10^{-10}$ = $10^{13}$ years.

It is evident that a considerable length of time is required, with the assumed conditions and simplifications, to accumulate methane hydrate in the fractures over a 500 metre-thick section of rock in and below the permafrosted thickness. On this basis, it seems very unlikely that methane hydrate could be significant in these conditions.

## C.7 Implications for a long-term safety case

In summary, the main facts and estimations are:

- Methane hydrate is thought to occur mainly in ocean floor sediments at certain locations where P and T conditions and production of $CH_4$ are favourable;

- Methane hydrate also occurs, probably less frequently, in onshore sedimentary rocks where the T and P conditions are also favourable to hydrate stability; the T conditions are indicated by the occurrence of permafrost, but methane hydrate may also be stable beneath permafrost as well as in it;

- No reported observations of methane hydrate in permafrosted fractured crystalline rocks could be found in this brief literature survey;

- Where methane hydrate does occur in porous media, i.e. oceanic sediments or permafrosted sedimentary rocks, it occupies a small fraction of the pore space, typically <10 %;

- A mathematical model for methane hydrate formation explains why the hydrate occupies only a small fraction of pore space and also suggests a very long time, typically millions of years, for it to accumulate;

- Deep groundwaters in fractured crystalline rocks in the Fennoscandian Shield are known to contain low to fairly high, i.e. close to saturation, concentrations of dissolved methane, which is thought to have a deep thermogenic origin;

- It is thought that the flux of methane in these crystalline rock environments is low, because only the highly saline almost stagnant deep groundwaters show the near-saturation concentrations, taking possibly a million years or more to accumulate;

- On the basis of these data and estimations, it would take a very long time for methane hydrate to accumulate significantly in the fracture rocks above and around a repository, probably longer than the timescale of one or several glacial cycles;

- The possibility that methane hydrate could form in the repository itself if there were more void spaces than in natural rock porosity needs to be considered also, as well as the possibility that methane gas (dissolved or as a discrete gas phase) could accumulate under the gas cap provided by permafrost and/or methane hydrate. However the rate of methane accumulation would be similarly controlled by the inwards flux of deep-sourced methane into the repository system, unless there were a source of significant additional amounts of methane in the re-

pository itself, e.g. from biogeochemical degradation of introduced organic materials.

The implications for a long-term safety case are:

- Permafrost itself (which certainly occurs in fracture crystalline Shield rocks) has implications for evolution of repository conditions through the glacial part of the normal evolution scenario, e.g. reduced infiltration, lowered bedrock permeability, diversion of groundwater flow directions and radionuclide transport pathways, salinization due to freeze-out of dissolved solutes, freezing of the repository components such as bentonite buffer and backfill;

- Due to hydrate formation and/or methane trapping, methane could accumulate at repository depth, either in rocks adjacent to a repository and/or in the repository voids;

- The potential impact on repository processes would probably be an acceleration of the processes that depend on methane abundance, i.e. redox and other microbially mediated reactions such as sulphate reduction to sulphide;

- Another physical impact of methane release from hydrate or from trapped gas as permafrost thaws might be the opening up of gas pathways between repository depth and the surface; amongst other impacts, these new pathways could accelerate C-14 and radon release (though the sources of C-14 in the wastes would by this time have probably decayed substantially);

One mechanism for rapid release of methane from hydrate would be the pressure release due to removal of an overlying ice sheet which could destabilise the hydrate.

# Appendix D. Additional Pourbaix diagrams for the system Fe-S-O-H

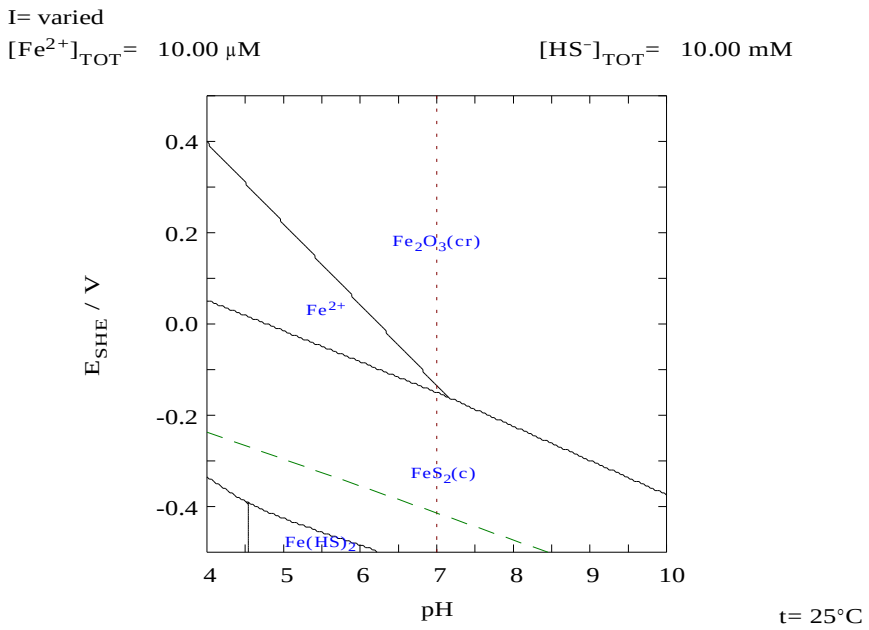


***Figure D1***. *Stability of iron sulphides and oxides in the simple system Fe-S-O-H at shown conditions. This diagram shows the case in which $HS^-$ concentration is extremely high (10 mM ≈ 350 mg/L).*

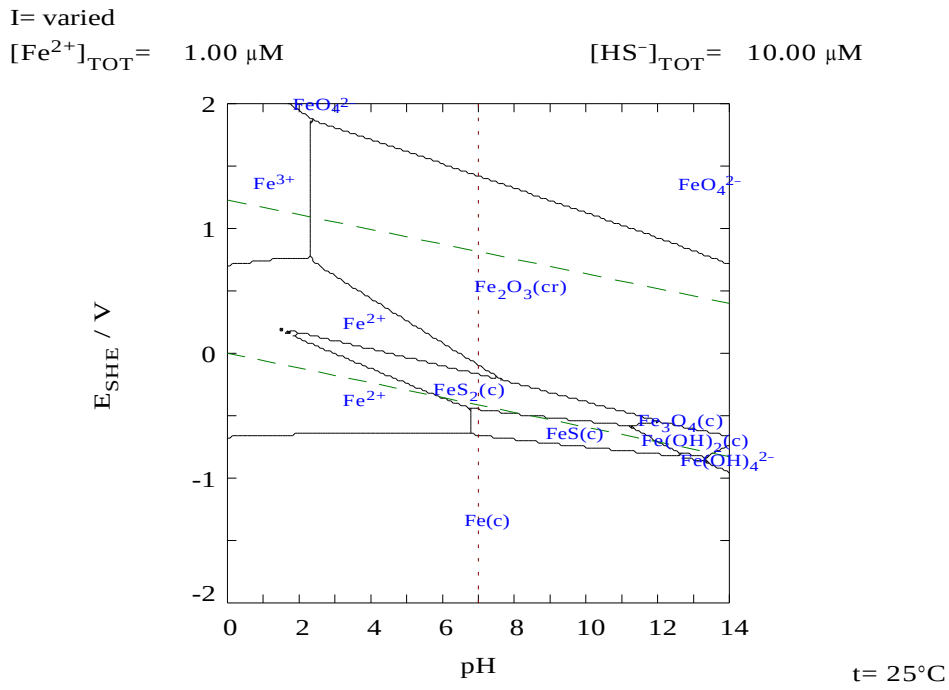


***Figure D2.*** *Stability of iron sulphides and oxides in the simple system Fe-S-O-H at shown conditions. This diagram shows the case in which [HS$^-$] is at the upper end of its range (10 µM ≈ 0.35 mg/L) and [Fe$^{2+}$] is at the low end of its range (1 µM ≈ 0.056 mg/L).*

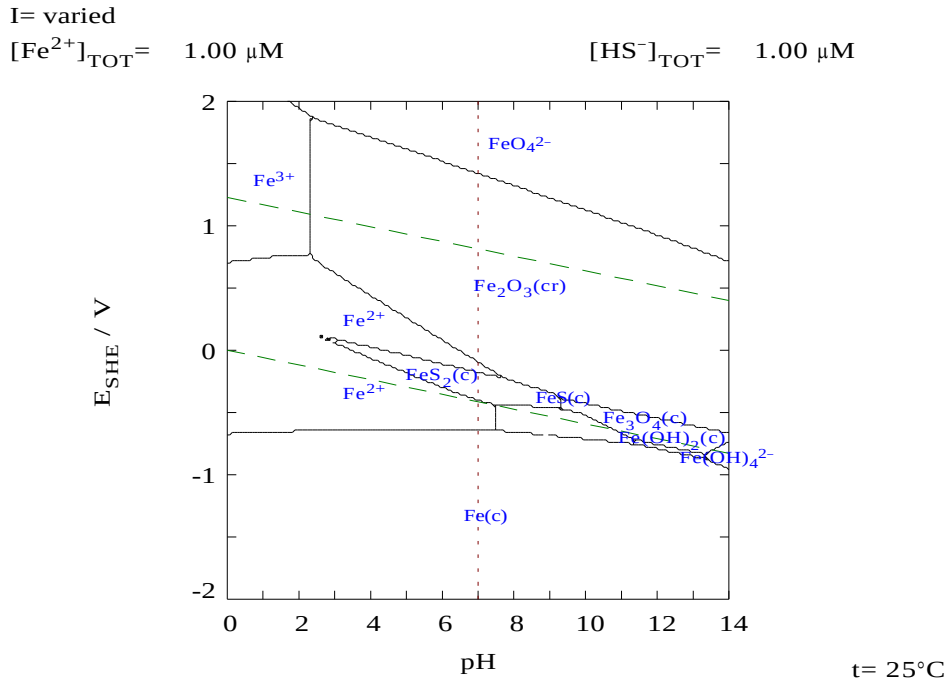


***Figure D3.*** *Stability of iron sulphides and oxides in the simple system Fe-S-O-H at shown conditions. This diagram shows the case in which both [HS$^-$] and [Fe$^{2+}$] are at the lower end of their ranges (0.035 mg/L and 0.056 mg/L respectively).*

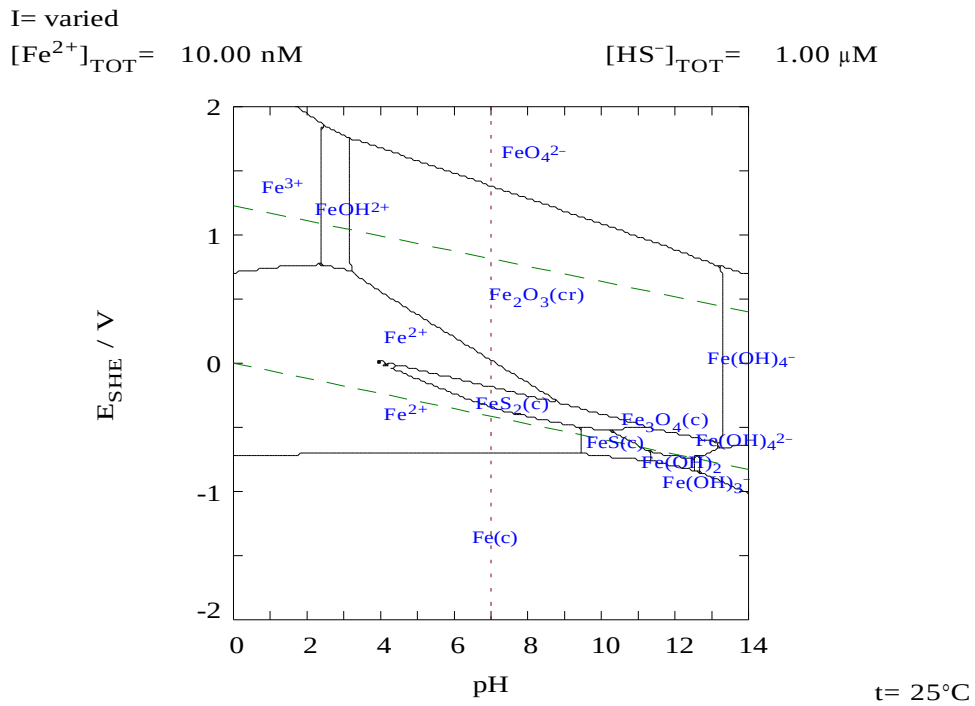


***Figure D4.*** *Stability of iron sulphides and oxides in the simple system Fe-S-O-H at shown conditions. This diagram shows the case in which [HS⁻] is at the lower end of its range (1 µM ≈ 0.035 mg/L) and [$Fe^{2+}$] is extremely low (10 nM ≈ 0.056 µg/L).*

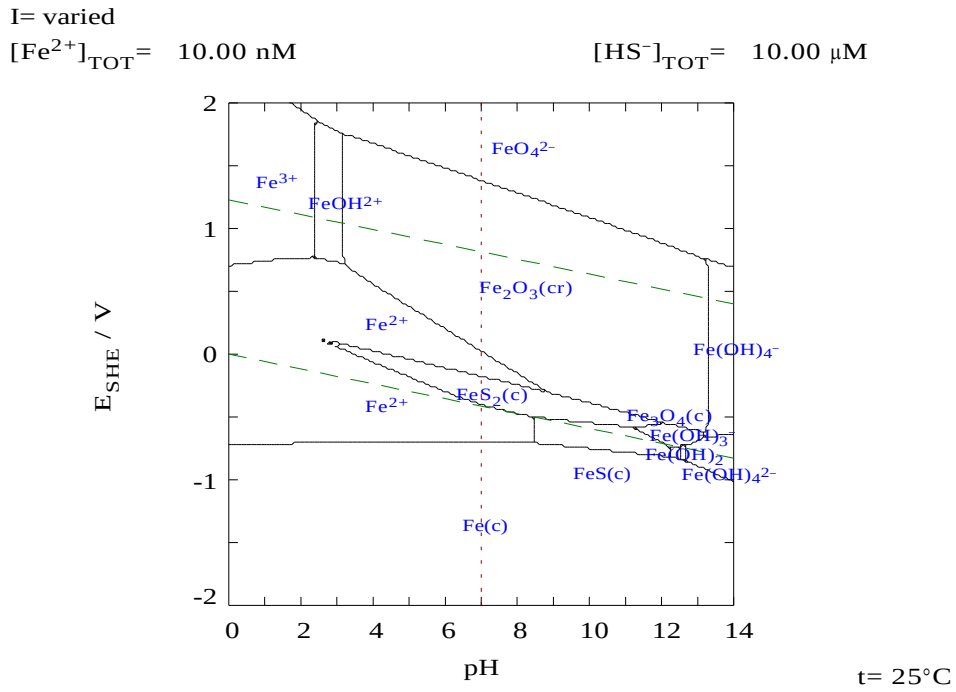


***Figure D5.*** *Stability of iron sulphides and oxides in the simple system Fe-S-O-H at shown conditions. This diagram shows the case in which [HS⁻] is at the upper end of its range (10 µM ≈ 0.35 mg/L) and [$Fe^{2+}$] is extremely low (10 nM ≈ 0.056 µg/L).*

# Appendix E. Additional Pourbaix diagrams for Cu-Fe-Cl-N-S-C-H-O

## E.1 The sub-system Cu-S-H-O

I= varied

$[HS^-]_{TOT}$= 0.10 µM $[Cu^+]_{TOT}$= 1.00 µM

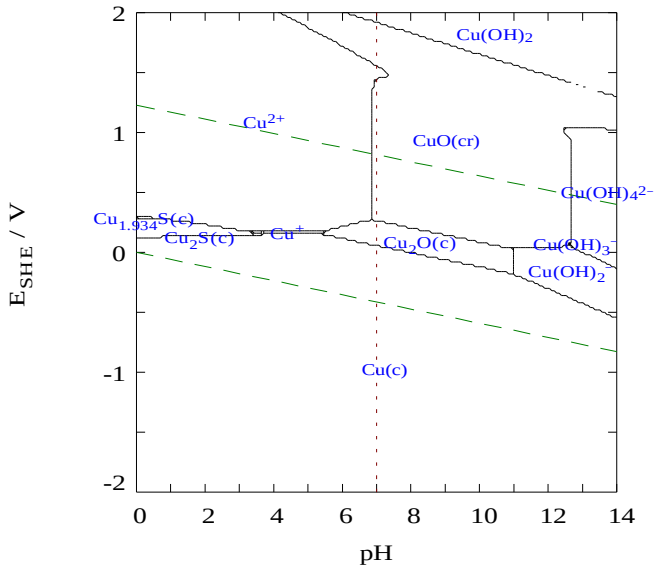


t= 25°C

***Figure E1.*** *Pourbaix diagram for the system Cu-S-H-O at indicated conditions. This diagram shows the case in which [HS$^-$] is much lower (0.10 µM ≈ 3.5 µg/L) than typical values and [Cu$^{2+}$] is much higher (1 µM ≈ 64 µg/L) than its likely range.*

## E.2 The sub-system Cu-Fe-S-Cl-H-O

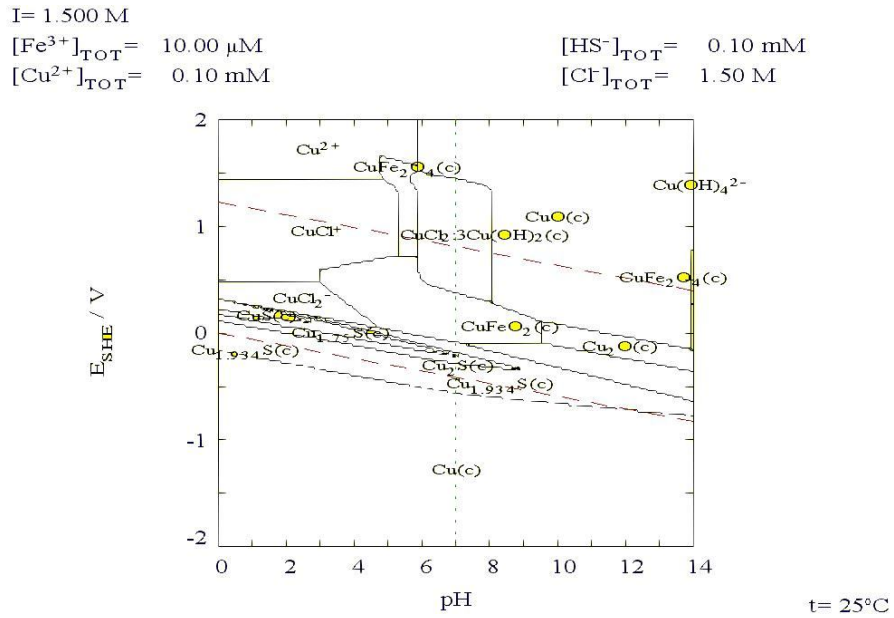


***Figure E2.*** *Pourbaix diagram for the system Cu-Fe-Cl-S-H-O at indicated conditions. This diagram shows the case in which [HS⁻] is [HS⁻] is at the high end (0.1 mM ≈ 3.5 mg/L) of the typical range, [$Fe^{2+}$] is typical (10 µM ≈ 0.56 mg/L) and [$Cu^{2+}$] is extremely high (0.1 mM ≈ 6.4 mg/L).*

## E.3 The sub-system Cu-Cl-C-H-O

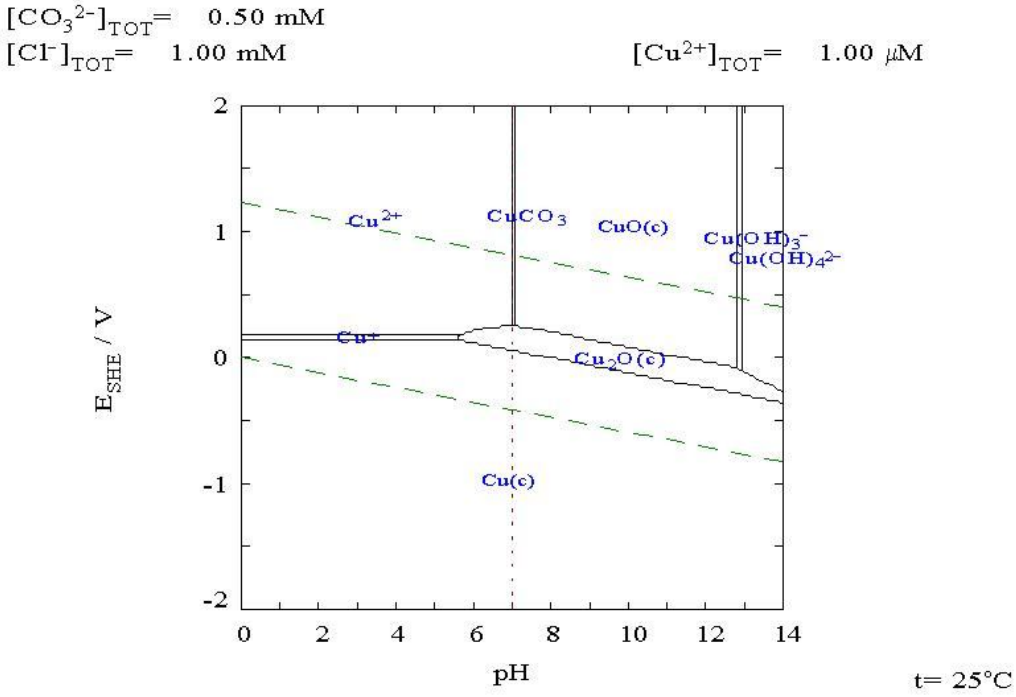


***Figure E3.*** *Pourbaix diagram for the system Cu-Cl-C-H-O at indicated conditions. This diagram shows the case in which [$CO_3^{2-}$] is higher (0.50 mM ≈ 30 mg/L) than typical for normal pH, [$Cl^-$] is low, i.e. fresh water(1 mM ≈ 35 mg/L) and [$Cu^{2+}$] is much higher (64 µg/L) than its likely range.*

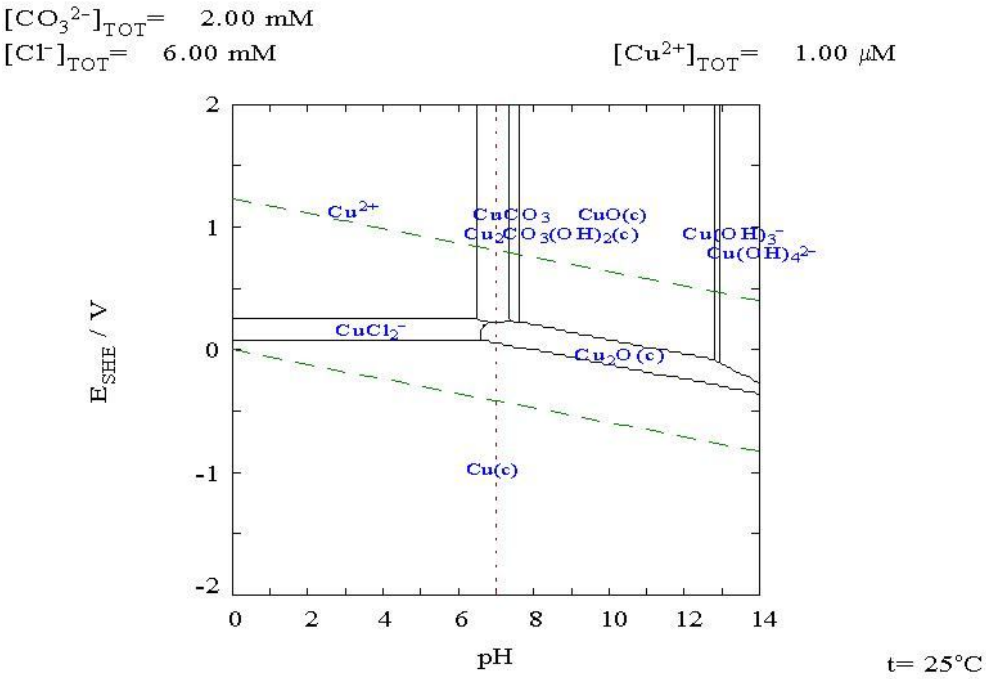


***Figure E4.*** *Pourbaix diagram for the system Cu-Cl-C-H-O at indicated conditions. This diagram shows the case in which [$CO_3^{2-}$] is extremely high (2 mM ≈ 120 mg/L) than typical for normal pH, [$Cl^-$] is low (6 mM ≈ 210 mg/L) and [$Cu^{2+}$] is much higher (64 µg/L) than its likely range.*

## E.4 The sub-system Cu-Cl-S-C-H-O

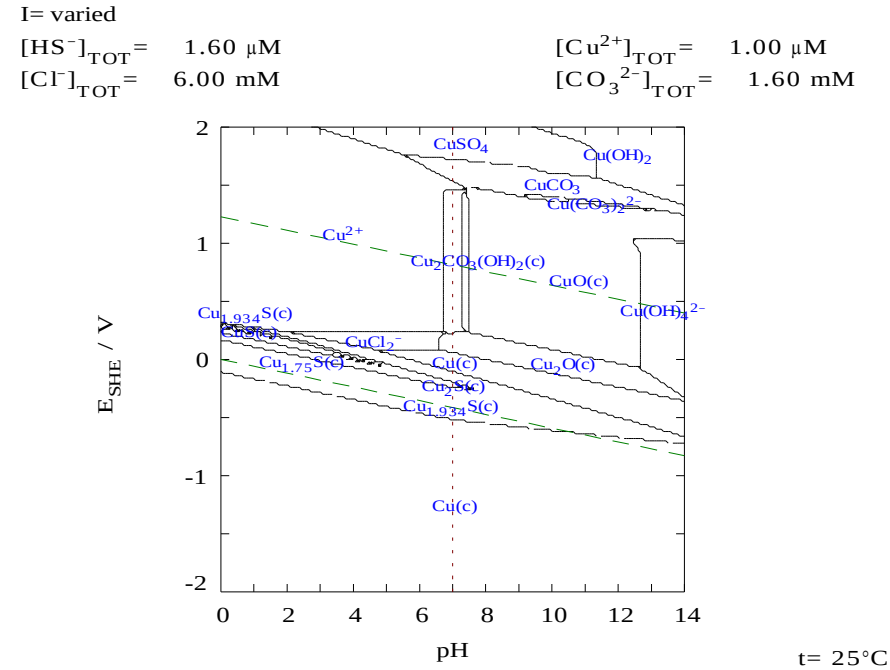


***Figure E5.*** *Pourbaix diagram for the system Cu-Cl-S-C-H-O at indicated conditions. This diagram shows the case in which [$CO_3^{2-}$] is extremely high (1.6 mM ≈ 96 mg/L) than typical for normal pH, [$Cl^-$] is low (6 mM ≈ 210 mg/L), [$HS^-$] is lower (56 µg/L) than typical values and [$Cu^{2+}$] is much higher (64 µg/L) than its likely range.*

## E.5 The sub-system Cu-Fe-Cl-S-C-H-O

$[CO_3^{2-}]_{TOT}$= 100.00 mM
$[HS^-]_{TOT}$= 1.00 mM
$[Cl^-]_{TOT}$= 20.00 mM
I= varied
$[Fe^{2+}]_{TOT}$= 1.00 µM
$[Cu^{2+}]_{TOT}$= 1.00 µM

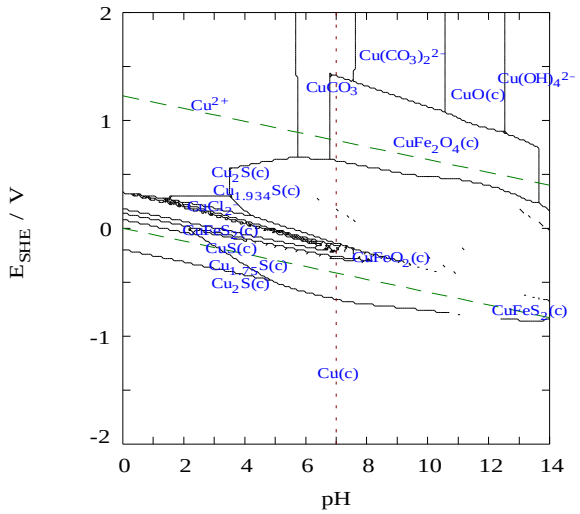


t= 25°C

***Figure E6.*** *Pourbaix diagram for the system Cu-Fe-Cl-S-C-H-O at indicated conditions. Low salinity water. Cu-containing species are shown. This diagram shows the case in which $[CO_3^{2-}]$ is unrealistically high (6000 mg/L), $[Cl^-]$ is brackish (700 mg/L), $[HS^-]$ is much higher (35 mg/L) than typical values, $[Fe^{2+}]$ is lower (0.056 mg/L) than typical values, and $[Cu^{2+}]$ is much higher (64 µg/L) than its likely range.*

$[CO_3^{2-}]_{TOT}$= 100.00 mM
$[HS^-]_{TOT}$= 1.00 mM
$[Cl^-]_{TOT}$= 5.00 M
I= varied
$[Fe^{2+}]_{TOT}$= 1.00 µM
$[Cu^{2+}]_{TOT}$= 1.00 µM

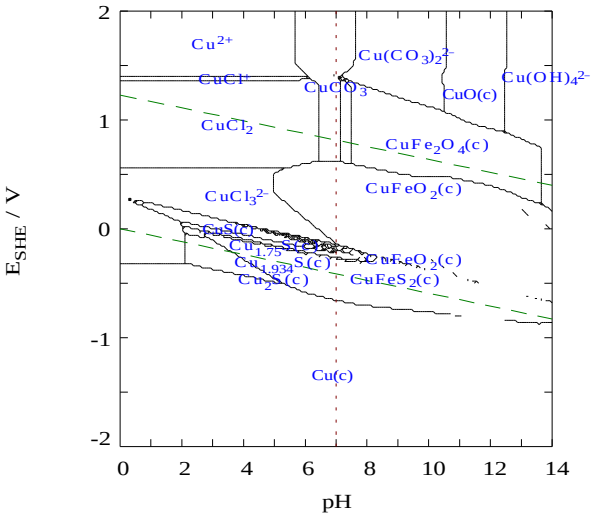


t= 25°C

**Figure E7.** *Pourbaix diagram for the system Cu-Fe-Cl-S-C-H-O at indicated conditions. High salinity water. Cu-containing species are shown. This diagram shows the case in which $[CO_3^{2-}]$ is unrealistically high (6000 mg/L), $[Cl^-]$ is very high, i.e. brine salinity (175000 mg/L), $[HS^-]$ is much higher (35 mg/L) than typical values and $[Cu^{2+}]$ is much higher (64 µg/L) than its likely range.*

## E.6 The sub-system Cu-Fe-N-S-H-O

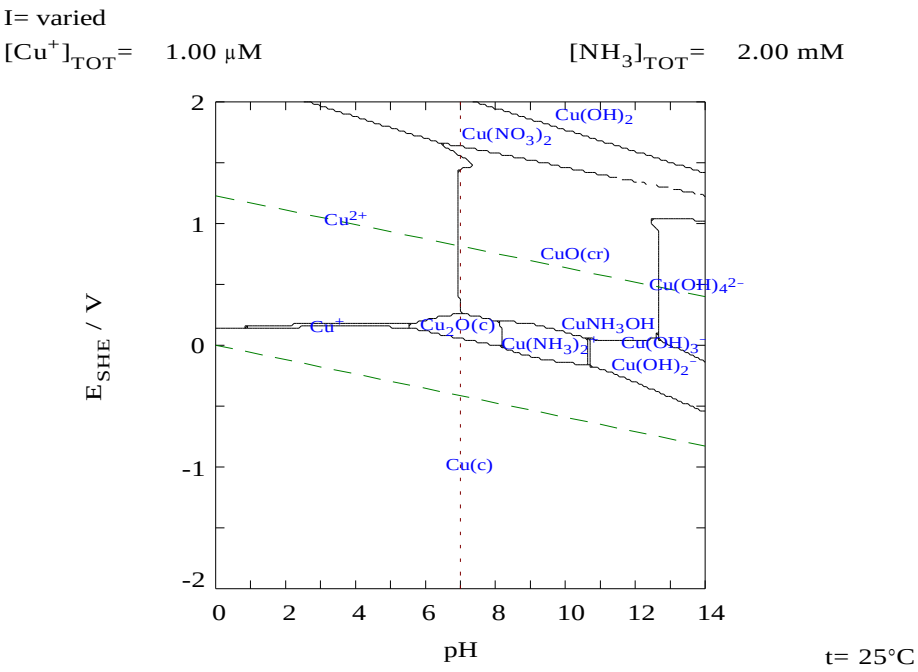


***Figure E8.*** *Pourbaix diagram for the system Cu-N-H-O at indicated conditions. Cu-containing species are shown. This diagram shows the case in which [$NH_3$] is very high (34 mg/L) and [$Cu^{2+}$] is much higher (64 µg/L) than its likely range.*

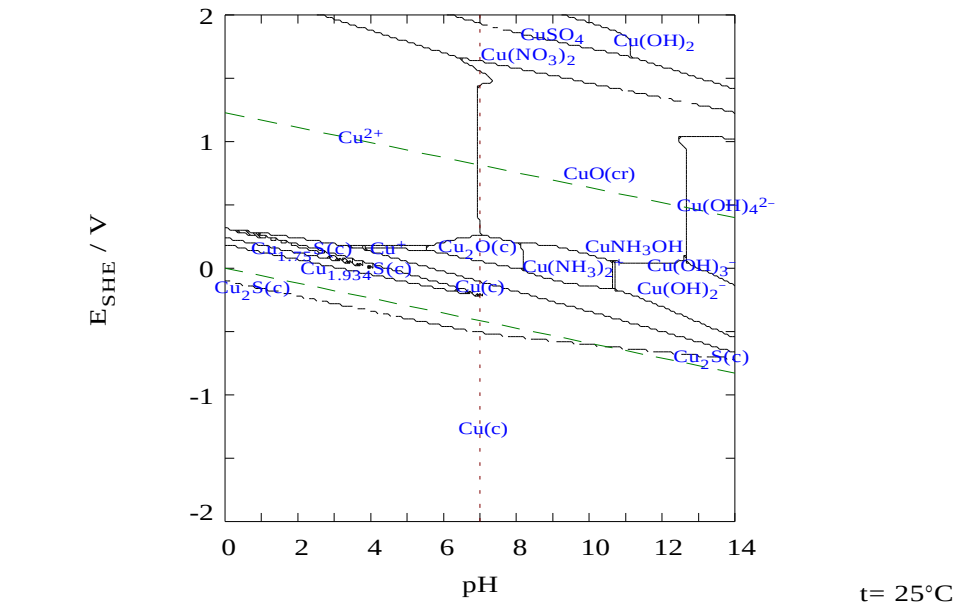


***Figure E9.*** *Pourbaix diagram for the system Cu-N-S-H-O at indicated conditions. Cu-containing species are shown. This diagram shows the case in which [$NH_3$] is very high (34 mg/L), [$HS^-$] is lower (35 µg/L) than typical values and [$Cu^{2+}$] is much higher (64 µg/L) than its likely range.*

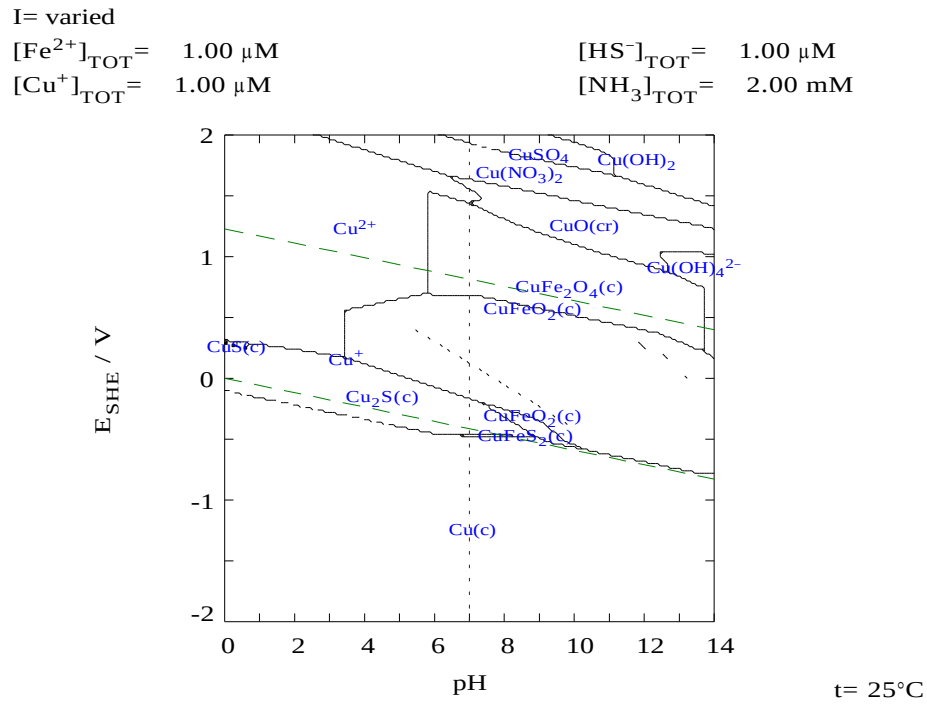


***Figure E10.*** *Pourbaix diagram for the system Cu-Fe-N-S-H-O at indicated conditions. Cu-containing species are shown. This diagram shows the case in which [$NH_3$] is very high (34 mg/L), [$HS^-$] is lower (35 µg/L) than typical values, [$Fe^{2+}$] is lower (0.056 mg/L) than typical values, and [$Cu^{2+}$] is much higher (64 µg/L) than its likely range.*

**Strålsäkerhetsmyndigheten**
**Swedish Radiation Safety Authority**

SE-171 16 Stockholm
Solna strandväg 96

**Tel**: +46 8 799 40 00
**Fax**: +46 8 799 40 10

**E-mail**: registrator@ssm.se
**Web**: stralsakerhetsmyndigheten.se